Inhibition of heterotrimeric Gs proteins by FR900359 - more than a simple transfer of the inhibitor binding site

Dissertation
zur
Erlangung des Doktorgrades (Dr. rer. nat)
der
Mathematisch-Naturwissenschaftlichen Fakultät
der
Rheinischen Friedrich-Wilhelms-Universität Bonn

vorgelegt von
Funda Eryilmaz
aus
Bonn

Bonn 2022

1. Gutachterin: Prof. Evi Kostenis
2. Gutachter: Prof. Hanns Häberlein

Tag der Promotion: 25.01.2023

Erscheinungsjahr: 2023

Die vorliegende Arbeit wurde in der Zeit von April 2018 bis Juli 2022 am Institut für Pharmazeutische Biologie der Rheinischen Friedrich-Wilhelms-Universität Bonn unter der Leitung von Frau Prof. Dr. Evi Kostenis angefertigt.

Für meine Familie

Abstract

A plethora of vital functions of the human body, including blood pressure, cell proliferation and metabolism are regulated by G protein-mediated signaling cascades. These cascades form a complex network of cause and effect that allows our bodies to adapt to, function and thrive in a wide range of environments and circumstances. However, this network of signals does not always run flawlessly, and when off balance, pathological changes and diseases are often the consequence such as cancer or hypertension. To treat these diseases, the thorough study of G protein-mediated signaling cascades is an important component of basic research, to understand their influence or contribution to certain cellular events. Such in depth investigations could be accomplished, for example, with specific G protein inhibitors. However, despite the discovery of G proteins about 30 years ago, only specific inhibition of Gi and Gq, two of the four G protein families, could be achieved by PTX or FR900359 (FR) / YM-25489 (YM), respectively. To bridge the lack of such highly cell permeable specific inhibitors of a third G protein family, $G\alpha_s$ (Gs) proteins with artificial FR/YM-binding sites, such as $G\alpha_{s11}$ (Gs 11), $G\alpha_{s10}$ (Gs 10), respectively, have been developed.

To this end, we investigated the suitability of Gs 11 and Gs 10 as chemogenetic tools for further possible studies. The idea behind chemogenetics is generally described as the approach in which engineered molecules interact with previously unrecognized molecules that are pharmacologically inert in the absence of the designed protein. Using CRISPR/Cas9-generated $G\alpha_s$-null or $G\alpha_{s/olf/q/11/12/13/z}$ - null cells along with several cutting-edge tools such as label-free whole-cell biosensing, HTRF based cAMP accumulation or real-time BRET-based G protein activation, we determined conditions for the use of Gs 10 as a possible chemogenetic tool.

However, intriguingly despite the transfer of the inhibitor binding site, FR´s inhibitory properties could not be entirely transferred. While Gq protein- dependent signaling events could be abolished completely, comparable conditions, such as the maximum activation of the overexpressed β2 adrenergic receptor (β2AR) resulted in partial inhibition for the artificial FR-sensitive Gs proteins. Moreover, we noted biologically distinct activities for FR and YM,

despite close structural similarities. Thus, the lack of full inhibition was pronounced for the studies done with YM as compared with FR.

Our results suggest that the simple transfer of the inhibitor binding site is not sufficient to transfer the properties of inhibition. Thus, possible FR scaffold-based inhibitors which mimic the interaction of FR with Gα proteins accommodating engineered FR-binding sites are not sufficient to perform studies on the same scale as would be possible with Gq.

As a result, our study provides an important basis for the understanding of G protein activation and inhibition thus demonstrating the uniqueness of each individual G protein family since although they share an identical inhibitor binding site, Gq but not Gs 11 and Gs 10 could be fully inhibited by FR.

Zusammenfassung

Eine Vielzahl lebenswichtiger Funktionen des menschlichen Körpers, darunter der Blutdruck, die Zellproliferation und der Stoffwechsel, werden durch G-Protein-vermittelte Signalkaskaden reguliert. Diese Kaskaden bilden ein komplexes Netz von Ursache und Wirkung, sodass unserem Körper ermöglicht wird, sich an eine Vielzahl von Umgebungen und Umständen anzupassen, zu funktionieren und zu entfalten. Dieses Netzwerk von Signalen funktioniert jedoch nicht immer einwandfrei, und wenn es aus dem Gleichgewicht gerät, sind pathologische Veränderungen und Krankheiten wie Krebs oder Bluthochdruck oft die Folge. Um diese Krankheiten zu behandeln, ist die sorgfältige Untersuchung von G-Protein-vermittelten Signalkaskaden ein wichtiger Bestandteil der Grundlagenforschung, um ihren Einfluss oder Beitrag zu bestimmten zellulären Ereignissen zu verstehen. Solche eingehenden Untersuchungen könnten zum Beispiel mit spezifischen G-Protein-Inhibitoren durchgeführt werden. Trotz der Entdeckung der G-Proteine vor etwa 30 Jahren konnte jedoch nur eine spezifische Hemmung von Gi und Gq, zwei der vier G-Proteinfamilien, durch PTX bzw. FR900359 (FR) / YM-25489 (YM) erreicht werden. Um den Mangel an solchen hoch zelldurchlässigen spezifischen Inhibitoren einer dritten G-Protein-Familie zu überbrücken, wurden Gαs (Gs)-Proteine mit künstlichen FR/YM-Bindungsstellen namens $G\alpha_{s11}$ (Gs 11) bzw. $G\alpha_{s10}$ (Gs 10), entwickelt.

Zu diesem Zweck untersuchten wir die Eignung von Gs 11 und Gs 10 als chemogenetisches Tool für weitere mögliche Studien. Die Idee hinter chemogenetischen Tools wird ganz allgemein als der Ansatz, bei dem konstruierte Moleküle mit zuvor unbekannten Molekülen interagieren beschrieben. Unter Verwendung von CRISPR/Cas9-generierten $G\alpha_{s}$-Null- oder $G\alpha_{s/olf/q/11/12/13/z}$ -Null-Zellen sowie verschiedener modernster Techniken, wie markierungsfreie Ganz-Zell Massenumverteilung, HTRF-basierte cAMP-Akkumulation oder BRET-basierte G-Protein-Aktivierung in Echtzeit, ermittelten wir die Bedingungen für die Verwendung von Gs 10 als mögliches chemogenetisches Tool.

Interessanterweise konnten jedoch trotz der Übertragung der Inhibitor-Bindungsstelle die hemmenden Eigenschaften von FR nicht vollständig übertragen werden. Während Gq-Protein-abhängige Signalereignisse vollständig gehemmt werden konnten, führten vergleichbare Bedingungen, wie die maximale Aktivierung des überexprimierten adrenergen β 2-Rezeptors (β2AR), zu einer teilweisen Hemmung der künstlich erzeugten

FR-empfindlichen Gs-Proteine. Darüber hinaus konnten wir trotz enger struktureller Ähnlichkeiten biologisch unterschiedliche Aktivitäten für FR und YM feststellen. So war partielle Hemmung bei den mit YM durchgeführten Studien im Vergleich zu FR deutlich ausgeprägter.

Unsere Ergebnisse deuten darauf hin, dass die einfache Übertragung der Inhibitor-Bindungsstelle nicht ausreicht, um die Eigenschaften der Hemmung zu übertragen. Mögliche Inhibitoren auf der Basis eines FR-Gerüsts, die die Interaktion von Gα-Proteinen, welche artifizielle FR-Bindungsstellen besitzen nachahmen, reichen also nicht aus, um Studien in demselben Umfang durchzuführen, wie es mit Gq möglich wäre.

Demzufolge liefert unsere Studie eine wichtige Grundlage für das Verständnis der Aktivierung und Hemmung von G-Proteinen und zeigt die Einzigartigkeit jeder einzelnen G-Protein-Familie, denn obwohl sie eine identische Inhibitor-Bindungsstelle besitzen, konnten Gq, aber nicht Gs 11 und Gs 10 vollständig durch FR gehemmt werden.

Table of Contents

Introduction

Signal transduction

How do cells convert extracellular into intracellular signals? And how do different cells exchange information in order to work together effectively? Martin Rodbell was the first who characterized the term “signal transduction” in 1980, to describe how cells receive, process, and finally transmit information from the outside to the interior of the cell (Rodbell 1980; Cooper 2000).

The barrier of a cell, a phospholipid bilayer, disconnects the cell interior from the outside milieu. Because membranes are semipermeable barriers only small and lipophilic ligands such as steroid hormones can freely overcome the boundaries. Yet, large, and hydrophilic ligands cannot pass the barrier (Alberts 2015; Escriva et al. 2000). Thus, to be able to detect and respond to such larger hydrophilic ligands, cells have evolved different strategies. A possible way to transfer those messages are via receptors, such as G-protein-coupled receptors (GPCRs) that are embedded into the membrane. Therefore, one form of a signal, the so-called first messenger, “binds” to the receptor which causes a change in its conformation that subsequently triggers a response in the cell by producing a second form of the signal (second messenger). Second messengers in turn are molecules that relay signals to further signaling partners, so-called effector proteins that trigger distinct signaling pathways that ultimately elicit a cellular response (Ashcroft 1997), (Newton et al. 2016)

G protein-coupled receptors and G proteins

G protein-coupled receptors (GPCRs) are the largest family of membrane proteins with over 800 members encoded in the human genome, and over 30 % of FDA-approved drugs target directly GPCRs (Hauser et al. 2017; Rosenbaum et al. 2009). All GPCRs share the same basic structure and are characterized by the presence of seven transmembrane helices, an extracellular N terminus, an intracellular C terminus and three interhelical loops on each side of the membrane (Rosenbaum et al. 2009; Oldham und Hamm 2008).They represent one of the most essential nodes to transduce signals from the extracellular to the intracellular environment. Thus, each GPCR binds and thereby detects a specific set of extracellular

ligands, wherein activation is typically mediated by the binding of an agonist that stabilizes receptor conformations which recruit and finally activate intracellular transducers (Wacker et al. 2017). Such transducers are heterotrimeric G proteins composed of three subunits, usually referred to as the Gα, Gβ and Gγ subunits (Simon et al. 1991; Marinissen und Gutkind 2001). The Gα subunit composed of two domains, a GTPase “Ras-like” domain that is conserved in all members of the GTPase superfamily and an α-helical domain that is unique to heterotrimeric G proteins. The guanine nucleotide, GDP or GTP, that gives G proteins their name, is tightly sandwiched between both domains (Syrovatkina et al. 2016b; Oldham und Hamm 2008). In the inactive state, Gα is GDP-bound and in complex with the βγ-subunit (Fig. 1A). Upon binding of an activated GPCR by a ligand on the external side of the membrane, the Gα subunit undergoes a conformational change and releases GDP. As a result, guanosine triphosphate (GTP) accommodates spontaneously the uncovered nucleotide-binding site (Fig. 1B) (Dror et al. 2015). Since the GTP-bound Gα subunit has a lower affinity for the Gβγ subunit the heterotrimer undergoes a structural rearrangement. Both subunits, Gα(GTP) and Gβγ in turn bind to intracellular effector proteins and modify their properties, thus transducing extracellular stimuli into an intracellular signaling cascade (Fig. 1C) (Oldham und Hamm 2008; Rosenbaum et al. 2009). To prevent sustained stimulation, the signal is terminated by the GTPase activity of the Gα subunit, which hydrolyzes GTP to GDP. Moreover, this process is supported by GTPase-activating proteins (GAP). As a result, the Gα subunit loses affinity for its effectors and re-associates with the Gβγ subunit. The formation of the heterotrimer in turn allows the engagement of a G protein to a GPCR and thus a reactivation to transmit a signal (Fig. 1D). This fast off-rate and subsequent potential for reactivation has evolved in animals for allowing quick, time-resolved responses to the environment.

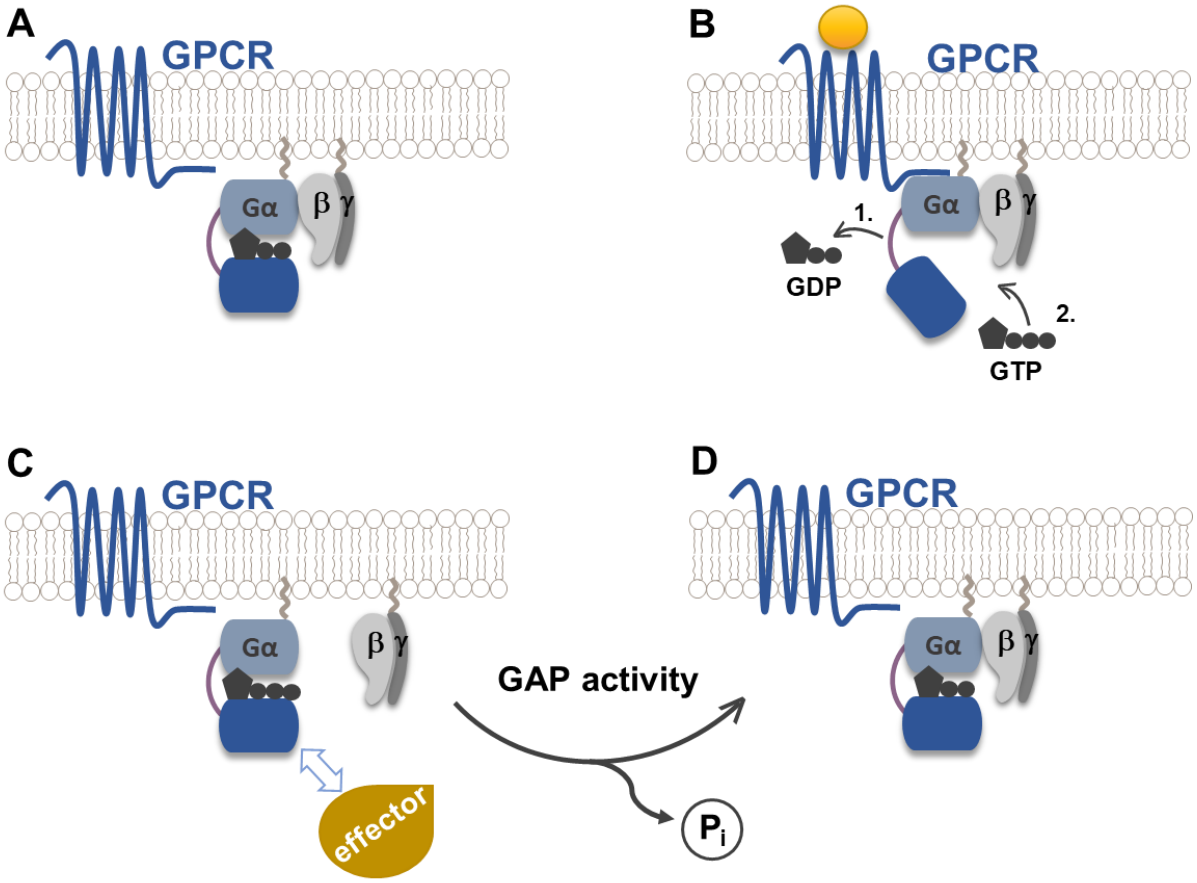

Figure 1: G protein activation via G protein-coupled receptor. Based on (Oldham und Hamm 2008; Syrovatkina et al. 2016b; Rosenbaum et al. 2009) The inactive state**,** depicted in (A) forms a heterotrimeric G protein composed of the GDP-bound Gα and Gβγ subunit, anchored to the cellular membrane by a prenylated residue of both Gα and Gγ subunit. (B) Upon ligand mediated activation of the G protein-coupled receptor (GPCR), a conformational change is provoked in the Gα subunit that accelerates the GDP release and thus (C) allows guanosine triphosphate (GTP) to accommodate spontaneously the uncovered nucleotide-binding site. The GTP loaded Gα subunit dissociates and binds to its effector proteins. (D) Both the GTPase activity of the Gα subunit and GTPase-activating proteins (GAP) hydrolyze GTP to GDP resulting in a re-association with the Gβγ subunit and thus formation of the heterotrimer.

Gαs signaling pathway

Based on the sequence similarity and their functional properties the Gα proteins are divided into four major classes $G\alpha_{q/11}$, $G\alpha_{s}$, $G\alpha_{i/o}$ and $G\alpha_{12/13}$ (here after Gq, Gs, Gi/o, G12/13) (Oldham und Hamm 2008) Each family is associated with a certain signaling cascade initiated by a GPCR and a GTP-bound Gα protein. The G protein at the center of this work, the ubiquitously expressed Gs protein, binds and stimulates upon receptor activation the adenylyl cyclase (AC), an enzyme that converts ATP to the second messenger cyclic adenosine monophosphate (cAMP) that directly regulates a variety of cell functions such as metabolism, ion channel activation, cell growth and, gene expression. Binding of cAMP to e.g. protein kinase A (PKA), the best-understood target, which is an inactive serine/threonine kinase that is composed of two regulatory and two catalytic subunits, causes the release of the catalytic subunits which in turn allows phosphorylation of proteins to modify their biological activity both cytosolic and nuclear (McKnight 1991; Taylor et al. 1992). As a result, PKA regulates signaling pathways, for example, by phosphorylating and thereby inactivating phospholipase C (PLC) β2 or by decreasing the activity of Raf and Rho or by activating MAP kinases through promotion of phosphorylation and dissociation of an inhibitory tyrosine phosphatase (PTP). Translocation of the catalytic subunits to the nucleus leads to regulation of transcription through direct phosphorylation of the transcription factor cAMP-response element-binding protein (CREB). This transcription factor binds CRE regions (cAMP response element), which are promoters of specific genes whose expression can be up- or down-regulated by the increase in cAMP (Sassone-Corsi 2012). Hence, the multiple influences dependent on Gs signaling suggest that mis-regulation within the signaling cascade could have enormous pathophysiological consequences, thus making it an extremely attractive target for in-depth investigations (Gold et al. 2013; Bock et al. 2020).

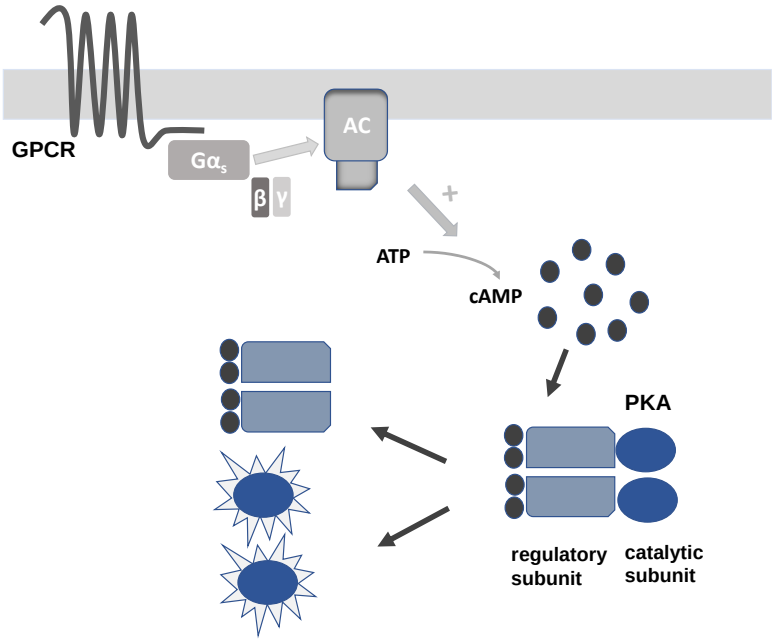

Figure 2: Gs protein signaling pathway. The Gα subunit binds and stimulates upon receptor activation the adenylyl cyclase (AC), which converts ATP to the second messenger cyclic adenosine monophosphate (cAMP). Binding of cAMP to protein kinase A (PKA), an inactive serine/threonine kinase that is composed of two regulatory and two catalytic subunits, causes the release of the catalytic subunits which in turn allows phosphorylation of proteins to modify their biological activity.

G Protein modulator

Despite the discovery of heterotrimeric G proteins about 30 years ago and their important role in the GPCR-mediated signal transduction, only few pharmacological agents exist for precision G protein modulation. However, targeting GPCR signaling on the level of heterotrimeric G proteins instead of the receptor may actually have several advantages. Thus, the pathology of numerous diseases is multifaceted and results in dysregulation of more than one receptor (Stone und Molliver 2009; Dorsam und Gutkind 2007; Druey 2009). Of the four major G protein families (Gi/o, Gs, Gq, and G12/13) only the Gi/o and Gq proteins are effectively hampered from signal transduction by pertussis toxin (PTX) through covalent modification (Katada und Ui 1982) and FR900359 (FR) (Schrage et al. 2015) or YM-254890 (YM) via noncovalent binding (Taniguchi et al. 2003) respectively (Patt et al. 2021). Both the bacterial toxin PTX, which selectively and irreversibly inactivates Gi proteins by ADP-

ribosylation of the alpha subunit, and FR/YM, which suppress Gq signaling by hindering GDP release in the Gα subunit, provided the possibility to unravel the involvement of Gi and Gq proteins in cellular processes.

Noncovalent control of G protein function has so far only been achieved for the Gq family by FR and YM. In 1988, the selective and cell-permeable Gq inhibitor, isolated from the evergreen plant Ardisia crenata, was first described by Fujioka et al. Even though the mechanism of action had not been elucidated at that time, the first pharmacological effects such as inhibition of platelet aggregation on rabbits in vitro and decrease of the blood pressure were observed (Fujioka et al. 1988). In 2003, YM, the highly structural similar depsipeptide, first isolated from the chromobacterial strain QS3666, was reported to inhibit ADP-induced platelet aggregation in human plasma (Taniguchi et al. 2003). In 2004, shortly after the discovery, Takasaki et al. elucidated the mechanism of action and characterized YM as a potent and selective Gq inhibitor (Takasaki et al. 2004). X-ray crystallographic evidence disclosed that YM docks into a hydrophobic cleft between the Linker I and Switch I (Linker II) loop that connect the GTPase and the helical domain of Gα, which harbors the bound nucleotide. Stabilizing of these interdomain linkers suppresses the hinge motion of the helical domain away from the GTPase domain which is required for the GDP release. Therefore, noncovalent binding of YM leads to inhibition of GDP, thus trapping the Gα subunit in its GDP bound inactive state. Consequently, YM was classified by Nishimura et al. as a guanine nucleotide dissociation inhibitor (GDI) (Nishimura et al. 2010a). A few years ago, in 2015, the comprehensive study by Kostenis and her co-workers revealed that FR likewise functions as GDI (Schrage et al. 2015), and that FR operates via comparable mechanism of action as compared with YM to accomplish its specific Gq inhibition (Malfacini et al. 2019).

Pharmacological control over Gs

Such pharmacological agents, i.e., FR and YM do not exist for Gs proteins even though cholera toxin (CTX), a bacterial toxin produced by Vibrio cholerae, has been used for defining the contribution of Gs proteins to biological processes (Chakraborty et al. 1991). While FR and YM leave Gq in the “off-state”, CTX actually induces the opposite effect

through irreversible ADP-ribosylation of the residue R201, leading to an abolished GTPase activity and consequently persistent activation rather than inhibition of the Gs protein. Thereby, CTX masks Gs signaling by freezing the $G\alpha_s$ subunit in its GTP bound state. As a result, the Gs protein is uncoupled and no longer available for the recruitment of GPCRs. While this disrupts the natural G protein cycle, the results should still be interpreted with caution because there is no proper inhibition of G protein, such as maintenance of the GDP bound and therefore inactive state (Seibel-Ehlert et al. 2021; Patt et al. 2021; Haan und Hirst 2004; Cassel und Pfeuffer 1978). Moreover, BIM-46174 and the more stable BIM-46187 or the anthelmintic drug Suramin were initially characterized as selective Gs inhibitors (Prévost et al. 2006; Freissmuth et al. 1996). However, neither BIM molecules nor Suramin proved to be selective Gs inhibitors, as further studies revealed that BIM targets not only the Gs family, but also the Gi/o, Gq/11 and G12/13, as do Suramin and its analogs, which have a low selectivity profile since in addition to partial Gs inhibition, the Gi/o family can also be inhibited (Ayoub et al. 2009; Freissmuth et al. 1996). Thus, studies addressing, for example, the involvement of the Gs signaling pathway in various cellular processes cannot be performed as precisely and effectively as has been done for several years to decipher the Gq signaling pathway by using FR and YM. Notable, several groups reported the emerging potential of FR as a therapeutical agent in studies on adipose tissue (Klepac et al. 2016) or uveal melanoma (Annala et al. 2019; Kostenis et al. 2020). Furthermore, inhalative application of FR revealed auspicious results by preventing airway constriction without side effects such as arrythmia and hypotonia (Matthey et al. 2017).

Chemogenetic approach

As mentioned above, effective Gs modulators do not exist. Therefore, scientists attempted to develop strategies to circumvent among other the lack of Gs inhibitors by developing FR and YM analogs. Since the common binding site of FR and YM in each Gα subunit is distinct but sufficiently conserved it is reasonable to speculate that the development of such analogs might inhibit other G proteins such as Gs by a similar mechanism of action (Malfacini et al. 2019). However, despite intense efforts none of the designed analogs showed specific inhibition apart from the Gq family (Gq, G11 and G14) (Kaur et al. 2015a; Rensing et al. 2015b; Zhang et al. 2018a; Zhang et al. 2017a; Taniguchi et al. 2004b). Because the rational design of such molecules is more difficult than expected, chemogenetic G16 (Taniguchi et

al. 2004b), Gi (Onken et al. 2018), and Gs (Boesgaard et al. 2020) proteins with artificial FR binding sites were developed, offering an alternative for specific studies to i.e., determine the G protein family that is responsible for a particular physiological effect. The idea behind chemogenetics is generally described as the approach in which engineered molecules interact with previously unrecognized molecules that are pharmacologically inert in the absence of the designed protein (Roth 2016). Following this strategy FR sensitive G proteins were engineered by exchanging eight residues in Gi (Onken et al. 2018), five residues in G16 (Malfacini et al. 2019), and eleven residues in Gs (Boesgaard et al. 2020) for the equivalent Gq amino acids of the inhibitor binding site.

Gs 11

In order to develop a FR-sensitive Gs protein, Boesgaard et al. analyzed first the differences between the defined inhibitor binding site in Gq and the presumed depsipeptide binding site in Gs by creating a homology model of Gs in complex with FR. They compared amino acids with side chains that interact or might interact with FR and mapped subsequently these positions in a sequence alignment. As a result, 11 positions near the inhibitor differ between Gq and Gs.

Figure 3: Amino acid sequence alignment of Gq WT, Gs WT and Gs 11.
Sequence alignment of the inhibitor binding site region in Gq WT and Gs WT with differing binding site residues in blue and okra, respectively. Gs 11 with the respective Gq residue in blue.

Finally, the authors reported that their attempt to introduce FR inhibition in Gs succeeded by altering the Gs protein at the respective relevant 11 positions. Hence, referring to the 11 mutations within the Gs protein the FR-sensitive Gs protein was named $G\alpha_{s11}$ (Gs 11). Because the goal of their study was to “investigate the molecular determinants for the Gq selectivity of FR by swapping selected Gαs and Gαq residues” (Boesgaard et al. 2020), the main focus of Boesgaad et al. was more structural rather than functional related contrary to our approach in this work.

Goal of the study

Since inhibition of Gs is needed to determine, e.g. the G protein family that is responsible for a particular physiological effect, chemogenetic tool characterizations are important to assess the suitability for such approaches in vitro, ex vivo and in vivo.

Firstly, we wondered whether the artificial FR-sensitive Gs protein might be suitable to serve as a chemogenetic tool since Gs11 has been reported to have a high basal activity (Boesgaard et al. 2020), which could affect its performance as a chemogenetic tool. Secondly, we examined the inhibition profiles of Gq, the natural target of FR, and Gs 11 to compare them under similar conditions. Because studies, in which FR was used as a Gq inhibitor, provided promising experiments (Annala et al. 2019; Klepac et al. 2016; Matthey et al. 2017) we wondered whether the transfer of the inhibitor binding site would result in similar inhibitor efficacy and potency, as these parameters are important for chemogenetic tools in studies where, for example, conclusions are to be drawn based on complete inhibition of the pathway.

Material

Chemicals and Reagents

Table 1: Chemicals and Reagents

Table 1: Chemicals and reagents

Name	Company	Ref. No.
Ampicillin	Roth	K.029.1
Carbachol	Sigma-Aldrich	C4382
FR900359	G König lab	N/A
GTPγS [^{35}S]	Perkin Elmar	N/A
Guanosine diphospate	provided by C. Müller lab	N/A
Hanks' buffered salt solution (HBSS)	Thermo Fischer Scientific	14175129
Isobutylmethylxanthine (IBMX)	Sigma-Aldrich	I5879
Isoprenaline	Sigma-Aldrich	I5627
Magnesium chloride	provided by C. Müller lab	N/A
Magnesium sulfate	provided by C. Müller lab	N/A
Nano-Glo Luciferase	Promega	N1110
Natrium chloride	provided by C. Müller lab	N/A

Pfu-DNA-PolymeRase	Promega	M774A
Poly-ethylene imine (PEI)	Polyscience	24313-2
YM-254890	Wako	253-00633

Cell Culture Media

Table 2: Media Bases

Name	Company	Ref. No.
DMEM - Dulbecco's Modified Eagle Medium	Thermo Fisher Scientific	11965092

Table 3: Media Supplements

Name	Company	Ref. No.
Penicillin/streptomycin solution	Thermo Fisher Scientific	15140
Fetal Bovine Serum (FBS)	Sigma Aldrich	804

Antibodies

Table 4: Antibodies

Name	Company	Ref. No.
mous anti-Gs	Santa Cruz	C2816
rabbit anti-α tubulin	LSBio	C368771

Plasmids

Table 5: Plasmids

Name	Company	Ref. No.
β2AR	Asuka Inoue	1516
$G\alpha_q$-pcDNA3.1	Evi Kostenis	1008
$G\alpha_s$-pcDNA3.1	Evi Kostenis	1530
$G\alpha_{s11}$-pcDNA3.1	Gene Cust	1549
$G\alpha_{s10}$-pcDNA3.1	Evi Kostenis	1572
$G\alpha_{sR201C}$-pcDNA3.1	Evi Kostenis	1580
masGRK3ct-Nluc	Kirill Martemyanov	1599
muscarinic M3	Asuka Inoue	1525
pcDNA3.1	Evi Kostenis	1218
PTXS1	Asuka Inoue	1464
venus/156-239-Gbeta1	Kirill Martemyanov	1601
venus/1-155-Ggamma2	Kirill Martemyanov	1602

Bacterial Strains

Table 6: Bacterial Strains

Name	Company	Ref. No.
DH5α Competent Cells	Thermo Fisher Scientific	18265-017

Experimental Models

Table 7: Cell lines

Name	Company	Ref. No.
Human: ΔGq/11 HEK	Asuka Inoue	N/A
Human: ΔGs/o HEK	Asuka Inoue	N/A
Human: ΔGs, Gq, G12/13, Gz HEK	Asuka Inoue	N/A

Commercial Assay Kits

Table 8: Commercial Assay Kits

Name	Company	Ref. No.
ECL Prime Western blotting detection reagent	GE Healthcare	RPN2236
HTRF-cAMP dynamic 2 kit	Cisbio International	62AM4PEC
Pierce BCA Protein Assay	Thermo Fisher Scientific	23225
black 96-well tissue culture plates with clear bottom	Corning	3603

Methods

Molecular biology protocols

Site directed mutagenesis

Site directed mutagenesis was utilized to introduce point mutations via primers, containing the desired modification in the nucleotide sequence.

A mixture of 5 µl Reaction buffer, 2 µl template DNA (0.01 µg/µl), 1.5 µl Forward and Reverse Primer, 1 µl dNTP 10 mM, 1.5 µl DMSO, 0.5 µl Pfu-Polymerase and 37 µl Rnase-Dnase free water were prepared to perform the Polymerase Chain Reaction (PCR). The reaction contains several steps as follows:

Steps	**Temperature (°C)**	**Time (min)**	
Initial denaturation	94	3	
Denaturation	94	1	16 x
Annealing	52	1	
Elongation	68	8	
Storage	4	∞	

Digestion of template DNA

To digest the template DNA 1 µl of digestion enzyme DpnI was added to each reaction tube. The mixture was gently vortexed, centrifuged and incubated for at least 1 hour at 37°C. Afterwards the DNA was either stored at -20°C or amplified by a transformation.

Site directed mutagenesis by overlap extension (for Gs 11^{V123E})

PCR-mediated overlap extension method was performed according to the previously published protocol (Ho et al. 1989). The Gs 11 gene was amplified and mutated in three PCR steps using four designed primers. Two segments of the target gene ((intermediate PCR products #1, #2) were produced from the template DNA by pairing of one flanking primer (a, d) and one mutagenic primer (used mutagenic primers are completely overlapping (b, c)). A third PCR, which amplified two fragments of PCR 1 and PCR 2 with the same both flanking primers (that mark the 5`and 3'end) was performed to generate the full mutated gene. The digestion of the final fragment with the appropriate restriction enzymes (*Hind*III, *Xho*I) and purification from the agarose gel allowed the ligation with the digested empty pcDNA3.1 vector. Finally, after transformation and plasmid preparation, the presence of the insert was checked by a control digest and nucleotide correctness had been proven by sequencing. Afterwards, the obtained DNA was either stored at -20°C or amplified by a transformation. All information provided by Dr. Nicole Merten

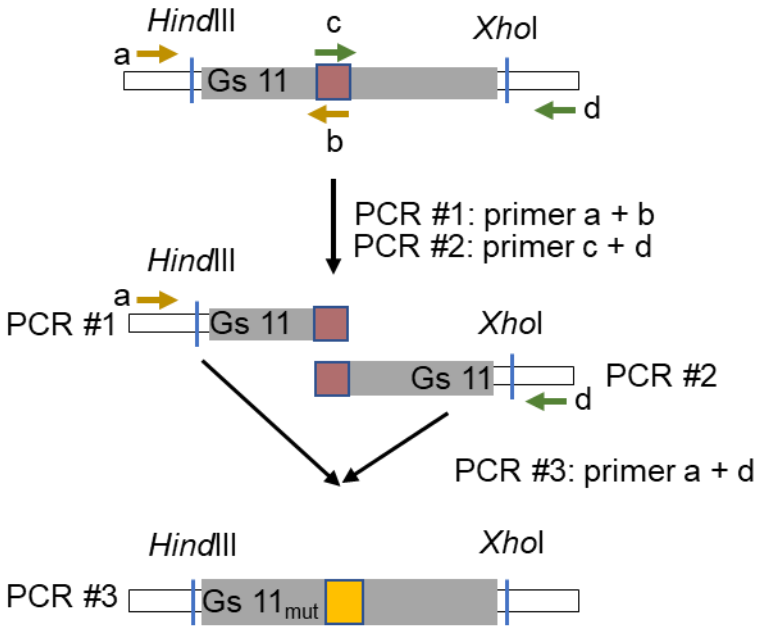

Figure 4: Graphical illustration of site directed mutagenesis by overlap extension adapted by Heckmann et al., 2007

Transformation of chemically competent bacteria

Transformation describes the inclusion of exogenous genetic material through the membrane of a host organism, in this case DH-5α.

Competent bacteria were thawn on ice for 5-10 min. Approximately 50 ng of DNA were added to the cells, mixed, and left to incubate on ice. After 30 minutes, cells were heat shocked for 60 seconds at 42°C and immediately put on ice for another 120 seconds. 500 µl of Luria broth medium (LB) (w/o antibiotic) was added to each tube and left to incubate at 37°C for 1 hour. 100 µl were then plated onto LB plates containing ampicillin for selection. Plates were incubated for 16-18 hours at 37 °C. The following day, a single colony was picked and added to an Erlenmeyer flask, containing 150 ml LB medium and 150 µl Ampicillin to be grown as a LB culture overnight at 37 °C and vigorous shaking 200 rpm.

Isolation of plasmid DNA

To achieve large amounts of pure and concentrated DNA, such as needed for transfection experiments, the NucleoBond® Xtra Midi kit was used. As described earlier, bacterial cultures were grown in 150 ml LB medium containing the selective antibiotic ampicillin for 16- 18 h at 37°C under thorough shaking (220 rpm). The entire 150 ml were harvested according to the manufacturer´s instructions.

Cell culture

Culture conditions

All cell lines were cultivated at 37°C in a 5% CO2 humidified atmosphere, either in standard sterile 75 cm^2 or 150 cm^2 cell culture flaks. Cells were passaged according to their grow rate, about 2-3 times per week to keep confluency below 80 % and replace the culturing media. Thus, under laminar air flow conditions, medium was removed, cells were washed with 3-5 ml PBS, and 1-2 ml trypsin was added to cover the cell surface in a thin layer. After cells were fully detached, the trypsination was stopped by addition of medium up to 10 ml total volume.

Cell culture media

Each cell line was cultured in a HEK standard medium containing the following mixture:

Constituent	Volume (ml)	Final concentration
Dulbecco's Modified Eagle Medium (DMEM)	500	
FCS	50	10%
Penicillin-Streptomycin mixture	5	100 U/ml penicillin, 0.1 mg/ml streptomycin

Transient Transfection of HEK 293 cells via Polyethlenimin

HEK cells were transiently transfected in suspension 48 h before experiments using Polyethlenimine (PEI, 1 mg/ml), a stable cationic polymer, which allows the entry of DNA into the cytoplasm by condensation of DNA into positively charged particles that bind to anionic cell surfaces. Consequently, the PEI:DNA complex is endocytosed by the cells (Longo et al. 2013). Transfection was performed by using 6 µg plasmid DNA in a final volume of 300 µl Opti-MEM. 18 µl PEI (DNA:PEI ratio 1:3) in a final volume of 300 µl Opti-MEM were added to the DNA mixture and incubated for 15 minutes before adding it to 10 cm dishes containing 3 mio cells diluted in 9 ml HEK medium.

If less or more cells were needed for an experiment, the cell number, amount of plasmid, media volume, and amount of transfection reagent were modified to sustain the constant ratio for transfections with higher or lower cell numbers.

Cell based methods

Western Blot

Lysates were collected from transfected cells, used either for cAMP or DMR measurements. 48 h after transient transfection cells were lysed on the day of the cAMP or DMR measurements. After running and blotting the gels onto nitrocellulose membranes, protein expression was detected as follows: to detect Gs expression, the membranes were incubated in N-Terminal anti-Gs mouse monoclonal antibodies diluted in Roti Block (1:1000) at 4°C overnight. Anti-mouse antibody diluted in Roti Block (1:20.000) was used as the second antibody and incubated for 1 h at room temperature on a slightly swiveling shaker before detection. After Gs detection using ECL detection reagent, the membranes were washed with PBS buffer once for 15 minutes at room temperature. Afterwards, to detect α-tubulin, anti-α-tubulin antibody was diluted in Roti Block (1:2500) to treat membranes overnight at 4 °C. Anti-rabbit antibody diluted in Roti Block (1:20.000) was used as the second antibody and incubated for 1 h at room temperature on a slightly swiveling shaker before detection.

cAMP accumulation

For cAMP assays, the Cisbio HTRF kit (Cisbio Codolet, France) was used according to manufacturer's instructions, with following modifications: 6 µg total cDNA amounts were used composed of 2 µg G protein with either 4 µg pcDNA or 2 µg β2AR + 2 µg pcDNA. Vector control was composed of either 6 µg pcDNA or 4 µg pcDNA + 2 µg β2AR unless otherwise marked in the figure. 2500 cells/well were preincubated with the indicated concentrations of FR or YM for 1 hour at 37 °C and stimulated afterwards with or without (buffer) varying concentrations of receptor agonist Isoprenaline for 30 min at 37°C. Then, lysis buffer and HTRF components were added and incubated at room temperature for 1 hour. The Mithras LB 940 multimode plate reader (Berthold Technologies, Bad Wildbad, Germany) was used to record HTRF values. Standard curve generated from the cAMP standard solutions provided by the manufacturer were used and all HTRF ratios were converted to nM cAMP concentrations.

Dynamic Mass Redistribution (DMR)

Dynamic mass redistribution assays (DMR) were performed using the corning Epic biosensor (Corning, NY, USA) according to a previously published protocol (Schröder et al. 2011). Briefly, unless otherwise marked in the figure total cDNA amounts were 6 µg, which were composed of 2 µg G protein encoding plasmid with either 4 µg pcDNA or 4 µg β2AR or 0.6 µg M3 + 3.4 µg pcDNA to equalize the total DNA amount. 24 hours post transfection 18. 000 cells/well were transferred and cultured in 384 well plates on top of an optical biosensor overnight. On the following day, cells were washed twice with Hank's Balanced Salt Solution (HBSS) (Life Technologies) containing 20 mM HEPES (Life Technologies) and plate was placed into the Epic DMR reader allowed to equilibrate for 1 hour until measurements stabilized. Afterwards, a new measurement was started to record 5 minutes of baseline read followed by the addition of compounds diluted in washing buffer using the Cybi-SELMA semi-automated electronic pipetting system (Analytik Jena AG, Jena, Germany). Each compound- provoked DMR alterations by ligand addition was recorded for 3600 seconds at 37 °C. Raw data were processed and evaluated with the GraphPad Prism software (GraphPad Inc.) and all optical DMR recordings were buffer corrected.

Membrane preparations

Competition binding and dissociation experiments: Membrane preparations obtained from (i) Gq/11 ko cells recombinantly co-expressing Gq proteins along with the muscarinic M3 receptor, and (ii) Gs/o ko cells co-expressing either Gs 11, or Gs 10, respectively together with the β2AR. 8.3 mio cells diluted in 19 ml HEK standard medium were transiently transfected with 5.5 µg of G protein DNA and 11 µg of receptor DNA (11 µg β2AR DNA, 1.66 µg M3 receptor DNA + 9.34 µg pcDNA) in a 150 mm dish using 49.5 µl PEI as transfection reagent.

[^{35}S]GTPγS binding experiments: Membrane preparations obtained from (i) Gq/11 ko cells recombinantly co-expressing Gq proteins along with the muscarinic M3 receptor and PTX-S1, and (ii) Gs/o ko cells co-expressing Gs 11 together with PTX-S1 and the β2AR. 8.3 mio cells diluted in 19 ml HEK standard medium were transiently transfected with 5.5 µg of G protein DNA together with 1.1 µg PTX-S1 and 11 µg of receptor DNA (11 µg β2AR DNA, 1.66 µg M3 receptor DNA + 9.34 µg pcDNA) in a 150 mm dish using 53 µl PEI as transfection reagent.

In each case 48 hours after transfection, the medium was discarded, and cells were frozen overnight at -20° C. After defrosting, the cells were harvested with a cell scraper while adding 5 mM Tris-HCl buffer containing 2 mM Na-EDTA, pH 7.4. The suspension was homogenized with an UltraTurrax® (IKA Labortechnik, Staufen, Germany) for 1 minute at level 4 and subsequently centrifuged at 1.000 g for 10 minutes. The pellet was discarded, and the supernatant was centrifuged for 1 hour at 48.400 g. The pellet was resuspended in 5 mM Tris-HCl buffer containing 2 mM Na-EDTA, pH 7.4. Protein concentration was determined with the Lowry method, and aliquots were frozen at -80°C until use.

Competition binding experiments.

Radioligand binding assays were performed essentially as previously described (Kuschak et al. 2019) in Tris-HCl buffer, pH 7.4, supplemented with 1 mM $MgCl_2$. The assay volume was 200 µl containing 2.5% DMSO. The experiments were performed at 37 °C, using 15 µg of protein (membrane preparation). For competition binding experiments, radioligand and several concentrations of FR were mixed. A 90-minute incubation was started by addition of membrane preparation. The incubation was terminated by rapid vacuum filtration through GF/C glass fiber filters using a Brandel-48 harvester. Filters were washed three times with 3 ml of ice-cold Tris-HCl buffer pH 7.4 containing 0.1% BSA and 0.1% Tween20. Subsequently, filters were transferred to scintillation vials and incubated with LumaSafe® scintillation cocktail for at least 6 hours prior to measurement in a liquid scintillation counter (PerkinElmer TriCarb 2810 TR, 53% counting efficiency).

Dissociation experiments.

Membrane preparation (15 µg of protein) and radioligand solution (5 nM final concentration in the assay) were mixed in a total volume of 195 µl Tris-HCl buffer pH 7.4 containing 1 mM $MgCl_2$. The mixture was preincubated for 90 minutes to reach the equilibrium. Dissociation was induced by the time-displaced addition of FR (final concentration: 5 µM) or a GPCR agonist, dissolved in 5 µl DMSO. Samples were harvested and treated as described above. Data were normalized to total binding (binding in the presence of DMSO) = 100% and non-specific binding (addition of 5 µM FR before addition of radioligand) = 0%. Non-specific binding amounted in all cases to less than 10 % of total binding.

[^{35}S]GTPγS Binding Assays

Gq and Gs 11 protein membrane preparations (1 µg and 3 µg of protein, respectively) were preincubated with FR (5 µM) for 30 minutes at room temperature. Afterwards, FR pretreated Gq membranes were incubated with CCh (30 µM) and 0.3 nM [^{35}S]GTPγS in Tris-HCl buffer pH 7.4 without NaCl addition for 60 minutes at room temperature, whereas Gs 11 membranes preparations were incubated with Iso (10 µM) and 0.3 nM [^{35}S]GTPγS in HEPES buffer pH 8 for 10 minutes at 30°C. 10 µM GDP was added to decrease the basal turnover rate of Gs 11.

Experiments were terminated by rapid vacuum filtration through GF/C glass fiber filters using a Brandel-24 harvester. Subsequently, filters were transferred to scintillation vials and incubated with LumaSafe® scintillation cocktail for at least 6 hours prior to measurement in a liquid scintillation counter (PerkinElmer TriCarb 2810 TR, 53% counting efficiency).

Real-time BRET-based G protein activation

BRET measurements were performed comparably to the published protocol (Masuho et al. 2015). Briefly, HEK293 $G\alpha_{\Delta 7}$ cells were transfected with 800 ng $G\alpha$, 400 ng Venus (156-239)-$G\beta_1$, 400 ng Venus (1-155)-$G\gamma$, 400 ng masGRK3ct-Nluc and 400 ng PTX-S1. Empty pcDNA3.1 vector was used to equalize the total amount of DNA to 5000 ng per transfection of 3 mio cells in a 10 cm dish. 24 hour post transfection, cells were harvested and resuspended in Hank`s Balanced Salt Solution (HBSS) supplemented with 20 mM HEPES. For agonist dose response curves, cells were transferred to a white 96-well plate with 80.000 cells per well. Nano-Glo nanoluciferase substrate (Promega) was added just before the recording of the baseline BRET. Then, maximum activating concentrations of CCh and Iso were added, and BRET signals were measured.

Data processing

All data were processed using Microsoft Exel and analyzed using GraphPad Prism 8 or 9. Representative traces were demonstrated as mean values + SEM, while quantified results are shown either as mean values + SEM or ± SEM. All kinetic data were baseline-corrected to a buffer control by subtracting the value of the buffer-stimulated curve from the respective ligand-stimulated curve for every timepoint. Data were analyzed as depicted in the respective y-axis title of each panel. Statistical analyzes were performed using the one-way ANOVA with Dunett´s or Turkey´s correction method. P values were determined and $P<0.05$ was considered significant (*) if, $P<0.01$ very significant (**), and $P<0.001$ extremely significant (***).

Results

Chapter 1: Evaluation of $G\alpha_{s11}$ and $G\alpha_{s10}$ - how do the mutations influence the $G\alpha_s$ protein?

Gs 11 shows elevated basal signaling in contrast to Gs WT.

The first goal of this work was to investigate whether $G\alpha_{s11}$ (Gs11), the artificially generated FR-sensitive Gs protein, might be suitable to serve as a chemogenetic tool since it has been reported that Gs 11 has a high basal activity (Boesgaard et al. 2020), which could affect its performance as a chemogenetic tool. Therefore, to evaluate the capability of Gs 11 to increase the intracellular basal levels of cAMP, we compared $G\alpha_s$ (Gs WT) and Gs 11 after transient transfection in CRISPR/Cas9 genome-edited HEK293 cells deficient in Gs (hereafter referred to as Gs ko´s or Gs ko cells). This cellular background allows analysis of Gs proteins without the confounding variable of endogenously expressed Gs. For a more informative comparison, we also analyzed in addition the most frequent cancer-causing mutation in Gs, R201C (hereafter “Gs RC”), which leads to constitutive activation by inhibiting ~30 fold the GTPase activity (Landis et al. 1989) and results in elevated intracellular cAMP levels (O'Hayre et al. 2013 Jun). Western blot analysis confirmed proper expression of the three Gs proteins (Fig. 5A), albeit Gs 11 was detected in lower abundance as compared to Gs WT and Gs RC (Fig. 5A$_i$). Expression of the three Gs proteins increased intracellular basal levels of cAMP as compared with those cells transfected with vector, pcDNA3.1 (Fig. 5B). However, both Gs 11 and Gs RC showed a higher increased intrinsic activity compared with that of Gs WT (Fig. 5B) since their intracellular basal cAMP levels were about 21 nM and 52 nM, respectively. Notably, normalization of cAMP levels with protein abundance displayed comparable basal activity of Gs 11 and Gs RC (Fig. 5C). Therefore, our results led us to conclude that basal signaling of Gs 11 is as high as that of the oncogene Gs RC.

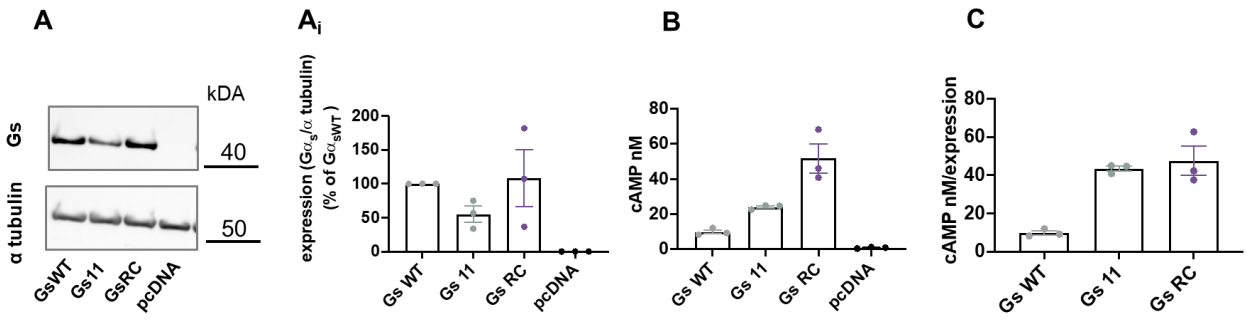

Figure 5: Gs 11 triggers elevated basal signaling.
(A) Representative western blot showing expression levels of Gs WT, Gs 11 and Gs RC detected in cellular lysates obtained from CRISPR-Cas9 $G\alpha_s$-null cells transiently expressing the indicated constructs. α- tubulin was used as loading control. (A_i) Western blot quantification from three independent experiments. (B) cAMP measurement (1000 cells/well) of HEK293 Gs ko cells expressing transiently Gs WT, Gs 11 or Gs RC displayed elevated basal activity for Gs 11 and Gs RC compared to Gs WT. (C) cAMP measurement shown in (B) was related to the respective expression level in (A_i), displaying comparable basal activity between Gs 11 and Gs RC. Error bars represent mean ± SEM from three biologically independent experiments.

Gs 11 significantly increases cAMP production upon GPCR activation.

Chemogenetic G proteins should behave as wildtype G proteins to preserve the cellular environment and signaling events that are intended to study. Based on the high magnitude of the basal activity (Fig. 5), we wondered whether Gs 11, which seems to prefer the active state, could lead to stronger cellular responses compared to those of Gs WT upon receptor activation.

With this in mind, we firstly used a classical readout for the canonical Gs signaling pathway and analyzed the production of the second messenger cAMP, which is generated from ATP by the action of several adenylyl cyclase (AC) isoforms (Patt et al. 2021), upon activation of the endogenously expressed β2 adrenergic receptor (β2AR) (Fig. 6A). We observed that in Gs ko cells transiently expressing either Gs 11 or Gs WT, the β2AR agonist Isoprenaline (Iso) led to a concentration-dependent increase of cAMP. Notably, in addition to its strong basal activity, Gs 11 stood out with a significantly higher maximum response (449 nM cAMP) as compared to Gs WT (Fig. 6B). Only by zooming in the y-axis of the figure, the cell

response of Gs WT became apparent (33 nM cAMP; Fig 6B$_i$), which was far below that of Gs 11.

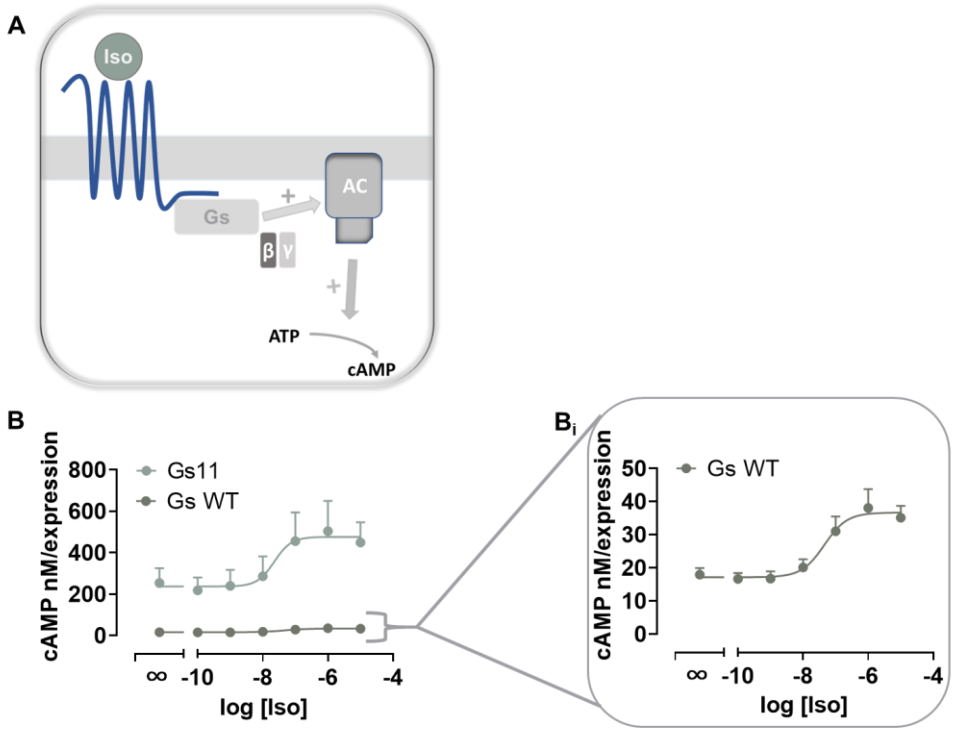

Figure 6: Gs 11 shows elevated GPCR-induced cAMP production.
(A) Graphical illustration of cAMP production upon GPCR activation by Isoprenaline and adenylyl cyclase conversion of ATP to cAMP. (B) cAMP measurement (2500 cells/well) in HEK293 Gs ko cells expressing transiently Gs WT or Gs 11, shown as mean + SEM of four biologically independent experiments, display distinct concentration-dependent isoprenaline-induced cAMP production of Gs 11 compared to Gs WT. (B$_i$) Zoom in of the dose response curve for Gs WT.

Gs 11 provokes GPCR-induced cell dynamic mass redistribution.

Secondly, we used a live-cell assay based on the dynamic mass redistribution (DMR) that occurs in the cell upon receptor activation (Fig. 7A). This assay detects in real-time changes in the mass of cells caused in response to a ligand which is measured as wavelength shifts (Δ λ) relative to the baseline at outset (Schröder et al. 2010; Schröder et al. 2011). Changes

in increase of the optical density associated with the accumulation on the biosensor results in a positive wavelength shift.

Stimulation with increasing Iso concentrations of endogenously expressed β2AR in Gs ko's expressing Gs WT or Gs 11 resulted in different degrees of mass accumulation at the biosensor, leading to different wavelength shifts between Gs WT and Gs 11 (Fig. 7B). Concentration-effect curves of the recorded traces represented as area under the curve between the time periods 500-2500 seconds showed higher mass redistribution values for Gs 11 compared to Gs WT (Fig. 7B_i).

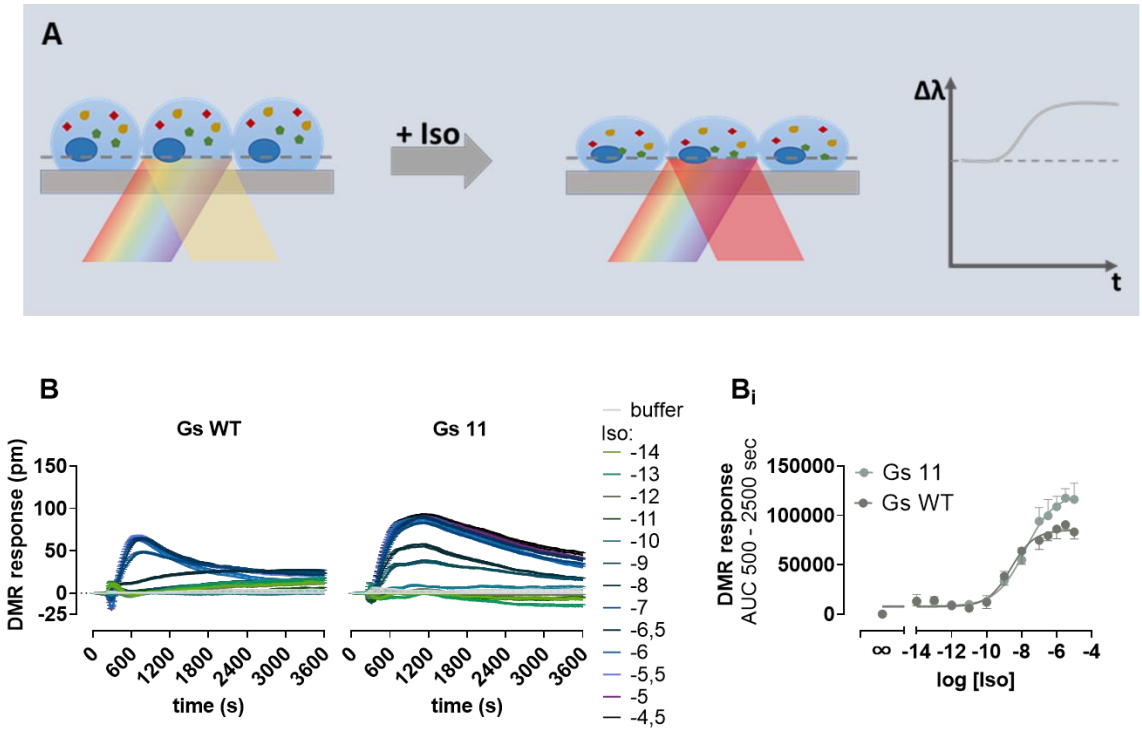

Figure 7: Gs 11 shows elevated GPCR induced dynamic mass redistribution. (A) Graphical illustration of DMR technology: Isoprenaline induces cellular cytoskeletal changes that are captured by the optical biosensor as a change in the reflected wavelength. Mass redistribution and, consequently, accumulation on the biosensor results in a positive wavelength shift. (B) Representative DMR kinetics obtained in Gs ko´s expressing Gs WT or Gs 11, shown as mean + SEM. (B_i) Summarized area under the curve (AUC) quantification as mean + SEM of four independent experiments.

In summary, our data demonstrated (Fig.5-7) that the 11 mutations within the Gs protein caused tremendous changes in its function compared to Gs WT. Therefore, the increased basal activity, equivalent to that of the Gs RC oncogene (Fig.5), and the enhanced GPCR-induced signaling (Fig. 6,7) displayed by the mutated Gs suggested that Gs 11 might not be an ideal designed chemogenetic tool.

Gs 10 shows comparable basal signaling as compared to Gs WT.

Hans Bräuner-Osborne´s group (Boesgaard et al. 2020) has reported the generation of another FR-sensitive Gs protein, $G\alpha_{s10}$ (Gs 10), that would display WT-like basal activity. Gs 10 is similar to Gs 11 with the difference that the amino acid proline at position 189, present in Gs 11, was mutated back to leucine, which occurs naturally in Gs WT (Fig. 8).

Figure 8: Amino acid sequence alignment of Gs WT, Gs 11 and Gs 10. Mutated amino acids in Gs 11 and Gs 10 are highlighted in blue. Box around position 189 shows reverse mutation of proline to the Gs WT original amino acid leucine in Gs 10.

Therefore, we decided to evaluate whether Gs 10 could be a better candidate than Gs 11 as a chemogenetic G protein tool. We initially evaluated Gs 10 basal signaling by expressing it in Gs ko cells. Western blot analysis confirmed proper expression of Gs WT and Gs 10 after transfection, although Gs 10 was detected in lower abundance as compared to Gs WT (Fig. 9A, B). In contrast to our previous findings with Gs 11 (Fig. 6), transient expression of Gs 10 in Gs ko cells increased basal intracellular levels of cAMP to a more similar extent as Gs WT transfected cells (Fig. 9C). Normalized cAMP levels with protein abundance displayed basal cAMP concentrations in the magnitude of 17 nM and 58 nM for Gs WT and

Gs 10, respectively, compared to Gs 11 that had an intrinsic cAMP level of 236 nM under similar experimental conditions (Fig. 6B).

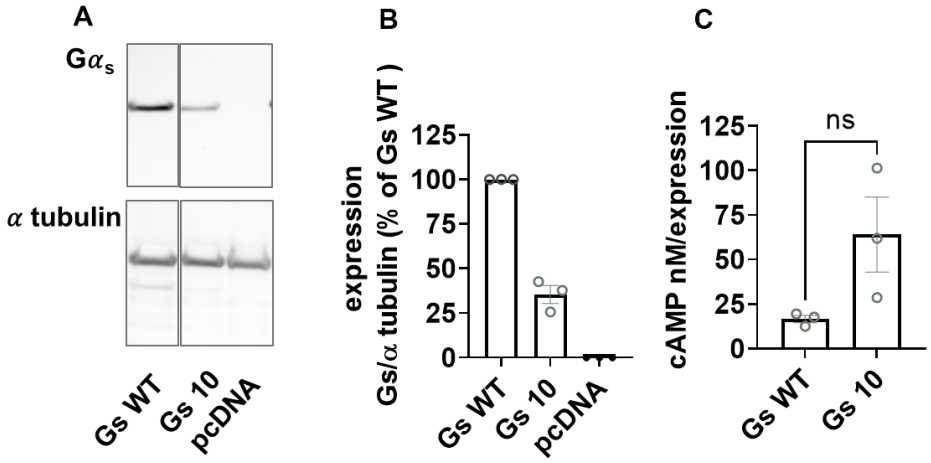

Figure 9: Gs 10 shows comparable basal signaling as compared to Gs WT.
(A) Representative western blot showing expression levels of Gs WT, Gs 10 and pcDNA detected in cellular lysates obtained from CRISPR-Cas9 $G\alpha_s$-null cells transiently expressing the indicated constructs. α- tubulin was used as loading control. (B) Western blot quantification from three independent experiments, shown as mean $\pm$ SEM. (C) Basal cAMP production, after normalization of cAMP levels with protein abundance, in HEK293 Gs ko cells (2500 cells/well) expressing transiently Gs WT or Gs 10, shown as mean ± SEM of three biologically independent experiments. Statistical analysis was performed with two-tailed unpaired t test, p value 0.0882, ns, not significant.

Chapter 2: Do artificially generated FR-sensitive Gs proteins display identical inhibition profiles as the natural FR- target Gq?

Basal activity of Gs 10 is entirely inhibited by FR with biphasic inhibition pattern.

Because Gs 10 behaved comparably to Gs WT, showing a similar increase in cAMP basal activity we were driven to test FR´s capability to inhibit Gs 10 under different conditions. Therefore, we decided to examine whether FR could inhibit the cAMP basal formation triggered by Gs 10. We transfected Gs ko´s with Gs WT, Gs 10, or vector (pcDNA3.1) and incubated them with increasing amounts of FR. In Gs 10 transfected cells, FR abolished the basal level of cAMP in a concentration-dependent manner at the level of vector (pcDNA3.1) transfected cells (Fig 10A). Interestingly, FR inhibition displayed a biphasic pattern, as shown by the inflection points pIC_{50} 7.0 and 5.7, respectively. As expected, Gs WT transfected cells did not show notable inhibition of basal signaling upon treatment with FR (Fig. 10B). Only, a minor decrease of the basal cAMP level could be also observed around the inflection point pIC_{50} 7.0. We wondered why the inhibition of basal cAMP levels i) follows a biphasic inhibition pattern and ii) why Gs WT and Gs 10 share their first inflection point around pIC_{50} 7.0.

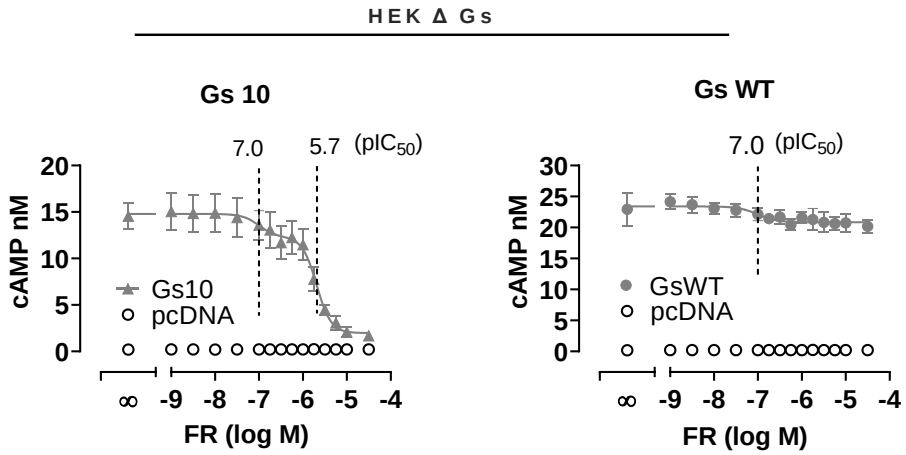

Figure 10: Basal activity of Gs 10 is entirely inhibited by FR with biphasic inhibition pattern.

cAMP measurements of HEK293 Gs ko cells expressing transiently Gs 10 or Gs WT, shown as mean ± SEM of three or four biologically independent experiments, displayed (A) complete inhibition of basal activity for Gs 10 with biphasic inhibition character and (B) incomplete inhibition of basal activity for Gs WT. Both Gs WT and Gs 10 show an inflection point at pIC_{50} 7.0 (constrained to 7). Additionally, Gs 10 shows a second inflection point at pIC_{50} 5.7.

FR inhibits Gs 11 triggered cAMP basal levels with a biphasic inhibition pattern.

Because we observed a biphasic FR inhibition pattern for Gs 10, we wondered whether this pattern was specific for Gs 10. Consequently, we questioned what FR inhibition pattern might follow for Gs 11. We expressed transiently Gs 11 in Gs ko´s and treated the cells with increasing amounts of FR. Similar to Gs 10, FR inhibition of basal cAMP levels induced by the expression of Gs 11 exhibited also a biphasic inhibition pattern, with identical inflection points (Fig. 11) as observed in Gs 10 expressing cells (Fig 10A). Therefore, biphasic inhibition by FR was not exclusive for Gs 10 since Gs 11 showed a similar pattern.

On a side note, the basal cAMP level was also almost completely reduced to the level of pcDNA in a concentration-dependent manner. One could speculate that the higher basal activity of Gs 11 indicates a tendency to retain the active conformation, and thus, a lower sensitivity to being inactivated by FR. However, Gs 11 could be transferred almost as equally effectively and potently from the ON state to the OFF state compared with Gs 10. Thus, we

concluded that the inhibition of basal activity is not less effective and potent the more the G protein prefers the active conformation.

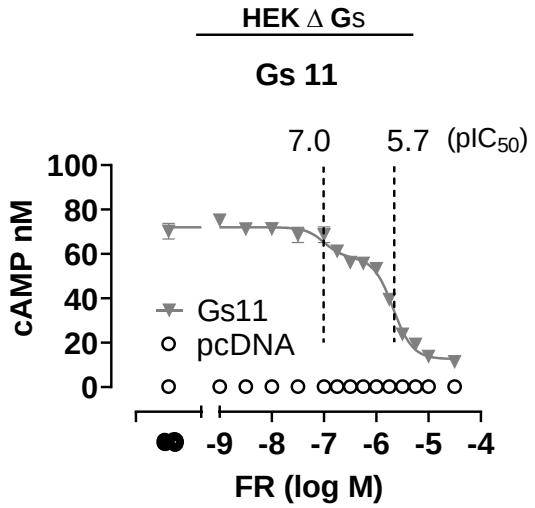

Figure 11: Gs 11 shows total basal inhibition with biphasic inhibition pattern.
cAMP measurement of HEK293 Gs ko cells expressing transiently Gs 11 shown as mean ± SEM of four biologically independent experiments, show complete inhibition of basal activity with biphasic inhibition character and pIC_{50} values around 7.0 (constrained to 7.0) and 5.7.

FR unmasks Gq contribution to Gs mediated cAMP production.

Why did FR inhibition of Gs 10 and Gs 11 basal cAMP levels follow a biphasic inhibition pattern? Considering that Gs WT, Gs 10 and Gs 11 have shared their first inflection point around pIC_{50} 7.0, we hypothesized that this inflection point might depend on the cellular background of Gs ko cells. Because Gs ko cells express endogenously $G\alpha_{q/11}$ (Gq), and all Gq dependent signals affect or enhance cAMP formation, we expected FR to unmask Gq components (Cooper et al. 1995; Wong et al. 2000; Mons et al. 1998; Tang und Gilman 1991; Steiner et al. 2006; Hurley 1999; Patt et al. 2021)
To test this assumption, we employed CRISPR/Cas9 genome-edited HEK293 cells deficient in Gs, Gq and G12/13, later referred to as ΔG_{seven}, which allow analysis of specific G proteins after transfection without the disturbing variable of endogenously expressed Gs and Gq. For

a better evaluation of our hypothesis, we decided to transiently transfect Gs 11 in ΔG_{seven} cells because of its higher cAMP -formation. After incubation with increasing amounts of FR, the basal level of cAMP was depleted in a concentration-dependent manner and to a similar level to that of ΔG_{seven} cells transfected with vector (pcDNA3.1; Fig. 12A). Notably, cAMP reduction displayed a monophasic inhibition pattern with a single inflection point around pIC_{50} 5.8, which is similar to the previously determined second inflection point of the biphasic FR-inhibition curves in Gs ko´s expressing Gs 11 (Fig. 11).

This result strongly indicated that endogenously expressed Gq was responsible for the observed first inflection point thus biphasic inhibition pattern. Congruently, reintroduction of Gq in ΔG_{seven} cells, by transiently expressing Gq WT together with Gs 11, resulted again in FR mediated biphasic inhibition curves (Fig. 12B). Moreover, both inflection points at pIC_{50} 7.0 and 5.7 respectively, are identical to those that were previously identified in the cellular background of Gs ko´s (Fig. 11).

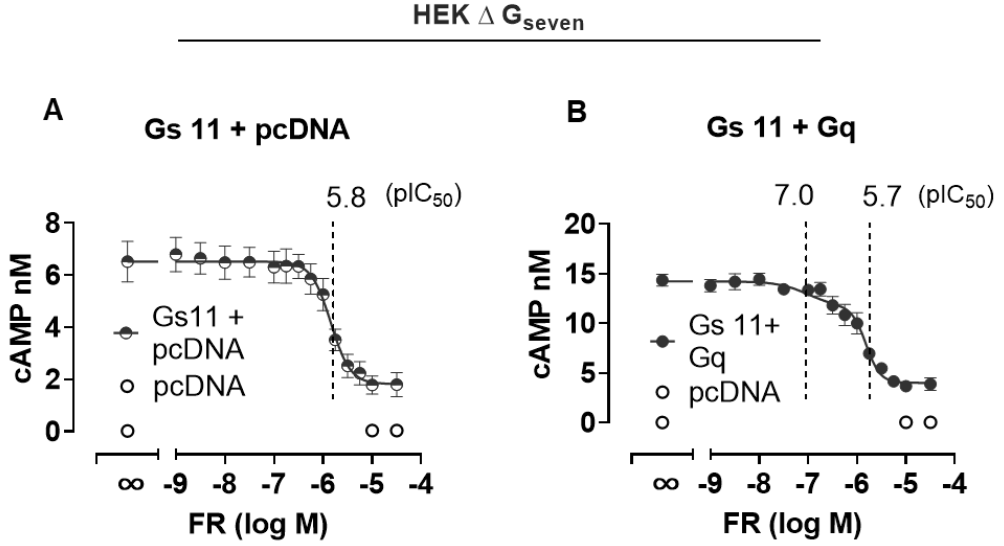

Figure 12: FR unmasks Gq contribution to Gs mediated cAMP production.
(A) cAMP measurement of HEK293 ΔG_{seven} cells expressing transiently Gs 11, shown as mean ± SEM of four biologically independent experiments, displayed monophasic inhibition of basal cAMP levels (B) cAMP measurement of HEK293 ΔG_{seven} cells expressing transiently Gs 11 + Gq WT, shown as mean ± SEM of four biologically independent experiments, displayed biphasic inhibition of basal cAMP levels with two inflection points, pIC_{50} 7.0 and 5.7, respectively.

Taking together, we concluded that the pIC_{50} value for Gs dependent cAMP inhibition is 5.7 - 5.8, whereas the pIC_{50} 7.0 belongs to the inhibition of Gq dependent cAMP formation that was unmasked by FR.

Isoprenaline (Iso) increases intracellular cAMP in Gs WT and Gs 10 transfected Gs ko cells with or without overexpressed β2AR.

Having decoded the FR-biphasic inhibition pattern of basal cAMP levels, we proceeded to investigate the suitability of Gs 10 to function as a chemogenetic tool. Inhibition of basal cAMP levels were fully under FR control; however, how does FR inhibit Gs-signaling after receptor activation? To this end, we decided to test the capacity of FR under conditions such as i) endogenously or overexpressed receptor with ii) maximal or 80% activating concentrations.

Initially we assessed whether β2AR overexpression might alter the expression of transiently transfected Gs WT and Gs 10 in Gs ko´s by Western blot analysis. These studies confirmed proper expression of both Gs proteins, regardless of the presence of endogenous or overexpressed β2AR (Fig. 13A). Even though we observed a trend of higher expression of Gs proteins in the presence of the overexpressed β2AR, no statistically significance was observed when comparing the expression of each G alpha subunit with endogenous vs. overexpressed receptor. (Fig. 13B). Therefore, we confirmed that overexpression of the β2AR had no significant influence on transfected Gs expression levels.

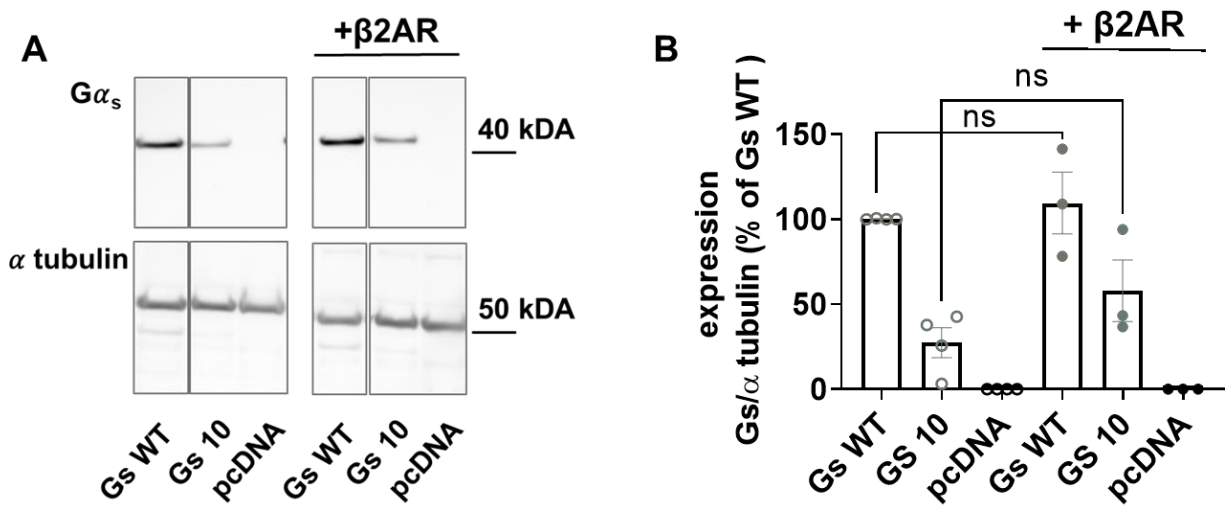

Figure 13: Expression of Gs proteins together with endogenous and overexpressed β2AR.

(A) Representative western blot showing expression levels of Gs WT, Gs 10 and pcDNA3.1 with or without overexpressed β2AR detected in cellular lysates obtained from CRISPR-Cas9 $G\alpha_s$-null cells transiently expressing the indicated constructs. α-tubulin was used as loading control. (B) Western blot quantification from three-four independent experiments showing expression of Gs proteins in the presence of endogenous or overexpressed β2AR, shown as mean ± SEM. trend Statistical analysis were performed with one-way ANOVA, followed by Dunnett´s test; ns, not significant

Next, in order to ascertain the precise agonist concentration for further investigations on receptor induced signaling inhibition by FR, Gs ko cells transiently expressing Gs WT, Gs 10 or vector (pcDNA3.1) along with or without overexpressed β2AR were incubated with increasing amounts of Iso up to a concentration of 10 µM. Both Gs WT and Gs 10 transfected cells increased intracellular cAMP amounts in a dose-dependent manner (Fig. 14A-D) compared to cells transfected with vector (pcDNA3.1) (Fig. 14E, F). Notably, cells overexpressing the β2AR (Fig. 14B, D) showed a more potent increase of the cAMP level upon Iso stimulation for both Gs proteins as compared to cells expressing the endogenous receptor (Fig. 14A, C). Determination of pEC_{80} and maximum activating values in all analyzed conditions for further investigations displayed that Gs WT and Gs 10 transfected cells expressing either the endogenous or overexpressed β2AR had comparable (Fig. 14A, C) or identical (Fig. 14B, D) activation values by Iso, respectively.

Overall, our data showed that Gs 10 functions similarly to Gs WT, again suggesting that Gs 10 could in principle be used as a chemogenetic tool.

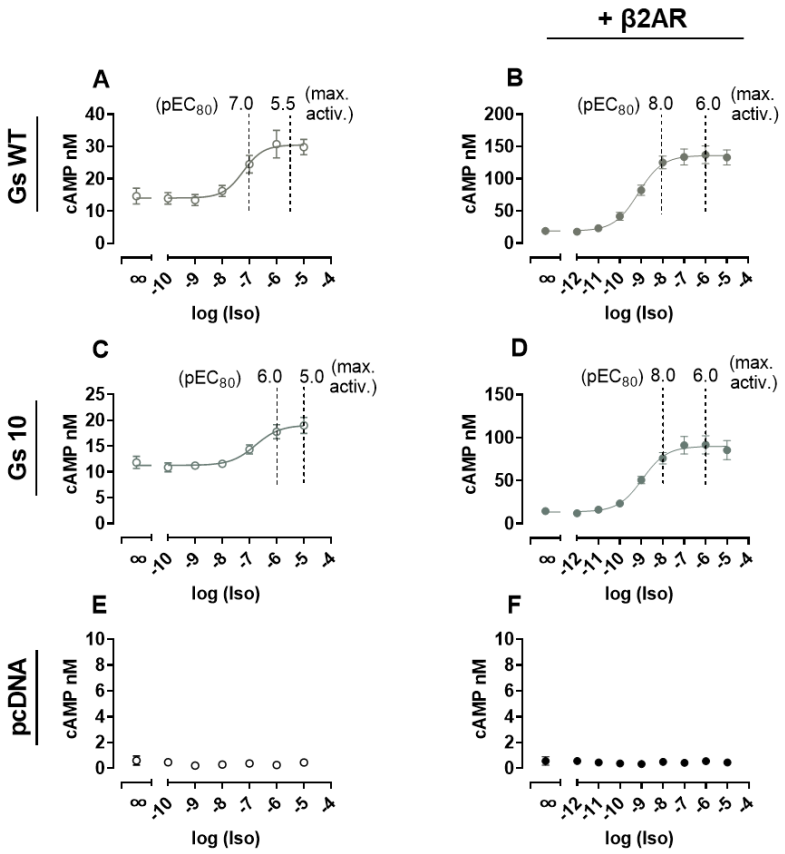

Figure 14: Isoprenaline (Iso)- induces increase in intracellular cAMP of GS WT and Gs 10 with or without overexpressed β2AR. cAMP measurement of HEK293 Gs ko cells expressing transiently Gs WT (A, B), Gs 10 (C, D) or pcDNA3.1 (E, F), shown as mean ± SEM of four-five biologically independent experiments, displayed Iso concentration-dependent increase of cAMP levels. (A, C, E) Dose-response curves in the presence of endogenously expressed β2AR. (B, D, F) Dose-response curves in the presence of overexpressed β2AR.

Maximum activation of overexpressed β2AR undermines FR´s inhibitory power on Gs 10.

After we determined the Iso concentrations to be used in our cAMP assays, we next analyzed whether FR was capable to abolish ligand-mediated cAMP accumulation in Gs ko cells expressing Gs 10, both in the presence of endogenous or overexpressed β2ARs. Therefore, we transfected Gs ko cells with vector (pcDNA3.1), Gs WT or Gs 10, preincubated them with increasing concentrations of FR and stimulated them either with an 80 % (≙ pEC_{80}) or a maximum activating concentration of Iso. Vector transfected Gs ko cells, lacking functional Gs proteins, were completely inactive upon stimulation of endogenous (Fig. 15A) or overexpressed β2AR (Fig. 15B). Non-FR sensitive Gs WT showed an increase of cAMP accumulation upon Iso stimulation that was not abolished by FR (Fig. 15C-D). Only a minor decrease of cAMP production was observed which was probably due to endogenously expressed Gq in Gs ko cells such as investigated in Fig.12.
In cells expressing Gs 10, activation of the endogenous β2AR with either maximum (10 µM Iso) or 80 % (1 µM Iso) activating concentrations led to a ligand-mediated cAMP production that was completely suppressed by FR in a concentration-dependent manner, starting at 1.8 µM ("total inhib.") for both agonist conditions (Fig. 15E). Surprisingly, the overexpressed and maximally activated β2AR undermined the ability of FR to completely diminish cAMP production (Fig. 15F). Thus, the maximum activating concentration (1 µM Iso) still triggered cAMP production in cells preincubated with even the highest FR concentration (30 µM), resulting in 33% residual activity. In contrast, cAMP accumulation induced by a lower Iso concentration, corresponding to the pEC_{80} value, was completely inhibited at the highest FR concentration.

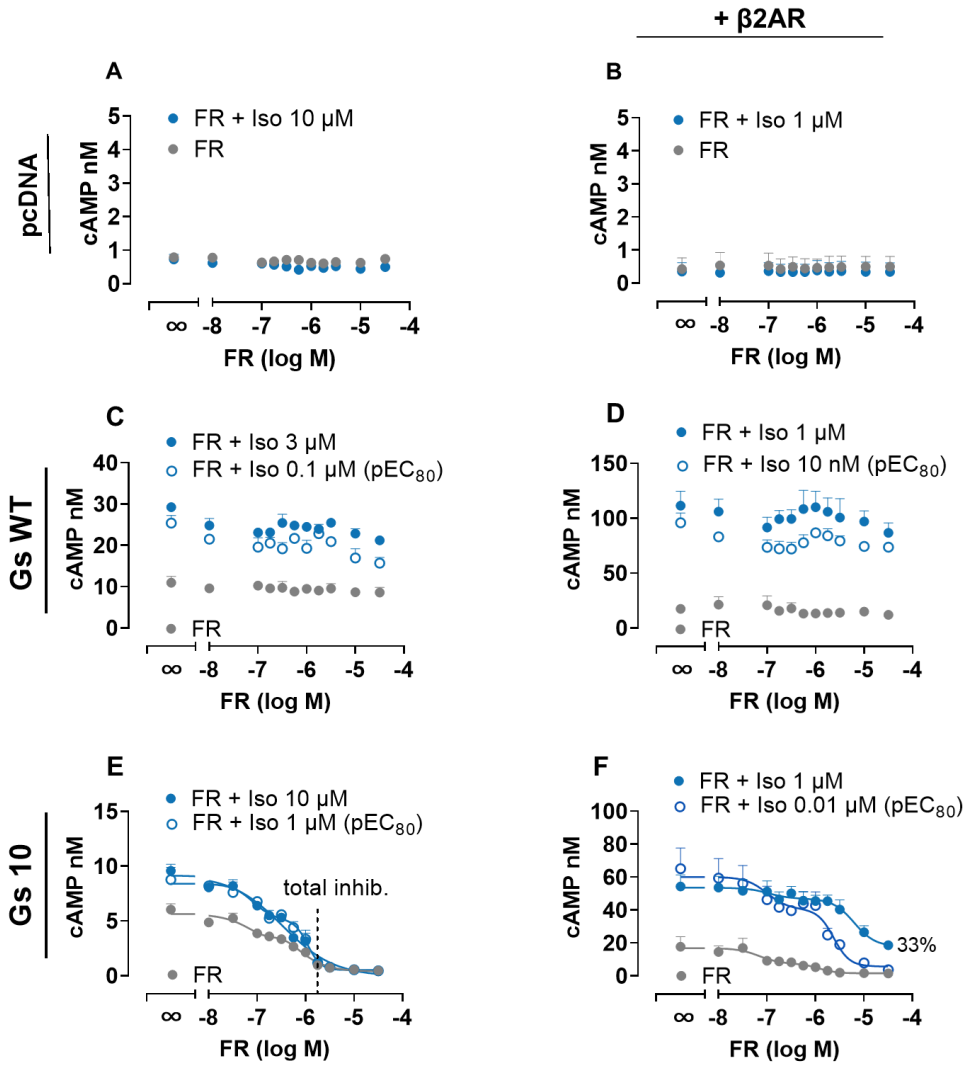

Figure 15: Maximum activation of overexpressed β2AR undermines FR´s inhibitory power on Gs 10. cAMP measurement in HEK293 Gs ko cells expressing transiently Gs WT, Gs 10, or pcDNA with endogenous or overexpressed β2AR, shown as mean + SEM of three biologically independent experiments, displayed total or partial inhibition of receptor induced signaling by FR. (A, B) Cells expressing vector pcDNA 3.1 displayed no response upon agonist stimulation. (C, D) Cells expressing Gs WT along with endogenous (C) or overexpressed (D) β2AR showed no decrease of Gs-dependent cAMP accumulation by FR. (E, F) Effect of FR on cells expressing Gs 10. Stimulation of endogenous β2AR (E) increased cAMP production that was completely inhibited in a concentration-dependent manner by FR. Stimulation of overexpressed β2AR (F) with 80 % activating concentration (0.01 µM Iso) of β2AR was completely inhibited at the highest FR concentration, whereas maximum activation (1 µM Iso) causes a partial inhibition by FR.

Overexpressing and maximum activation of the β2AR leads to partial inhibition of cAMP production by FR in cells expressing Gs 11.

Surprised by our previous result, since we were expecting a total inhibition by FR in Gs 10 expressing cells, we hypothesized that the presence of leucine instead of proline at position 189 in Gs 10 might be responsible for the inefficient inhibition by FR. Possibly, proline at this position plays a key role for FR´s efficient inhibitory power in Gq WT. To investigate our hypothesis, we decided to test FR´s capability to inhibit ligand-induced cAMP accumulation of endogenous or overexpressed β2AR in cells expressing Gs 11. To this end, we first determined the exact Iso concentrations, i.e., the maximum and 80% activating concentrations for our further investigations on receptor induced signaling inhibition by FR (Fig. 16). Based on the resulting dose response curves upon stimulation of endogenous (Fig. 16A) and overexpressed β2AR (Fig. 16B) with increasing amounts of Iso, pEC_{80} and maximum activating values were determined. Similar to our previous observations in cells expressing Gs 10 (Fig. 14), overexpression of the β2AR in cells expressing Gs 11 showed a more potent increase of the cAMP level upon Iso stimulation as compared to Gs 11 cells expressing the endogenous receptor (Fig. 16).

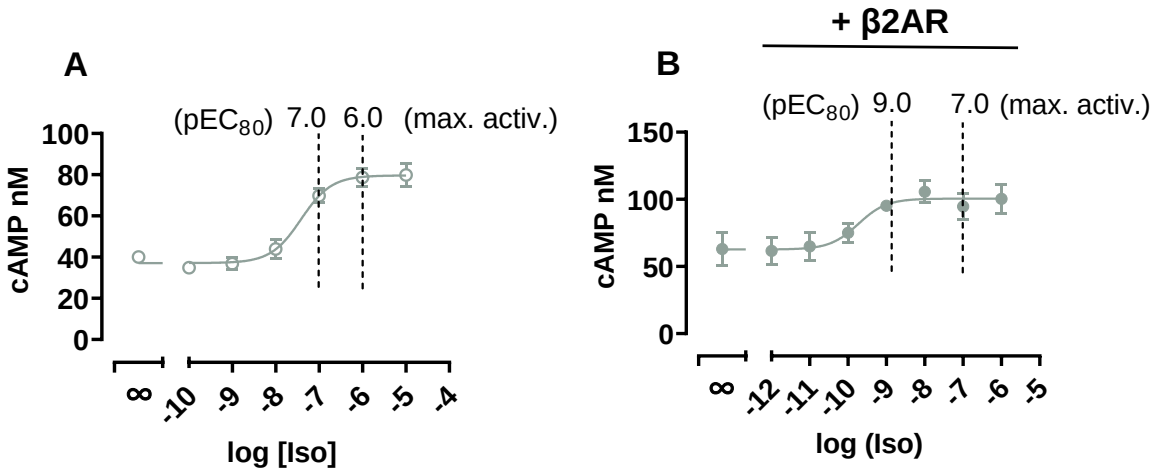

Figure 16: Iso-induced increase of intracellular cAMP in cells expressing GS 11 with endogenous or overexpressed β2AR. cAMP measurement of HEK293 Gs ko cells expressing transiently Gs 11 with endogenous (A) or overexpressed (B) β2AR, shown as mean ± SEM of four-five biologically independent experiments, displayed Iso concentration-dependent increase of cAMP levels.

Next, we analyzed whether FR was able to abolish ligand-mediated cAMP accumulation in cells expressing Gs 11. Consistent with the complete inhibition of ligand-induced signaling in cells expressing Gs 10 with the endogenous β2AR (Fig. 15E), cAMP accumulation triggered by Iso in cells expressing Gs 11 with endogenous β2AR was also completely inhibited by FR (Fig. 17A). Both maximum (1 µM Iso) and 80 % (0.1 µM Iso) activating concentrations were suppressed by FR in a concentration-dependent manner, showing complete inhibition at 3 µM ("total inhib"; Fig. 17A). Notable, the complete inhibition by FR of ligand-induced cAMP accumulation in cells expressing Gs 11 was minimally less potent (3 µM FR) than in cells expressing Gs 10 (1.8 µM FR), possibly due to Gs 11´s higher intrinsic activity in contrast to Gs 10.

Surprisingly, and akin to our observations in cells expressing Gs 10 with the overexpressed β2AR, the overexpressed and maximally activated β2AR also undermined FR´s ability to blunt cAMP production in cells expressing Gs 11 (Fig. 17B). Thus, whereas FR inhibited cAMP production when stimulated with 80% activating agonist concentration (1 nM Iso), the maximum activating concentration (0.1 µM Iso) resulted in activation of Gs 11 that remained about 38 % at the highest FR concentration (Fig. 17B). Differences related to the remaining activity between Gs 10 and Gs 11 could be again dependent on the altered basal activity

Altogether, we concluded that the partial inhibition by FR of cAMP levels in Gs 10 expressing cells upon maximum activation of the overexpressed β2AR was not due to the lack of proline at position 189 since Gs 11, containing proline, showed a comparable inhibitory behavior with FR.

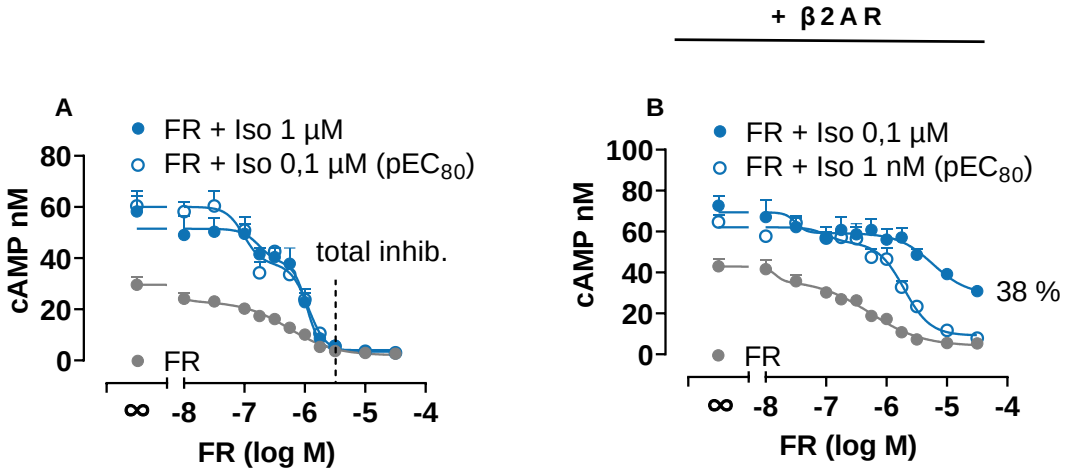

Figure 17: Maximum activation of overexpressed β2AR still triggers cAMP production in the presence of FR in cells expressing Gs 11. cAMP measurements of HEK293 Gs ko cells with endogenous (A) or overexpressed (B) β2AR and expressing transiently Gs 11, shown as mean + SEM of three biologically independent experiments. Stimulation of endogenous β2AR (A) increased cAMP production that was completely inhibited in a concentration-dependent manner by FR. Stimulation of overexpressed β2AR (B) with 80 % activating concentration (1 nM Iso) of β2AR was completely inhibited at the highest FR concentration, whereas maximum activation (0.1 µM Iso) causes partial inhibition by FR.

FR superior to YM by inhibiting Gs 10 and Gs 11 mediated increase of intracellular cAMP accumulation.

Previous findings of our group revealed biologically different activities of FR and YM despite a close structural similarity. Because FR inhibition was superior to YM (Malfacini et al. 2019) we wondered how YM performs its inhibitory power on cells expressing Gs 10 and Gs 11 and speculated that FR is also superior to YM in the case of Gs 10 and Gs 11 inhibition, respectively. Therefore, we assessed FR´s and YM`s capability to blunt ligand-mediated cAMP accumulation in Gs ko cells transiently expressing Gs 10 (Fig. 18A) and Gs 11 (Fig. 18B) in the presence of overexpressed and maximally activated β2AR. In line with earlier findings, increasing concentrations of FR and YM displayed distinct inhibition profiles in both Gs 10 and Gs 11 expressing cells (Fig. 18), with FR being superior to YM in reducing ligand-induced cAMP accumulation. Thus, partial inhibition of YM preincubated cells was more

pronounced than FR preincubated cells when stimulated with maximum activating Iso concentrations.

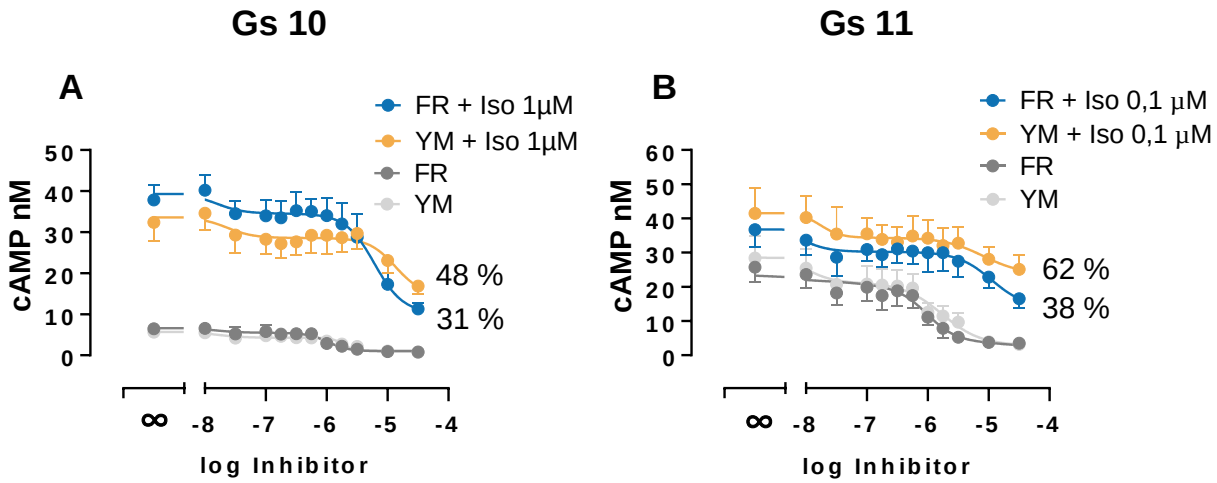

Figure 18: FR is superior to YM in blunting cAMP accumulation.
cAMP measurements in HEK293 Gs ko cells expressing transiently Gs 10 (A) or Gs 11 (B) with overexpressed β2AR, shown as mean + or - SEM of four biologically independent experiments, displayed more pronounced partial inhibition for cells preincubated with YM as compared to cells preincubated with FR when using the corresponding maximum activating agonist concentrations.

Next, we believed that the lower inhibitory ability of YM might cause a partial inhibition of ligand-induced cAMP accumulation triggered by an 80 % activating Iso concentration in contrast to FR, which inhibited the cAMP production totally at the highest inhibitor concentration (Fig. 15F, 17B). Indeed, in contrast to FR, which inhibited the cAMP production totally at the highest tested concentration in both Gs 10 and Gs 11 expressing cells along with the overexpressed β2AR, YM was not capable to fully attenuate the cAMP levels at its highest concentration (Fig 19A, B).

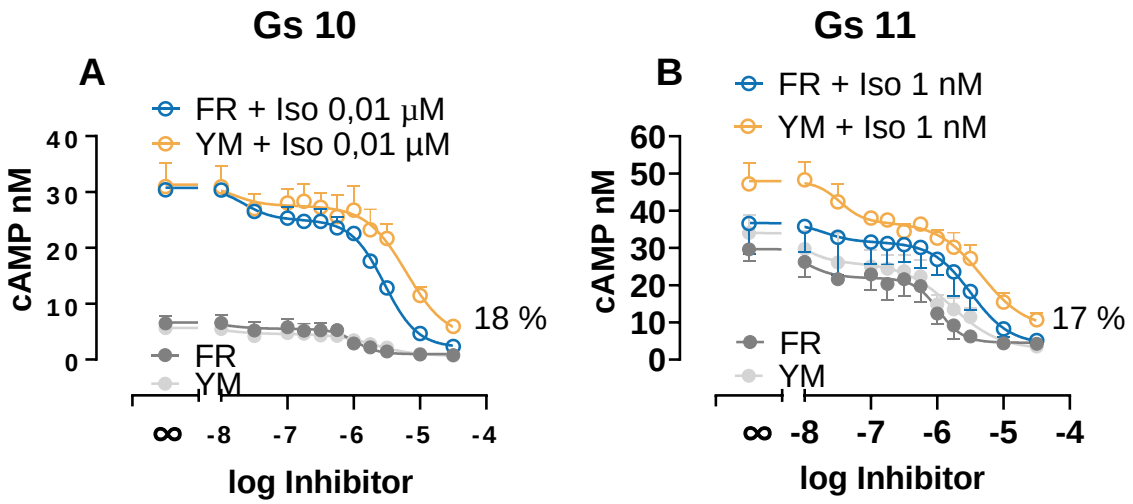

Figure 19: YM does not entirely inhibit pEC_{80} corresponding agonist concentrations. cAMP measurements in HEK293 Gs ko cells expressing transiently Gs 10 (A) or Gs 11 (B) with overexpressed β2AR, shown as mean + or - SEM of three- four biologically independent experiments, displayed partial inhibition in cells preincubated with YM in contrast to full inhibition in cells preincubated with FR when using the corresponding 80 % activating agonist concentrations.

Different expression levels of Gs 11 have no altering effect on FR´s responses registered in DMR assays.

Because partial inhibition of Gs 10 and Gs 11 by FR was observed upon maximum activation of the overexpressed β2AR, we wondered whether generally any overexpressed and maximally stimulated receptor would lead to partial inhibition of FR-sensitive G proteins. If this were the case, we would expect that Gq-signaling upon maximum activation of an overexpressed Gq-linked receptor would also result in partial inhibition by FR.

To test this hypothesis, we decided to compare the inhibition of Gs 10, Gs 11 and Gq signaling by FR upon maximum activation of the overexpressed β2AR or the established Gq-coupled muscarinic M3 receptor (M3). For this, we intended to use the holistic live-cell DMR assay (Fig. 7A), which records the cell changes triggered by GPCR stimulation of all G protein families (Schröder et al. 2010; Schröder et al. 2011) and thus provides the opportunity to compare FR´s capability to inhibit Gs- and Gq- signaling under the same conditions.

Since we had to transfect proteins from two different G protein families, a prerequisite for comparing FR´s ability to inhibit Gs- and Gq-signaling under the same condition was that the inhibitory effect of FR should not be affected by potential different expression levels of the transfected G proteins.

Hence, we transfected three different amounts of Gs 11 cDNA in Gs ko cells to assess the influence of variable expression levels for FR´s inhibitory potency for further DMR analysis. Careful titration of cDNA amounts up to 6 µg were used and Western blot analyses confirmed proper expression in correlation with the three amounts of the transfected Gs 11 cDNAs (Fig. 20A). Thus, normalization of expression levels with the highest transfected cDNA amount (6 µg Gs 11, 100% expression) displayed 7% expression when 0.6 µg Gs 11 was transfected and 42 % expression after 2 µg Gs 11 transfection (Fig. 20A_i). Next, the effect of increasing amounts of FR on the cells expressing the three different amounts of Gs 11 was analyzed by real time DMR assays. Real time recording of the dynamic mass redistribution revealed slightly different signaling strength at 10 µM and 30 µM FR within the different conditions (Fig. 20B) while concentration- effect curves of the recorded traces represented as negative area under the curve showed identical pIC_{50} (5.4) values for all three conditions (Fig. 20B_i). Correlation of pIC_{50} values with relative cellular abundance confirmed identical IC_{50} values despite increasing Gs 11 protein abundance (Fig. 20C).

Thus, we concluded that possible varying expression levels of Gq and Gs 11 would not influence the inhibitory potency of FR.

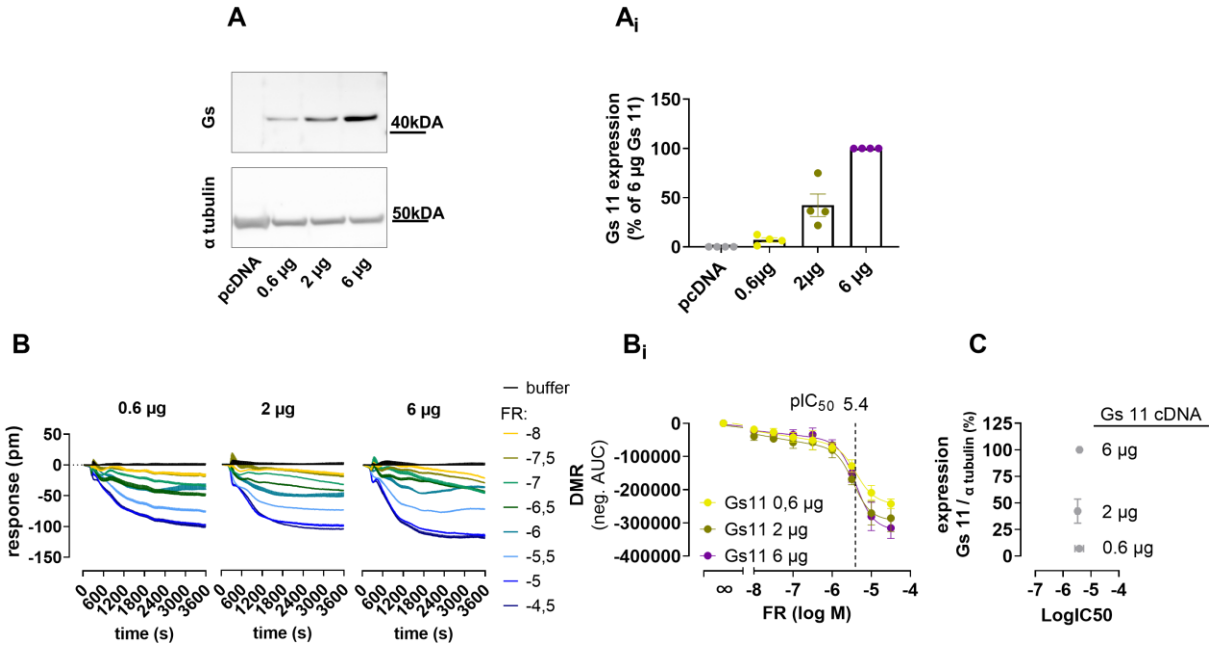

Figure 20: Different expression levels of Gs 11 have no effect on FR´s inhibitory responses. (A) Representative western blot showing expression levels of transiently expressing different transfected Gs 11 amounts detected in cellular lysates obtained from CRISPR-Cas9 $G\alpha_s$-null. α- tubulin was used as loading control. (A_i) Western blot quantification, shown as mean ± SEM displayed proportional increase in expression with increasing transfected DNA amount. (B) Concentration-dependent responses by FR at different transfected DNA amounts of Gs 11. DMR recordings are representative (mean + SE) of four independent biological replicates conducted in triplicates; pm, wavelength shift in picometer. (B_i) Concentration-response relationships for the traces shown in (*B*), shown as means ± SEM from four independent biological replicates. (C) Correlation of expressed Gs 11 amount, relative to the maximum transfected Gs 11 amount (6 µg, 100%), with the respective IC_{50} value.

Expression of Gs mutants and Gq along with overexpressed β2AR and M3 receptors, respectively, triggered agonist induced cell mass redistribution.

The inhibitory effect of FR should only be compared when the Gq and the modified Gs proteins are activated to a similar extent by their respective receptors and under comparable conditions. Therefore, we determined the precise agonist concentration to be used in our further DMR assays to analyze ligand-induced signaling inhibition by FR.

Firstly, Gs ko cells were transiently transfected with either Gs 10 or Gs 11 together with the β2AR in a DNA ratio of 2 µg: 4µg, respectively, and subsequently incubated with increasing amounts of Iso up to a concentration of 0.3 µM. Dose-dependent activation profiles of Iso revealed different maximal signaling strength for the individual Gs mutants (Fig. 21A). Nevertheless, concentration-effect curves of the traces depicted in figure 21A_i displayed similar maximum activating concentrations. Thus, for Gs 10 expressing cells a maximum activating concentration of 10 nM (“max. activ. 8”) was calculated whereas for Gs 11 expressing cells the maximum activating concentration was determined as 3 nM (“max. activ. 8.5”).

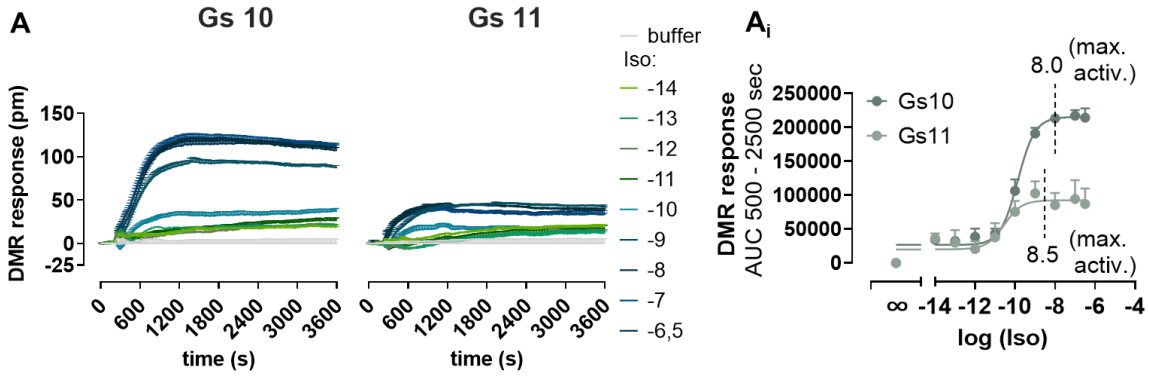

Figure 21: Recording of Isoprenaline induces mass redistribution in cells expressing Gs 11 and Gs 10 along with overexpressed β2AR. (A) concentration-dependent activation profiles of Iso in HEK-ΔGs cells transiently transfected to express Gs 10 or Gs 11 with the overexpressed β2AR in a DNA ratio of 2:4 µg using label-free DMR biosensing. A_i, concentration-effect curves of the traces depicted in (A), showing the area under the curve between the time period 500-2500 seconds. DMR recordings are representative (mean + SEM) of four independent replicates conducted in triplicate; concentration-effect relationships are the means + SEM from at least three independent experiments. pm, wavelength shift in picometer

Secondly, concentration-dependent activation profiles of carbachol (CCh) were recorded from Gq ko cells transiently expressing Gq and M3 receptor in a DNA ratio of 2 µg: 4 µg (Fig. 22A), i.e., identical to the ratio used in cells expressing the Gs proteins and the β2AR (Fig. 21). Surprisingly, despite the identical DNA ratios of G protein and receptor, no concentration-effect curve with a defined pEC_{50} value could be observed (Fig. 22A_i), since the lowest chosen CCh concentration (10^{-14}) triggered already a remarkable mass redistribution response of approximately 100 pm.

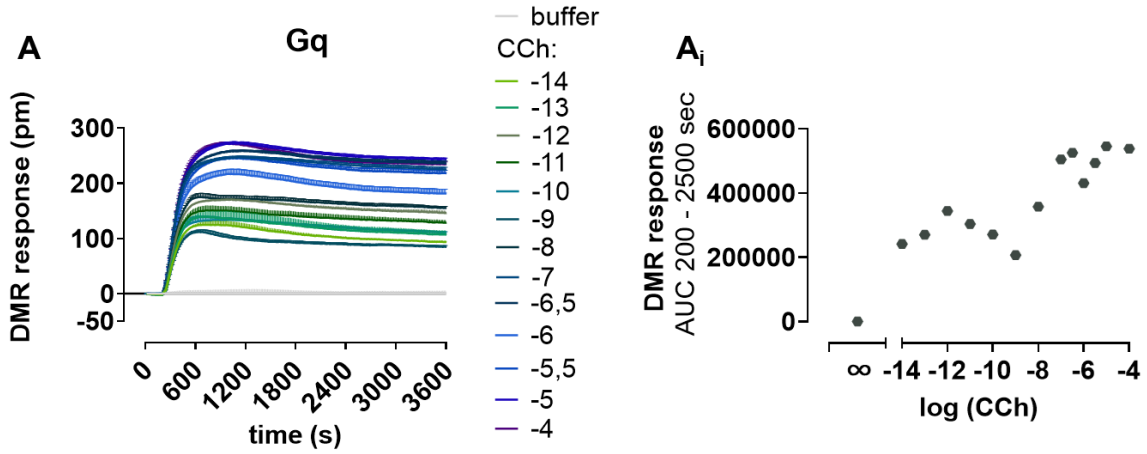

Figure 22: Identical chosen G protein-receptor ratio does not lead to a dose-response curve. (A) Concentration-dependent activation profiles of CCh in HEK-ΔGq/11 cells transiently transfected to express Gq along with the overexpressed muscarinic M3 receptor in an DNA ratio of 2:4 µg using label-free DMR biosensing. (A_i) concentration-effect curves of the trace depicted in (A), shows the area under the curve between the time period 500-2500 seconds with no defined pEC_{50} value. DMR recordings are representative (mean + SEM) one replicate conducted in triplicate; concentration-effect relationship is from one independent experiment. pm, wavelength shift in picomete22

We thought that a possible explanation for such an increased sensitivity upon agonist stimulation could be an extremely high expression level of the M3 receptor. If this were the case, lower amounts of transfected M3 receptor should result in a dose-response curve with a defined pEC_{50} value. Consequently, we tested our assumption by performing a new gene dosing with reduced cDNA amounts of transfected M3 receptor. Gq ko cells were transfected with 2 µg of Gq along with either 0.6 µg, 1 µg or 2 µg of M3 receptor, up to a total amount of 6 µg completed with vector (pcDNA3.1). As hypothesized, recording of dose-dependent activation profiles for all conditions (Fig. 23A) revealed a concentration dependent increase

of signaling strength, starting with significantly lower amplitudes after incubation with the lowest CCh concentrations. Analyses of the concentration-effect curves of the traces depicted in Fig. 23A displayed similar agonist efficacy and potency (Fig. 23A$_i$). However, the pEC$_{50}$ value for cells transfected with the lowest M3 receptor amount (0.6 µg) showed slightly higher agonist potency compared to cells transfected with either 1 µg or 2 µg M3 receptor. Therefore, we decided to select the DNA ratio with the proportionally lowest M3 receptor amount for the following analyses.

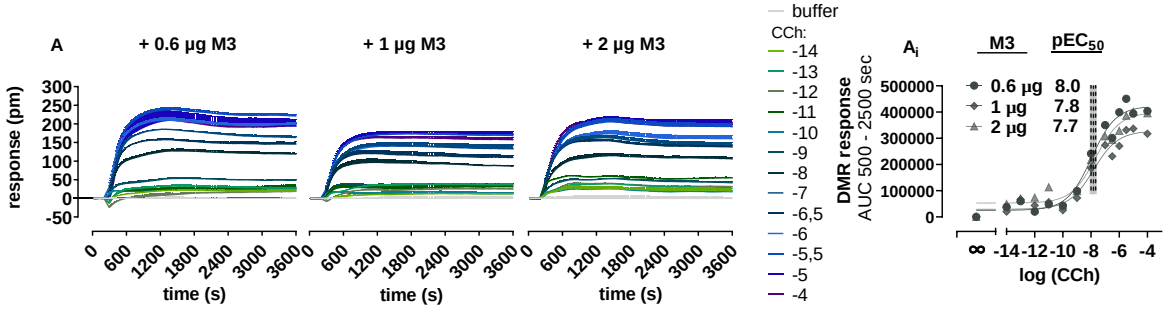

Figure 23: Gene dosing of the M3 receptor revealed ideal G protein-receptor ratio.
*(*A) Concentration-dependent activation profiles of CCh using label-free DMR biosensing in HEK-ΔGq/11 cells transiently transfected to express Gq in increasing amounts, i.e., 0,6 µg, 1 µg and 2 µg, along with the overexpressed muscarinic M3 receptor. (A$_i$) Concentration-effect curves of the traces depicted in (A), shows the area under the curve between the time period 500-2500 seconds. DMR recordings are representative (mean + SEM) from one independent replicate conducted in triplicate; concentration-effect relationships are from one independent experiment. pm, wavelength shift in picometer

Overexpression of both β2AR and M3 receptors lead to higher agonist potency.

Our preliminary analyses showed that a much smaller amount of the M3 receptor than the β2AR should be used to evaluate FR´s capability to inhibit Gq and Gs signaling. However, we wondered whether this small amount of M3 receptor would have an equivalent activating power as the β2AR since we wanted to compare FR inhibition of ligand-induced signaling between Gq and modified Gs proteins under comparable conditions.

To investigate this, we decided to evaluate and compare in DMR assays the potency shift triggered by the overexpressed β2AR and M3 receptors as compared to the endogenous

expressed receptors, since we previously found that overexpressing a receptor led to higher agonist potency in our cAMP data (Fig. 14, 16). Thus, dose-dependent activation profiles of Gs ko's transiently expressing Gs 10 or Gs 11 in the presence or absence of overexpressed β2AR, and Gq ko's transiently expressing Gq along with or without overexpressed M3 receptor were recorded. Traces registered from cells expressing overexpressed receptors (Fig. 24A- C) clearly differed from those, recorded from cells expressing endogenous receptors (Fig. 24A_i- C_i). Thus, stimulation of overexpressed receptors with their respective agonists resulted in traces that remained constant throughout the measured time period after reaching the maximum DMR response (Fig. 24A- C). Conversely, in cells expressing endogenous receptors the maximum signaling strength did not remain the same throughout the measured time period upon receptor activation but dropped afterwards (Fig. 24A_i- C_i). However, as expected, concentration-effect relationships from the traces shown in (Fig. 24A-C_i) displayed for both Gs mutants and Gq a left shift of the agonist potency in those cells expressing the overexpressed receptors compared to cells expressing the endogenous receptors. (Fig. 24A_{ii}- C_{ii}). Notably, this potency shift was similar (more than 400-fold) for Gs 11 (Fig. 24B_{ii}) and Gq (Fig. 24C_{ii}). Therefore, we concluded that the small amount of transfected M3 receptor had a comparable activating power as compared to the β2AR, which allowed us to determine for both Gs mutants and Gq the maximum agonist concentration to be used in our further investigations on ligand-induced signaling inhibition by FR.

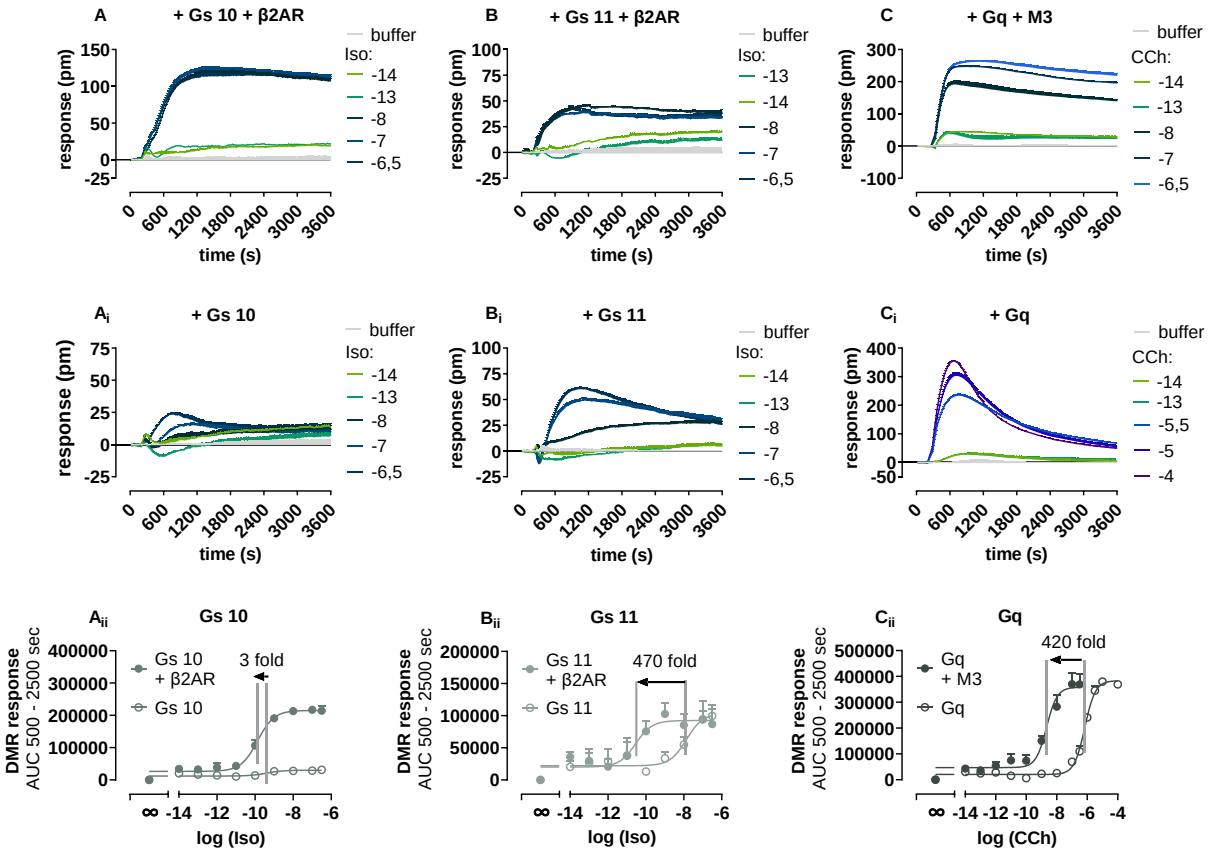

Figure 24: Overexpression of both β2AR and M3 receptor leads to higher agonist potency. (A, B & A_i, B_i) Representative label-free DMR biosensing showing concentration-dependent activation profiles of Iso in HEK-ΔGs cells transfected to express Gs 10 or Gs 11 in the presence of overexpressed β2AR (A, B) or endogenous β2AR (A_i, B_i). (C, C_i) Concentration-dependent activation profiles of CCh in HEK-ΔGq/11 cells transiently transfected to express Gq with overexpressed muscarinic M3 receptor (C) or endogenous M3 receptor (C_i). (A_{ii}-C_{ii}) concentration-effect curves of the traces depicted in A-C_i. Fold shifts above the curves denote the increase of agonist potency by overexpressing the respective receptor. Maximum activating agonist concentration were determined as 0.01 µM Iso for Gs 10 + β2AR, 3 nM Iso for Gs 11 + β2AR, 0.1 µM CCh for Gq + M3, 30 nM Iso for Gs 10, 1 µM Iso for Gs 11 and 30 µM CCh for Gq. DMR recordings are representative (means + SEM) of at least four independent biological replicates conducted in triplicate. Concentration-effect relationships are means (means + SEM) from at least four independent biological replicates. pm, wavelength shift in picometer.

FR inhibits entirely Gq but not Gs 10 or Gs 11-signaling upon maximum activation of overexpressed receptor.

Once we have determined the ideal G protein-receptor ratio as well as the maximum activating agonist concentrations for both receptors, we initiated our comparative studies of FR´s capability to inhibit Gq signaling upon maximum activation of the overexpressed M3 receptor in Gq ko cells. Priming these cells with increasing FR concentrations caused changes in the optical density as a result of DMR (Fig. 25A). Applying of a maximum activating concentration of the muscarinic M3 receptor agonist CCh did not result in a cellular response in cells primed with at least 1 µM FR (Fig. 25A, A_i), thus showing full inhibition. Furthermore, the half-maximal inhibitory concentration (IC_{50} value) of FR was hardly changed by maximal stimulation of the M3 receptor compared to inhibition of basal activity. Therefore, we concluded that, in contrast to our initial hypothesis, not any maximally activated and overexpressed receptors lead to partial FR inhibition.

However, we wondered whether FR could also suppress cellular DMR responses in cells expressing Gs 10 and Gs 11 with overexpressed β2AR upon challenge with Iso at its maximum activating concentration, in contrast to our previous cAMP results. Consequently, Gs ko cells transiently expressing Gs 10 or Gs 11 along with the overexpressed β2AR were treated with increasing FR concentrations. Akin to Gq expressing cells, real time recording of both Gs 10 (Fig. 25B, B_i) and Gs 11 (Fig. 25C, C_i) expressing cells revealed changes in the optical density as a result of DMR. Notably, the recorded negative wavelength shift was more pronounced in β2AR overexpressing cells that were transfected with Gs 11 (Fig. 25C) than in Gs 10 transfected cells (Fig. 25B), presumably due to Gs 11 ´s higher intrinsic activity. In contrast to our observations in cells expressing Gq and M3, Iso at its maximum activating concentration triggered a DMR response in FR treated cells expressing Gs 10 (Fig. 25B, B_i) or Gs 11 (Fig. 25C, C_i). Thus, partial inhibition of both FR-sensitive Gs proteins was observed even at the highest used FR concentration (30 µM). Furthermore, we noticed that the partial inhibition in cells expressing Gs 10 or Gs 11 along with the β2AR was more pronounced than observed in previous cAMP measurements (Fig. 15F and 17B).

Figure 25D-F illustrates both cellular and physical processes that occur during DMR measurements, which register in real time cytoskeletal rearrangement and mass redistribution in cells in response to the inhibitor FR and the agonists Iso or CCh (Schröder et al. 2010; Schröder et al. 2011).

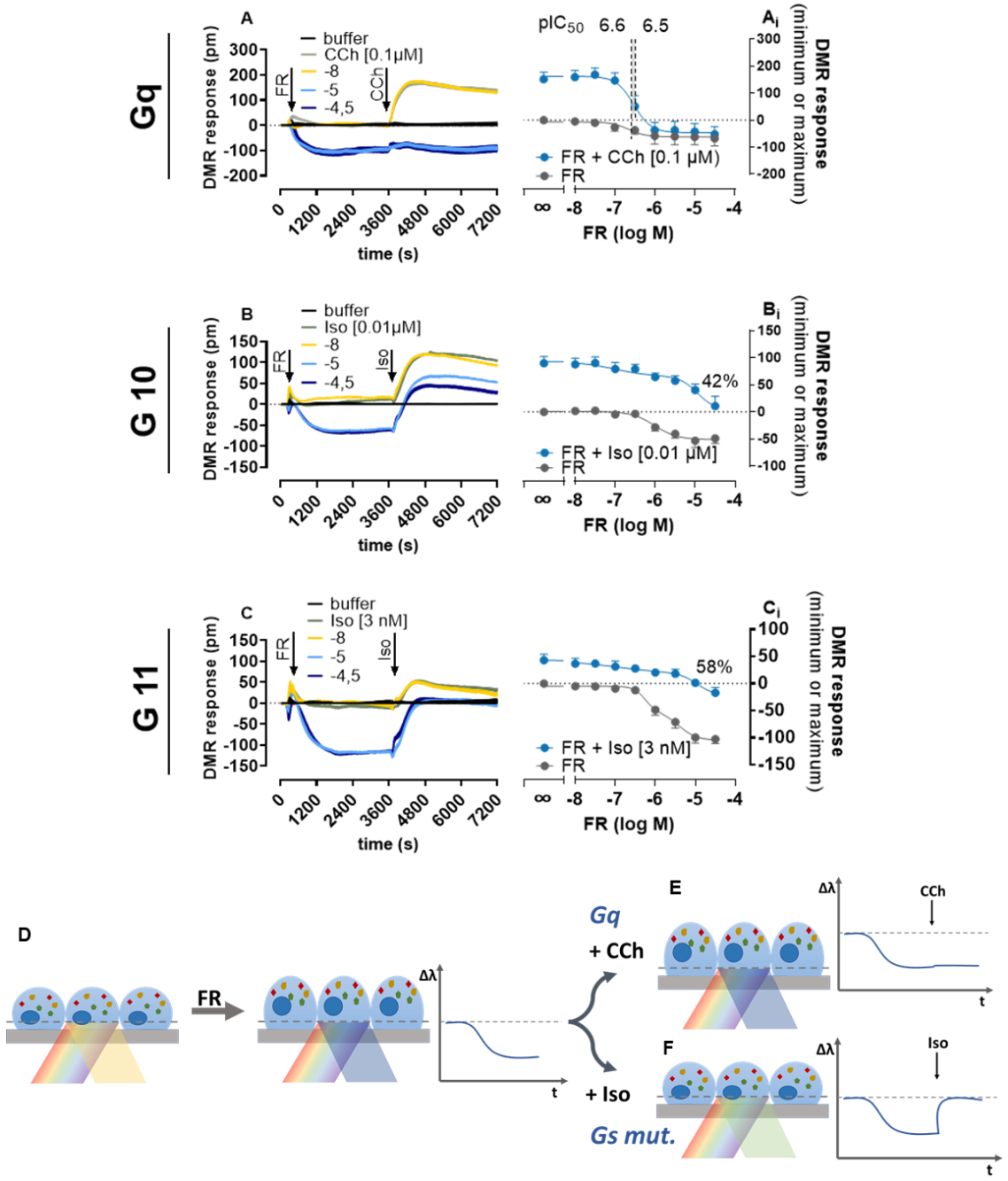

Figure 25: FR inhibits entirely Gq but not Gs 10 or Gs 11-signaling upon maximum activation of overexpressed receptors.

(A-C) inhibition by FR of G protein–dependent whole-cell activation profiles in HEK-ΔGq/11 (A) or HEK-ΔGs (B-C) cells transfected to express the Gq with overexpressed muscarinic M3 receptor (A) and Gs 10 (B) or Gs 11 (C) with overexpressed β2AR. G proteins were activated via overexpressed M3 receptors upon challenge with CCh at its maximum activating concentration (A) or via overexpressed β2AR upon challenge with Iso at its maximum activating concentration (B). Shown are representative whole-cell recordings (A,

B) along with concentration-inhibition curves for Gq, Gs 10 or Gs 11 (A_i–C_i). DMR recordings are representative (means + SEM) of at least three independent biological replicates conducted in triplicate. Concentration-effect relationships are means (means + or SEM) from at three independent biological replicates. pm, wavelength shift in picometer. (D-F) Graphical illustration of the DMR assay. Cells located on the resonant waveguide grating biosensor are exposed to polychromatic light that in part is reflected while the rest is absorbed. For both Gq and Gs mutant expressing cells, addition of FR decreases the optical density proximal to the biosensor and shifts the reflected light to shorter wavelengths (D). Second addition of the agonist CCh at its maximal activating concentration onto cells expressing Gq does not lead to changes in the optical density and wavelength shifts (E). In contrast, the addition of Iso at its maximum activating concentration onto cells expressing Gs 10 or Gs 11 causes a renewed increase in cellular mass on the biosensor and thus a shift to longer wavelengths (F).

Partial FR-inhibition of Gs 10 and Gs 11 upon maximum activation of endogenously expressed β2AR in DMR assays.

As mentioned above, DMR responses in the presence of the overexpressed and maximally stimulated β2AR displayed partial inhibition by FR, which was greater than observed in cAMP measurements. Therefore, we wondered whether DMR responses could be entirely inhibited by FR upon activation of the endogenously expressed β2AR at its maximum activating Iso concentration, since total inhibition of cAMP production by FR has been successfully demonstrated before (Fig. 15E & 17A). Consequently, Gs ko cells transiently expressing Gs 10 (Fig. 26A, A_i) or Gs 11 (Fig. 26B, B_i) were primed with increasing FR concentrations, which again caused changes in the optical density as a result of cellular mass redistribution. Notably, applying the maximum activating concentration of Iso for the endogenous β2AR caused a DMR signal, even in cells treated with 30 µM FR. Therefore, in cells expressing Gs 10 and Gs 11 together with the endogenous β2AR, DMR responses could not be completely inhibited in contrast to cAMP production, which was successfully blunted in comparable conditions. Furthermore, consistent with our previous analyses with the M3 receptor, FR-primed Gq ko cells transiently expressing Gq showed full inhibition of DMR upon maximum activation of the endogenously expressed M3 receptor (Fig. 26C, C_i). Based on our results, we concluded that the extent of FR inhibition of Gs mutants is method dependent, which should be consequently considered when using Gs 10 or Gs 11 in future studies.

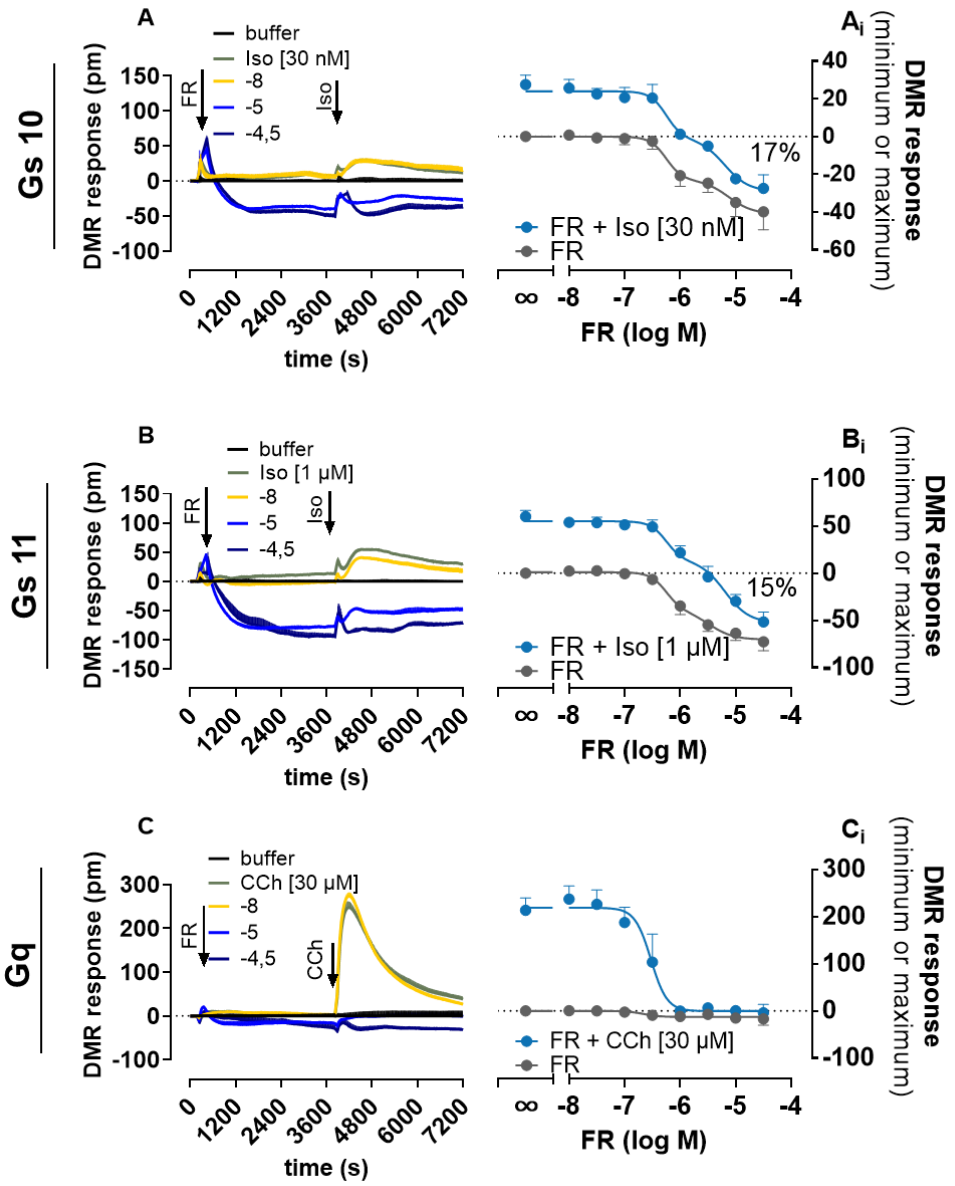

Figure 26: FR-partial inhibition of Gs 10 and Gs 11 upon maximum activation of endogenously expressed β2AR in DMR assays. (A-C) Inhibition by FR of G protein–dependent whole-cell activation profiles in HEK-ΔGs (A-B) or HEK-ΔGq/11 (C) cells transfected to express Gs 10 (A) or Gs 11 (B) or Gq (C). G proteins were activated via endogenous β2AR upon challenge with Iso at its maximum activating concentration (A-B) or via endogenous M3 receptors upon challenge with CCh at its maximum activating concentration (C). Shown are representative whole-cell recordings along with concentration-inhibition curves for Gs 10, Gs 11 or Gq (A_i–C_i). DMR recordings are representative (means + or - SEM) of at least three independent biological replicates conducted in triplicate. pm, wavelength shift in picometer

Introducing new Gq exclusive amino acids in Gs 10 and Gs 11 do not increase FR´s inhibitory power.

Our data has demonstrated that artificially generated FR-sensitive Gs proteins did not exhibit identical FR-inhibition profiles as Gq proteins. Although Gs 11 is endowed with the entire inhibitor binding site, cellular responses such as cAMP accumulation or DMR were possible upon agonist stimulation despite FR treatment, in contrast to the full FR-inhibition of Gq.
In a recent study, Müller and co-workers (Voss et al. 2021) highlighted two Gq exclusive residues E119 and K120 (amino acids and sequence numbers are from Gq) located in the helical domain that showed an entropy increase upon FR and YM binding, even though both positions are not in a proximate distance to both inhibitors. We hypothesized that these residues might support the stabilizing impact of the inhibitors via allosteric effects, preventing the separation between the αH and the RasD domains of Gq (Voss et al. 2021). Consequently, we decided to introduce both Gq exclusive positions by site directed mutagenesis in Gs 10 and Gs 11 for further analyses. We generated the single mutants Gs 10^{V123E}, Gs 10^{P124K}, Gs 11^{V123E} and Gs 11^{P124K}, as well as the double mutants Gs $10^{V123E,P124K}$ and Gs $11^{V123E,P124K}$. First, we analyzed the expression and functionality of all new constructs to evaluate the capability to increase the intracellular basal levels of cAMP compared with Gs 10 and Gs 11, respectively. Western blot analysis confirmed proper expression of all Gs mutants (Fig. 27A, B). Gs 11 constructs displayed comparable abundance among them (Fig. 27D), whereas Gs 10^{P124K} and Gs $10^{E1234V\ P124K}$ showed increased expression levels compared to Gs 10 (Fig. 27C). Subsequently, the functionality of the new designed Gs mutants was evaluated by measuring intracellular cAMP accumulation. Thus, Iso led to a robust and concentration-dependent increase of cAMP accumulation in Gs ko cells expressing Gs 10, Gs 11 and their respective new mutants (Fig. 27E, F). Even though Gs 11^{P124K} and Gs $11^{V123E\ P124K}$ showed a slight decreased efficacy (Fig. 27F), all mutants exhibited the same potency as compared to Gs 10 and Gs 11, respectively. Thus, all Gs 10 dependent mutants displayed a pEC_{50} value at 9.0 (Fig. 27E) whereas all Gs 11 related mutants revealed a higher potency with a pEC_{50} value at 9.9 (Fig. 27F). Moreover, the maximum activating concentration for all Gs 10 derived mutants was determined to be the same as Gs 10 (1 µM Iso).

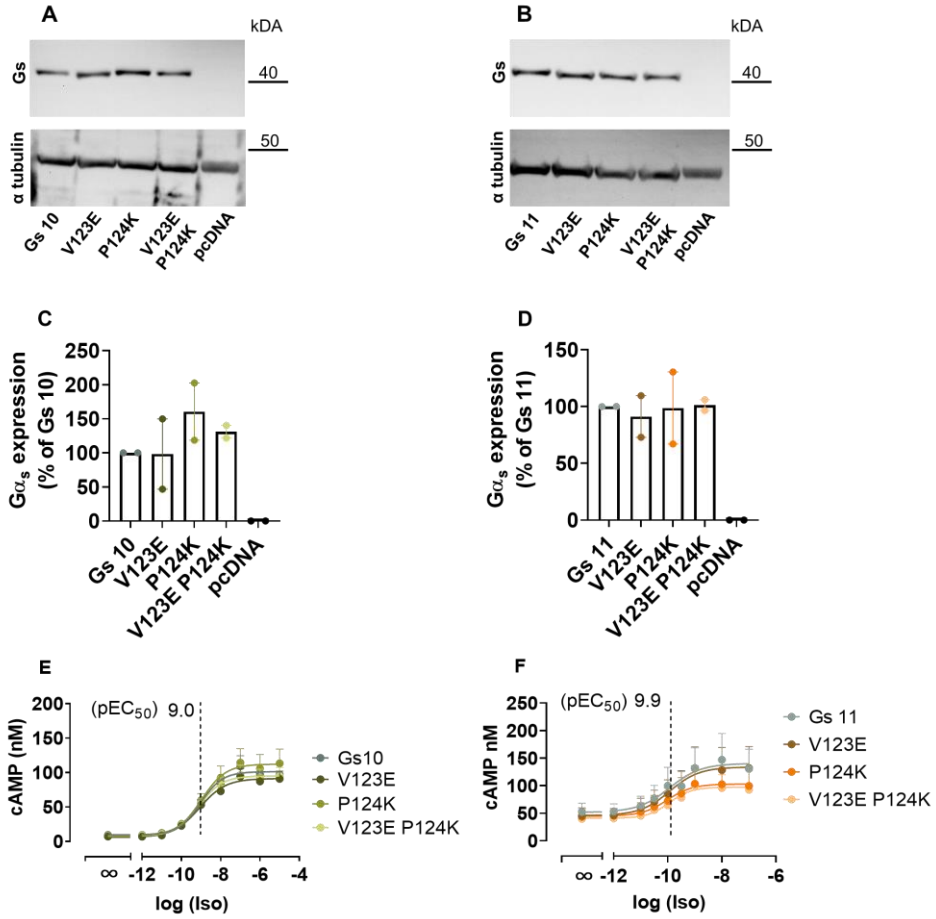

Figure 27: Expression and function of new single and double mutants of Gs 10 and Gs 11.

(A,B) Representative western blot showing expression of (A) Gs 10, $\mathrm{Gs\ 10^{V123E}}$, $\mathit{Gs}\ 10^{\mathrm{P124K}}$, $\mathrm{Gs\ 10^{V123E\ P124K}}$, and (B) Gs 11, $\mathrm{Gs\ 11^{V123E}}$ $\mathrm{Gs\ 11^{P124K}}$, $\mathrm{Gs\ 11^{V123E\ P124K}}$ detected in cellular lysates obtained from CRISPR-Cas9 Gαs-null cells transiently expressing the indicated constructs in the presence of overexpressed β2AR. α- tubulin was used as loading control. (C, D) Western blot quantification, shown as mean ± SEM of two independent biological replicates. (E, F) cAMP measurements of the indicated Gs mutants along with overexpressed β2AR, shown as mean ± SEM of three biologically independent experiments, displayed concentration-dependent increase of cAMP levels. Maximum activating concentration for Gs 10 and all Gs derived mutants calculated as: 1 µM ≙ 10^{-6}. Performed by Dr. Nicole Merten.

After confirming the proper expression and functionality of all Gs mutants, next we tested FR´s capability to inhibit receptor-mediated cAMP. First, we preincubated cells transiently expressing Gs 10, $\mathrm{Gs10^{V123E}}$, $\mathrm{Gs10^{P124K}}$ and $\mathrm{Gs10^{V123E\ P124K}}$ with increasing concentrations of FR and stimulated them afterwards with 1 µM Iso. Notably, none of the new Gs 10-derived

mutants resulted in complete inhibition or even significantly better inhibition by FR upon maximum activation of the overexpressed β2AR (Fig 28A-D).

Gs 11 and the corresponding mutants were tested via a schild analysis. We chose this method because the calculated maximum agonist concentration differed within the mutants despite identical EC50 values due to different slopes of the agonist curves (Fig 28F). Thus, cells were preincubated with a fixed concentration of FR (30 µM) and then stimulated with increasing concentrations of Iso. Our analysis revealed that the Gs 11 derived mutants $Gs11^{V123E}$, $Gs11^{P124K}$ and $Gs11^{V123E\ P124K}$ also did not show any significant better inhibition by FR as compared with Gs 11.

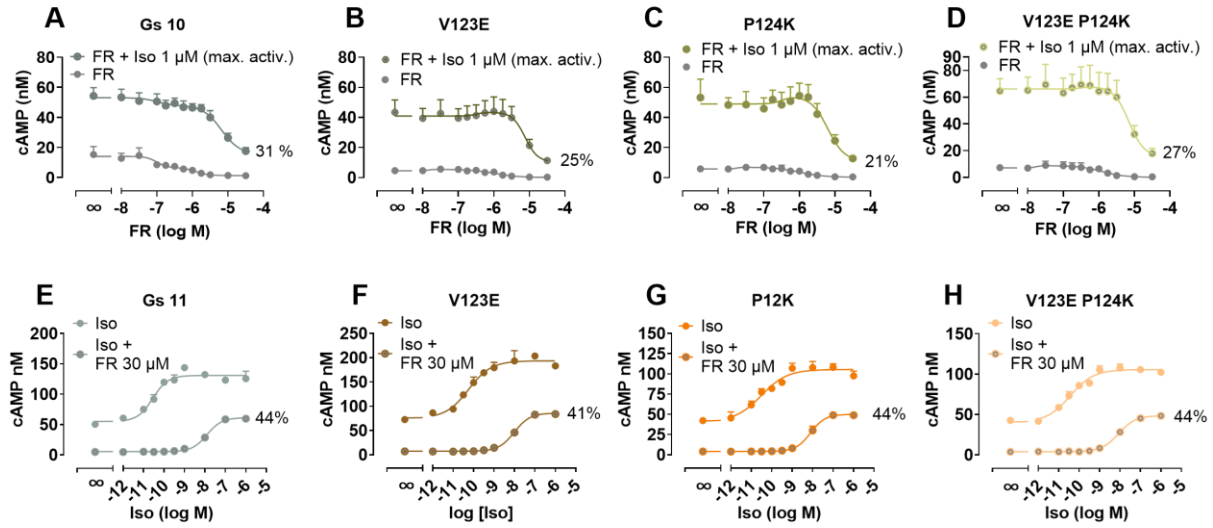

Figure 28: Introducing Gq exclusive amino acids in Gs 10 and Gs 11 do not increase FR´s inhibitory power.

cAMP measurement of HEK293 Gs ko cells expressing transiently Gs 10 (A), $Gs10^{V123E}$ (B), $Gs10^{P124K}$ (C), $Gs10^{V123E\ P124K}$ (D), Gs 11 (E), $Gs11^{V123E}$ (F), $Gs11^{P124K}$ (G), and $Gs11^{V123E\ P124K}$ (H) along with the overexpressed β2AR, shown as mean + SEM of two- three biologically independent experiments, revealed no significant differences on FR inhibition between the respective new engineered mutants and Gs 10 or Gs 11. Performed by Dr. Nicole Merten.

In summary, our comprehensive analysis revealed that transplanting the inhibitor binding site does not lead to identical inhibition profiles as the natural FR target Gq.

Chapter 3: Why are Gs 11 and Gs 10 not completely inhibited? What is behind it mechanistically?

FR displays equal affinity for all tested Gα proteins.

From our data, we concluded that FR is not able to inhibit completely the artificially generated FR-sensitive Gs proteins Gs 10 and Gs 11, in contrast to the potent and complete inhibition of its natural target Gq. We wondered whether FR affinity might differ between the Gα subunits, which could cause and explain this discrepancy. Thus, membrane samples were prepared (i) from Gs ko cells transiently expressing Gs 10 and Gs 11 along with the overexpressed β2AR, and (ii) from Gq ko cells transiently expressing Gq and the overexpressed muscarinic M3 receptor. Membrane preparations were subsequently used to perform competition binding experiments, testing 5 nM [^{3}H] PSB-15900 (labeled FR) versus increasing concentrations of unlabeled FR. We observed that FR displayed similar affinities in the low nanomolar range with no significant differences between Gq and the Gs mutants (Fig. 29).

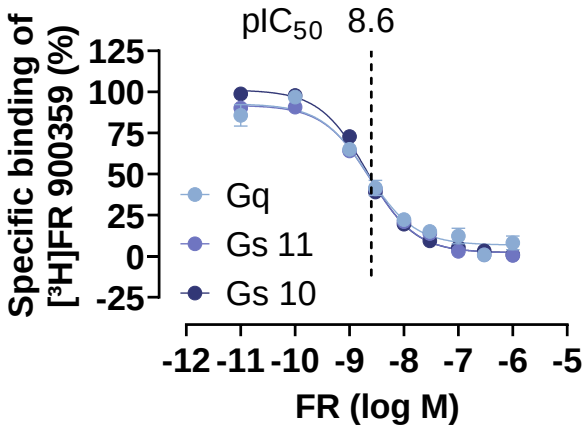

Figure 29: FR displays equal affinity for all tested Gα proteins.
Competition binding experiments of 5 nM [^{3}H] PSB-15900 versus multiple concentrations of FR using membrane preparations (15 µg protein) from cells transiently expressing Gq + M3, Gs11 + β2AR, or Gs10 + β2AR proteins after incubation at 37 °C for 90 min. Data points represent means ± SEM of three independent experiments. Performed in Christa Müller´s lab by Jan Hendrik Voß.

FR adheres to Gs mutants comparably well as to Gq.

Since FR affinity does not change between the Gα subunits, we next investigated whether the residence time of the inhibitor differs between them. A shorter residence time, i.e., a faster dissociation of the inhibitor, could give us insight into the discrepancies between Gq and the Gs mutants. To this end, same membrane preparations as described in figure 29 were used for dissociation experiments. After incubation of the membranes with 5nM labeled FR, the dissociation was induced by the time-displayed addition of 5 µM unlabeled FR (Fig. 30A-C). In all cases, displacement by addition of unlabeled FR was observed. Interestingly, our analysis revealed that the half-life ($t_{1/2}$) for the natural FR target Gq (Fig. 30A) was shorter than those for the FR sensitive Gs mutants (Fig. 30B, C). Consequently, the observed FR partial inhibition for Gs 10 and Gs 11 was not the result of a reduced inhibitor-residence time.

We also wondered whether activation of the G proteins could displace the bound FR-radioligand, thus explaining the different inhibition pattern by FR. Therefore, after preincubation of membrane preparations with labeled FR, either CCh (Fig. 30D) or Iso (Fig. 30E, F) were added in excess. In all cases labeled FR was barely displaced by receptor activation with the respective agonists and only an approximate decrease of 10 % in binding was observed for all Gα subunits (Fig. 30D- F).

Overall, our data show that FR adheres to the artificially generated FR-sensitive Gs mutants comparably well as to Gq, indicating that the adhesion capacity of the inhibitor was successfully transferred by transplanting the FR-binding site, although activation of the Gs mutants was still possible despite FR residence, in contrast to Gq.

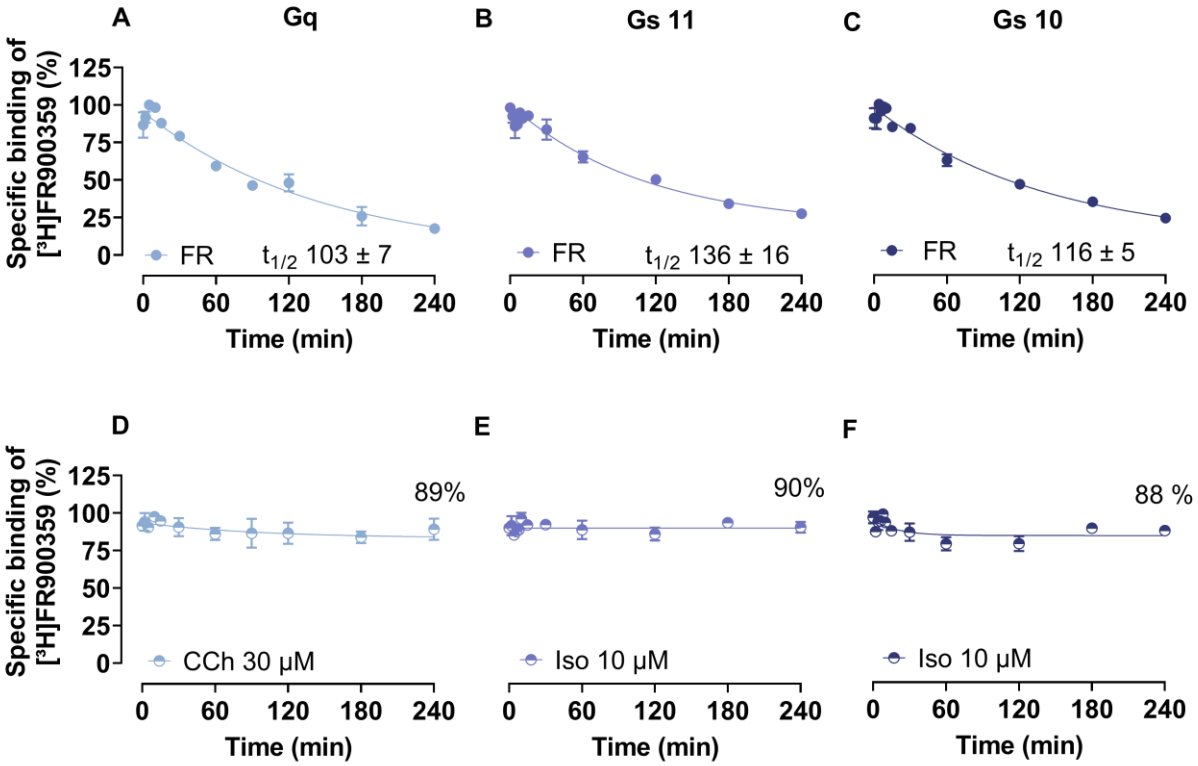

Figure 30: FR adheres to Gs mutants comparably well as to Gq.
Dissociation experiments of 5nM [³H] PSB-15900 in membrane preparations (15 µg of protein) from cells recombinantly expressing Gq + M3 (A, D), Gs 11 + β2AR (B, E), Gs 10 + β2AR (C, F) at 37° C. Dissociation was induced either by the time-displaced addition of 5 µM FR (A-C) or by addition of CCh 30 µM (D) and Iso 10 µM (E, F). Data points represent means ± SEM of four independent experiments. Performed in Christa Müller´s lab by Jan Hendrik Voß.

CCh increases [^{35}S] GTPγS binding only in the absence of FR.

Knowing that FR adheres to the Gs mutants comparably well as to Gq, we continued our investigations to elucidate why activation of FR-sensitive Gs proteins occurs despite excellent FR binding as opposed to Gq. Considering FR´s mechanism of action, it is known that FR traps the G protein into the GDP-bound fraction (Nishimura et al. 2010a), thus allowing neither nucleotide exchange nor dissociation of the heterotrimer Gαβγ. Therefore, we hypothesized that in Gs 10 and Gs 11 either (i) nucleotide exchange is possible despite FR binding or (ii) Gs 10 and Gs 11 bind and activate their downstream effectors in the GDP-bound state such as the oncogenic Gs mutation R201C, which allows GDP-bound-Gs to activate the adenylyl cyclase (Hu und Shokat 2018).

To address these hypotheses experimentally, we decided to perform nucleotide exchange analyses in the presence of FR. However, investigation of Gq- and Gs-dependent nucleotide exchange by the [^{35}S] GTPγS binding assay is technically challenging. Mostly Gi proteins, which are known for their rapid nucleotide exchange, are associated with the [^{35}S] GTPγS binding assay. Gs-dependent [^{35}S] GTPγS binding studies have also been performed in the past, but in most cases fusion proteins have been used since β2AR couples poorly to the endogenous Gs protein, according to the literature (Seifert et al. 1998).

Therefore, to establish an assay system that displays a robust and substantial amount of [^{35}S] GTPγS binding, we first used membrane preparations obtained from Gq ko cells transiently expressing Gq and the overexpressed M3 receptor. We compared the M3 receptor mediated binding of [^{35}S] GTPγS triggered by CCh in both the presence and absence of FR, anticipating that nucleotide exchange is not possible in the presence of FR. Based on the literature (Min et al. 2017; Liu et al. 2012; Katritch et al. 2014; Miller-Gallacher et al. 2014), we used a NaCl and GDP free Tris buffer to enhance the [^{35}S] GTPγS binding triggered by 30 µM CCh. Under these conditions, the M3 receptor agonist increased the [^{35}S] GTPγS binding in membrane preparations pretreated with DMSO, whereas it could not enhance the [^{35}S] GTPγS binding in FR (5 µM) pretreated membrane preparations (Fig. 31), indicating that the nucleotide exchange by FR was hampered.

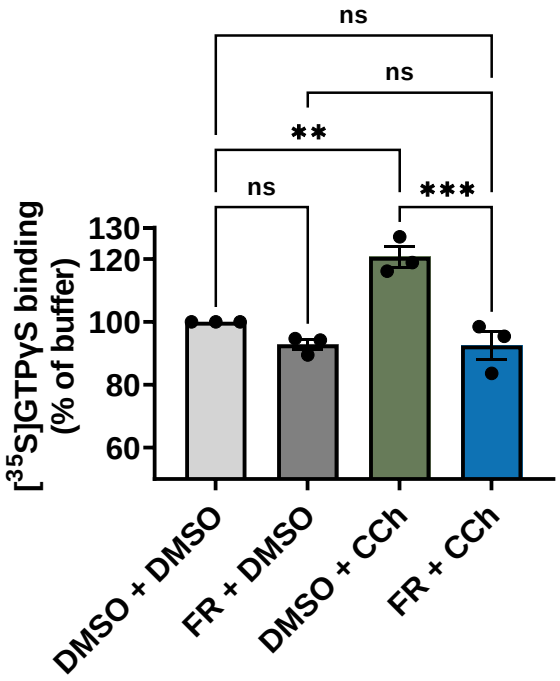

Figure 31: CCh increases GTPγS binding only in the absence of FR.
[^{35}S] GTPγS binding measurements in membrane preparations (1 µg of protein) from transiently expressing Gq, the muscarinic M3 receptor and the PTX S1 catalytic subunit, which inhibits the Gi/o family that is expressed in Gq ko cells. The CCh induced increase of [^{35}S] GTPγS binding was inhibited by preincubating with 5 µM FR. Statistical analysis was performed by one-way ANOVA followed by Dunnett´s test; **, $p < 0.01$; ***, $p < 0.001$; ns, not significant. Data points represent means ± SEM of three independent experiments. Performed in Christa Müller´s lab with the assistance of Jan Hendrik Voß.

Gs 11 allows nucleotide exchange in the presence of FR upon receptor stimulation.

To shed light on our previously obtained data, in which Gs-signaling was still possible despite FR, we interrogated whether FR inhibits the β2AR mediated binding of [^{35}S] GTPγS triggered by Iso. Consequently, membrane preparations were prepared from Gs ko cells transiently expressing Gs 11 along with the overexpressed β2AR.
Nevertheless, before examining the influence of FR, two different set ups for binding of [^{35}S] GTPγS in Gs 11 membrane preparations were tested: on the one hand, with identical experimental conditions as described in figure 31 (Fig. 32A), and on the other hand, with addition of 10 µM guanosine diphosphate (GDP) as buffer supplement (Fig. 32B). GDP has

been reported to maintain the inactive G protein conformation (Harrison und Traynor 2003), which should be considered due to Gs 11´s elevated intrinsic activity. However, and to our surprise, 10 µM Iso could not enhance significantly the [^{35}S] GTPγS binding compared with membrane preparations treated only with DMSO in both set ups. Therefore, we concluded that the chosen conditions were not suitable to address our investigation.

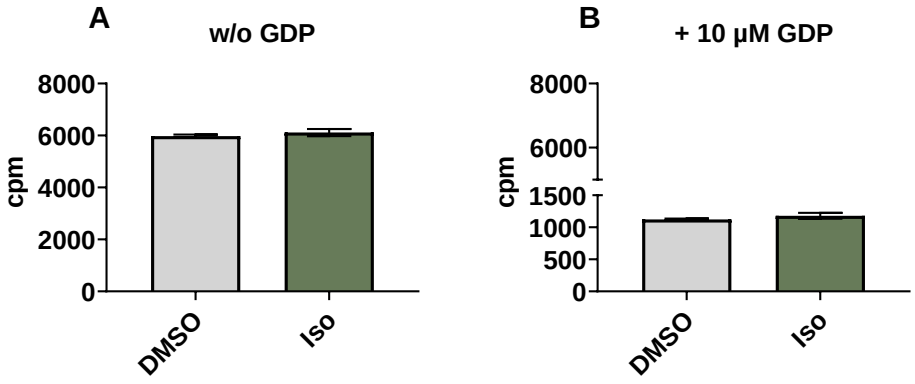

Figure 32: No increase of [^{35}S] GTPγS binding triggered by Iso in Gs 11 expressing cells.

[^{35}S] GTPγS binding assays performed with membrane preparations (2 µg of protein) collected from Gs ko cells transiently expressing Gs 11 and the β2AR. Assay was performed either in the absence (A) or in the presence of 10 µM GDP (B). Upon stimulation with 10 µM Iso, no increase of [^{35}S] GTPγS binding was observed in both conditions after an incubation time of 60 minutes at room temperature.

Accordingly, we modified our binding buffer by adding sodium ions and increasing the amount of magnesium ions. Sodium ions promote the Gα-Gβγ-GDP complex, helping to maintain the inactive receptor conformation (Nishimura et al. 2010a; Lorenzen et al. 1993; Min et al. 2017; Katritch et al. 2014), which could support an increase in [^{35}S] GTPγS binding triggered by Iso. Magnesium ions increase both basal and agonist-mediated [^{35}S] GTPγS binding but have a greater effect on agonist-stimulated binding, resulting in a stronger agonist-mediated response (Harrison und Traynor 2003). Therefore, 100 mM NaCl and 10 mM $MgSO_4$ were added to 20 mM Hepes buffer to be used for our investigation. We used identical Gs 11 membrane preparations as in figure 32 and preincubated them with either

DMSO or 5 µM FR for 30 minutes. A significant increase of Iso-mediated [^{35}S] GTPγS binding was now observed after 10 minutes in the membranes preincubated with DMSO (Fig. 33). Moreover, an increase of [^{35}S] GTPγS binding could be observed in FR-pretreated (5 µM) membranes. This is in perfect agreement with our previous cAMP and DMR data, in which partial FR inhibition was detected at FR´s highest used concentration.

Taken together, our data suggest that, despite the excellent binding properties of FR to Gs 11, nucleotide exchange is still possible upon receptor stimulation.

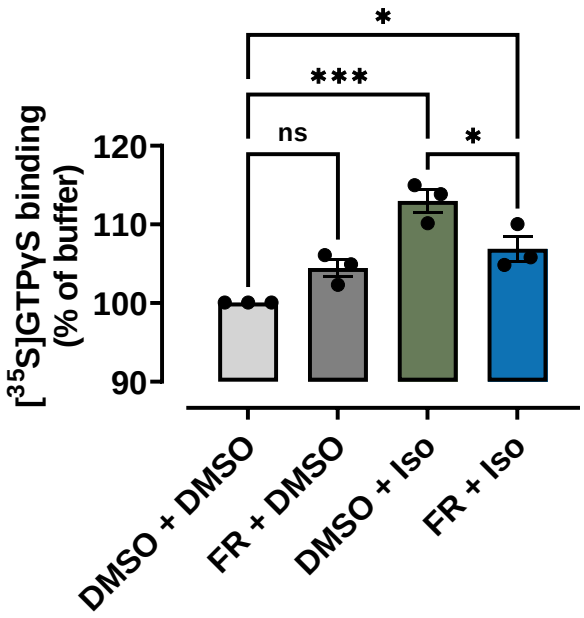

Figure 33: Gs 11 allows nucleotide exchange in the presence of FR upon receptor stimulation

[^{35}S] GTPγS binding measurements in membrane preparations (3 µg of protein) from transiently expressing Gs 11, the β2AR and the PTX S1 catalytic subunit, which inhibits the Gi/o family that is still expressed in Gs ko cells. Iso induced and increased of [^{35}S] GTPγS binding in DMSO preincubated membranes that was not observed when preincubating with 5 µM FR. Statistical analysis were performed with one-way ANOVA, followed by Turkey´s test; *, $p < 0.05$; ***, $p < 0.001$; ns, not significant. Data points represent means ± SEM of three independent experiments. Performed in Christa Müller´s lab with the assistance of Jan Hendrik Voß

Iso but not CCh induces conformational changes despite the presence of FR and YM.

Once GDP is released and GTP is recruited to the empty Gα subunit, a structural rearrangement occurs and dissociation of the Gαβγ heterotrimer takes place (Duc et al. 2015; Oldham und Hamm 2008). Because we have observed that nucleotide exchange is possible in Gs 11 despite the presence of FR, we hypothesized that if nucleotide exchange is possible, conformational changes in Gs 10 and Gs 11 should be detectible upon receptor activation in the presence of FR in contrast to Gq (Fig. 31). Moreover, because FR is superior to YM (Fig. 18, 19), in case of a detectable conformational change we also speculated that the magnitude of inhibition should be greater for FR than for YM.

To test these hypothesis, CRISPR/Cas9 genome-edited HEK293 cells deficient in $G\alpha_{s/olf/q/11/12/13/z}$ (ΔG_{seven}) were transiently transfected to express the BRET sensor pair Venus-tagged Gβγ and Nluc-labeled GRK3 together with (i) Gs 11 or Gs 10 along with the β2AR, or (ii) Gq and the muscarinic M3 receptor (Fig. 34A). Because ΔG_{seven} cells still express the proteins of the Gi/o family, we additionally co-expressed the PTX S1 catalytic subunit to inhibit them and thereby specifically isolate the activity of the respective overexpressed Gα proteins.

With this approach, we first needed to ascertain the precise agonist concentration to be used for our subsequent investigations on receptor induced signalling inhibition by FR and YM. Hence, increasing concentrations of either Iso, up to a concentration of 1 µM (Fig. 34B, C), or CCh, up to a concentration of 100 µM (Fig. 34D), were added to the respective cells, which triggered concentration-dependent BRET signals with diverse magnitudes and ligand potencies (Fig. 34B- D). Iso dependent activation of both Gs mutants (Fig. 34B, C) was less efficacious than activation of Gq by CCh (Fig. 34D), which was consistent with our earlier DMR data. Nevertheless, all Gα subunits were totally functionally active, so the maximum activating concentration of each Gα subunit could be determined (Fig. 34E-G).

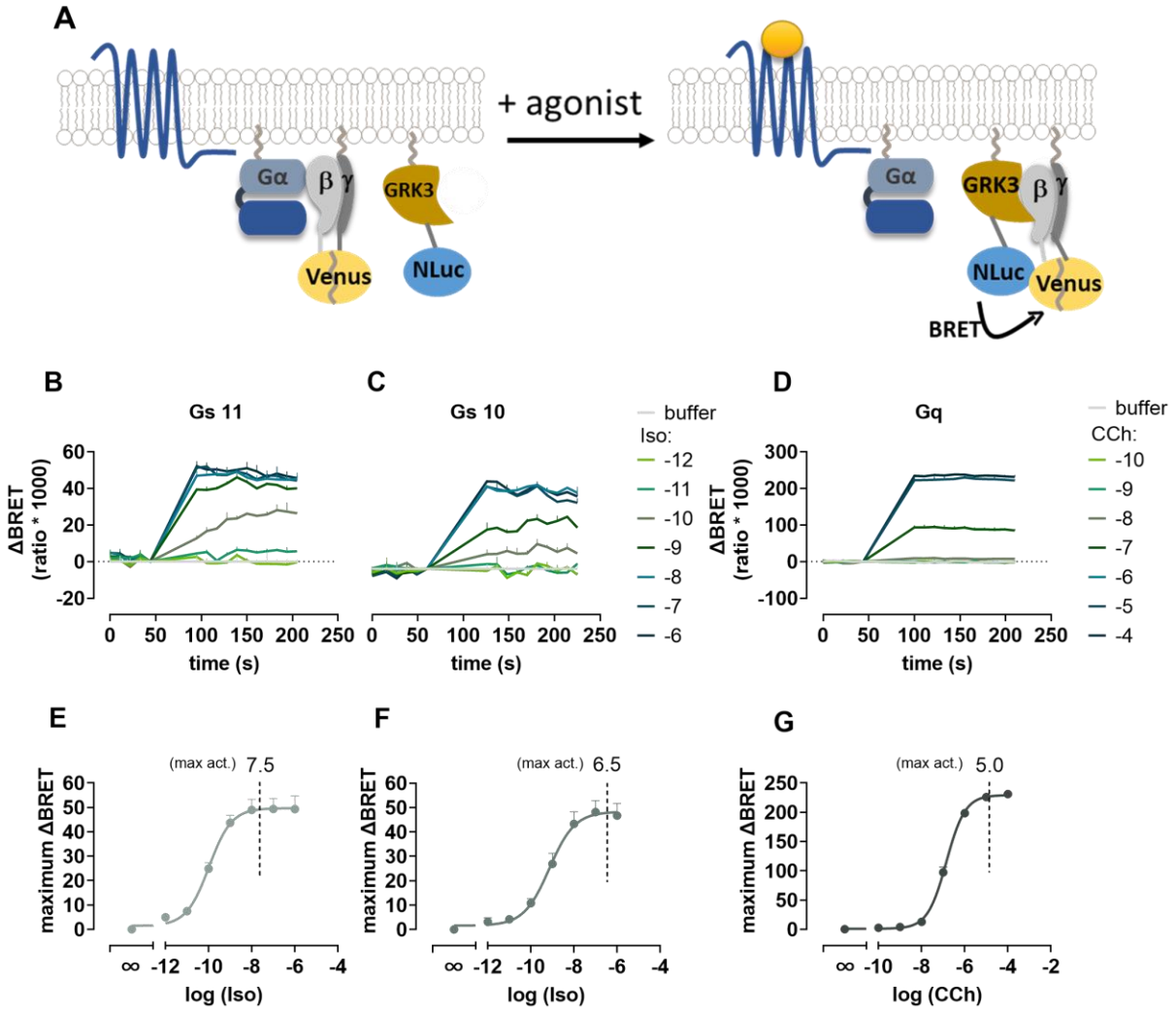

Figure 34: Iso and CCh- induces Gαβγ rearrangements in Gs 10, Gs 11 and Gq, respectively.

(A) Graphical illustration of the BRET assay that visualizes agonist-induced rearrangement of Gαβγ heterotrimers. Addition of the agonist, Iso or CCh, induces a rearrangement in the heterotrimer that approximates the Venus-tagged Gβγ to Nluc-labeled GRK3, which results in an increase of the BRET ratio that is recorded in real-time. (B-D) Representative BRET kinetics in response to Iso (B, C) or CCh (D) stimulation in ΔG_{seven} cells transiently expressing the BRET sensor pair and the PTX S1 catalytic subunit, together with the ß2AR and Gs 11 (B), the ß2AR and Gs 10 (C), or the muscarinic M3 receptor and Gq (D). (E-G) Concentration-effect curves of real-time BRET recordings, as shown in (B-D), displaying the corresponding maximum activating concentrations. Kinetic recordings are presented as mean + SEM and summarized concentration-effect relationships are means + SEM of at least three biologically independent measurements, each performed in duplicate.

As earlier discussed, we hypothesized that conformational changes and thus an activation of the Gs mutants upon receptor activation should be in the presence of FR and YM possible in contrast to Gq. To portray our hypothesis experimentally we used again the real-time BRET assay in the ΔG_{seven} cells with identical transfection conditions as previously described (Fig. 34) to test our hypotheses about FR and YM. Totally in line with our hypothesis, Gs 11 and Gs 10 expressing cells preincubated with FR and YM displayed a BRET increase over the time upon receptor activation (Fig. 35A, B) whereas no BRET increase of the sensor-pair in response to CCh was observed for cells expressing Gq (Fig. 35C). Moreover, we recognized different signalling strengths and kinetics between FR and YM. Consistent with our earlier cAMP data (Fig. 18, 19), inhibition of the BRET signal by FR was more pronounced than in the case of YM for both Gs mutants (Fig. 35A_i, B_i). In addition, activation of Gs 11 triggered by Iso was more rapid in cells preincubated with YM than in those cells that were preincubated with FR (Fig. 35A). This indicated that rearrangement of the Gs 11 heterotrimer was easier and quicker in the presence of YM than FR. Notably, these kinetic differences could not be observed in cells expressing Gs 10 (Fig. 35B) presumably because the strength of the BRET signal was lower than in cells expressing Gs 11 and, consequently, small kinetic differences were no longer clearly distinguishable.

Therefore, we concluded that FR and YM could only prevent the conformational change of their natural target Gq, but not of the artificially generated FR-sensitive Gs mutants Gs 10 and Gs 11, which underwent a Gαβγ rearrangement upon receptor stimulus.

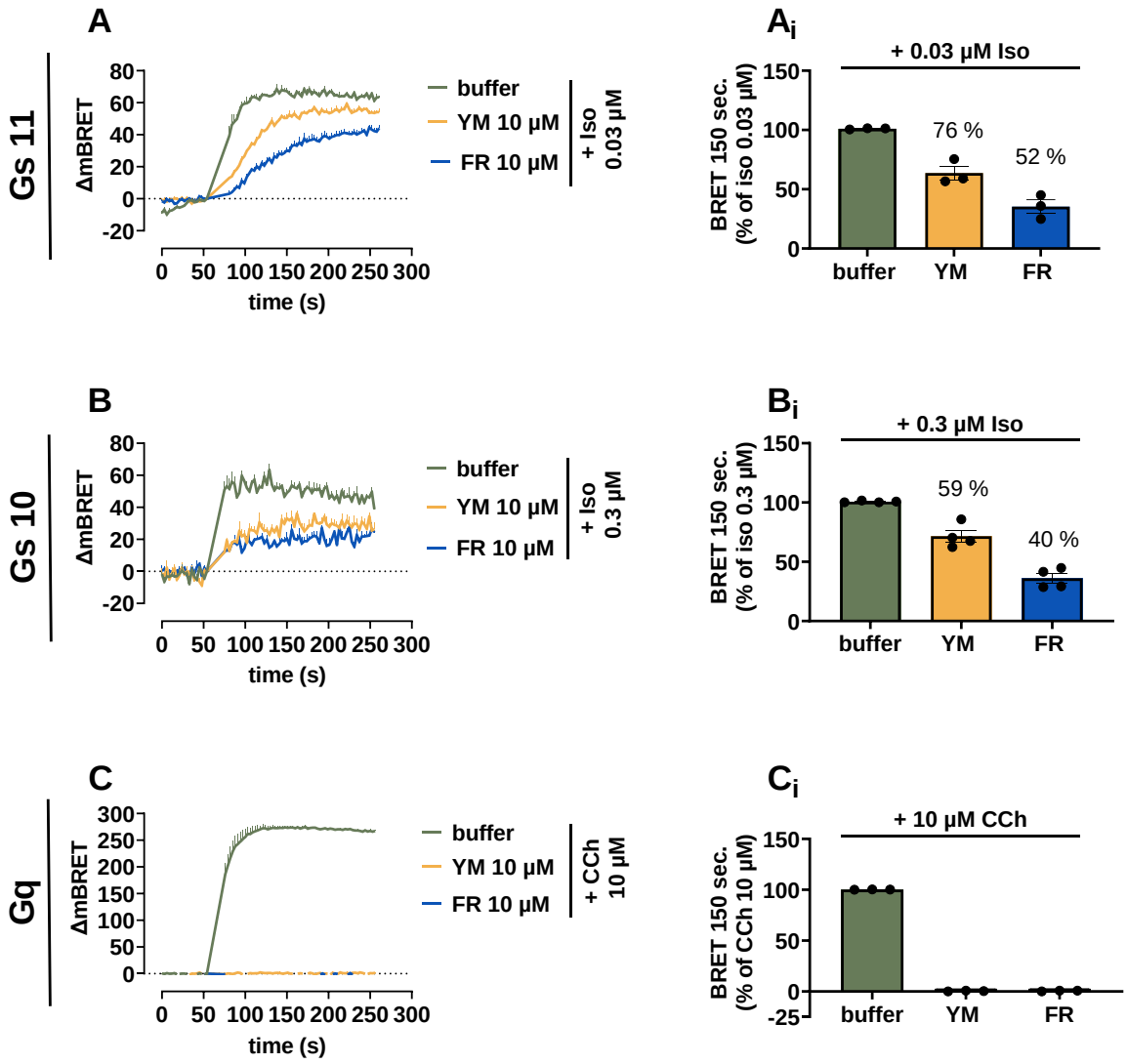

Figure 35: Iso but not CCh induces conformational changes despite FR and YM.
Real-time BRET-based G protein activation of ΔG_{seven} cells transiently expressing the BRET pair-sensor and the PTX-S1 subunit together with Gs 11 and ß2AR (A), Gs 10 and ß2AR (B) or Gq and the muscarinic M3 receptor (C). Shown are representative BRET kinetics either in response to Iso (A, B) or CCh (C) with the respective concentration-effect curves (A_i-C_i). Traces are shown as mean +SEM and summarized data are means ± SEM from at least three biologically independent experiments, each carried out in duplicates.

Discussion

Why are artificial FR-sensitive G proteins generated and what are the advantages of chemogenetic Gs proteins?

G protein-mediated signaling cascades are key regulators to a plethora of many physiological processes, including regulation of blood pressure or cell proliferation among many other vital functions (Uemura et al. 2006; Li et al. 2020; Syrovatkina et al. 2016a). Due to their involvement in various biological processes, G proteins caught the attention of the scientific community in recent years as potential targets. Consequently, identifying the responsible G protein family for a given physiological effect could contribute to close knowledge gaps.

How have been signaling pathway analyses performed so far? Designer Receptors Exclusively Activated by Designer Drugs (DREADDs) (Roth 2016; Zhu und Roth 2014; Meister et al. 2021; Atasoy und Sternson 2018), small interfering or short hairpin RNAs (Krumins und Gilman 2006), minigenes encoding C-terminal Gα peptide sequences (Gilchrist et al. 2002), dominant negative forms of Gα subunits (Barren und Artemyev 2007), and whole organism or individual cell knockouts (Wettschureck und Offermanns 2005; Schrage et al. 2015) (Schrage et al. 2015) were or are still employed to interrogate the GPCR-G protein signaling cascade. Even though those tools provided insightful results, conventional approaches based on interception of the target by chemical inhibition would provide more complementary insights into the role of proteins of interest, since they would allow biological measurements when proteins are functionally inhibited but physically intact (Schrage et al. 2015).

Indeed, the importance of physically intact proteins has recently been revealed by Lambert and co-workers (Okashah et al. 2020) showing that agonist activated GPCR activation formed complexes with specific G proteins that were not subsequently activated, an observation that they could not have made with G protein knockout cells. Moreover, they displayed that overexpressed but not activated G12 proteins reduced the AVP-induced interaction of G protein receptor kinase 2 (GRK2) and the vasopressin V_2 receptor (V2R), which consequently inhibited the V2R trafficking from the plasma membrane (Okashah et al. 2020)since phosphorylation of the V2R by GRK´s are a prerequisite for arrestin binding

and subsequent internalization (Oakley et al. 1999). The Gs signaling pathway is central to important physiological functions and consequently to many diseases thus, making it an extremely attractive target for in-depth investigations (Gold et al. 2013; Bock et al. 2020). Based on Lambert and co-worker's findings, one might wonder whether the presence of non-active Gs proteins, i.e., blocked by FR, would have a previously unknown signaling effect. If this were the case, it would be possible to identify which functions depend on Gs protein presence but not activation. Therefore, inactive Gs proteins would have an enormous advantage over e.g. knockouts.

Investigation of the Gs pathway

Utilizing cell-permeant inhibitors that specifically interact with Gs proteins would immensely contribute to unravel Gs specific signaling events. Such inhibitory properties are indeed possessed by the bacterial toxin, CTX, which freezes the $G\alpha_s$ subunit in its GTP bound state by irreversible ADP-ribosylation, thus leading to a permanent activation of the Gs protein, which is in turn uncoupled and no longer accessible for GPCR recruitment. However, despite immense contribution of CTX to understand the role of Gs proteins in biological processes (Lit. Schrage etc.), irreversible ribosylation leads rather to a maximum activation than inhibition of the Gs protein, which why these results should be interpreted with caution (Gill und Meren 1978; Seibel-Ehlert et al. 2021).

Hence, inhibitors such as the naturally occurring Gq specific cyclic depsipeptides, FR and YM, which act as guanine nucleotide dissociation inhibitors (GDI) that preserve GDP-bound heterotrimers in their inactive state, would represent more advantageous classes of inhibitors because they would interfere with the G protein when it is necessary, thus firstly allowing its activation by specific GPCRs and then its subsequent inhibition (Schrage et al. 2015; Malfacini et al. 2019). Thus, for example, using this strategy, Pfeil et al. recently reported that Gi-Gßy-Ca^{2+} signaling requires the presence of active Gq by showing that in the presence of FR no Ca^{2+} signals were elicited (Pfeil et al. 2020). This study largely depended on the use of the specific G protein inhibitors PTX and FR, alone or in combination, to reveal the hierarchical control of Gq for Gi-GPCR triggered Ca^{2+} signaling via PLCβ enzymes. Likewise, it could be envisaged that a specific Gs protein inhibitor could

allow to investigate whether Gs coupled GPCRs are also under hierarchical control by Gq. The possibility of inhibiting individual components could open up new crosstalk mechanisms or could even contribute to discover non-canonical Gs effects. However, to date, such G protein modulators for Gs do not exist and moreover, despite intense efforts (Kaur et al. 2015b; Reher et al. 2018a; Reher et al. 2018b; Rensing et al. 2015a; Zhang et al. 2017b), no single FR or YM analog could be developed with altered Gα specificity profiles apart from Gq, G11, and G14 (Zhang et al. 2018b; Taniguchi et al. 2004a), suggesting that rational design of such molecules may be more demanding than generally anticipated (Nishimura et al. 2010b; Xiong et al. 2016; Schrage et al. 2015) (Malfacini et al. 2019).

An additional strategy to bypass the lack of such inhibitors is to engineer Gα proteins with artificial sensitivity toward FR and YM via transplanting the inhibitor binding site. Based on this approach, pharmacological control over, Gi, G16 and Gs by FR/YM scaffolds could be achieved by exchanging their corresponding residues with the equivalent depsipeptide binding site in Gq (Onken et al. 2018; Malfacini et al. 2019; Boesgaard et al. 2020). Thus, following this strategy, fully functional inhibitor sites for FR/YM have been achieved by swapping a total of eight residues in Gi (Onken et al. 2018), five residues in G16 (Malfacini et al. 2019), and eleven residues in Gs (Boesgaard et al. 2020) for the equivalent Gq amino acids to stabilize the inactive state and hamper the nucleotide exchange. These comprehensive studies have provided guidance for the rational design of FR mimics, demonstrated by the modelled interactions between FR and the mutated Gs, G16 and Gi-proteins that accommodate engineered FR binding sites. However, the possibility to study signaling pathway specific events in detail by utilizing these artificially generated FR-sensitive G proteins, particularly for Gs, has to be demonstrated.

Gs mutants; models for further chemogenetic tools.

As mentioned above Boesgaard et al. addressed the question of whether the rational design of an artificially generated FR-sensitive Gs protein is possible. Based on their study, the main goal of our investigation was to analyze whether their artificially generated FR-sensitive Gs proteins could be suitable for pathway analysis.

Such tools have to follow certain rules, such as a wildtype like behavior to preserve the cellular environment and signaling events that are intended to be studied. It turned out that

the complete shift of the inhibitor binding site, which means a change of 11 positions in the Gs protein, causes a strong basal activity similar to that of the oncogene R201C (Fig. 5) and that restoring leucine at position 189 (Gs 10) reduced the basal activity tremendously (Fig. 9). We performed a comprehensive study by testing the chemogenetic Gs proteins under different inhibitory conditions. Starting with the distinction between inhibition of basal and acute activity, we found that regardless of their basal activity, both Gs 10 (Fig. 10) and Gs 11 (Fig. 11) expressing cells completely inhibit basal activity in the presence of FR. Such a result suggests that these FR-sensitive Gs proteins could serve as a model to analyze constitutively active Gs pathways, since severe biological effects are known to arise when G proteins became overactive. Thus, basally active G proteins have been associated with cancer or endocrine disorders, such as the oncogene Gs R201C, which leads to constitutive activation of Gs and substantial increase of adenylate cyclase activity and therefore an autonomous synthesis of cAMP resulting e.g., in tumor growth (Wilson et al. 2010),or the Gs A366S mutation, which causes an accelerated GDP dissociation in the testis that leads to autonomous production of testosterone (Iiri et al. 1998; Majumdar et al. 2004). Therefore, pathophysiological events whose origin is unknown and have not been associated with increased Gs activity could be identified by expressing FR-sensitive Gs proteins in specific cell or animal models. Because of the enormously high basal activity of Gs 11, Gs 10 would be expected to be more suitable for such approaches than Gs 11.

Limitations of FR-sensitive Gs proteins.

Although we observed that FR successfully facilitated inhibition of basal activity in cells expressing both Gs 10 and Gs11, we found that acute activation of the pathway could only be partially inhibited, depending on the quality of stimulation. This finding was novel and has not been previously discussed in the literature in relation to the described constructs. Thus, we observed that by challenging with a maximum stimulating concentration of agonist in the presence of a high receptor density (overexpression), the acute activation of the signaling pathway could not be completely inhibited by FR. More specifically, we observed that despite high FR concentrations, such as 10 or 30 µM, cAMP accumulation (Fig. 15, 17), mass redistribution (Fig. 25), nucleotide exchange (Fig. 33) and conformational changes

(Fig. 35) were still possible, in contrast to the natural FR target Gq. Consequently, and contrary to the findings previously described in the literature, we observed that both FR-sensitive Gs mutants could be transferred to the active state in the presence of FR. This occurred because FR could not trap the Gs protein in its GDP-bound form. Thus, our results i) define for the scientific community experimental conditions for the FR-sensitive Gs protein that can be considered as a guideline for the use of the chemogenetic Gs protein such as investigations in which endogenous receptor levels are required to draw conclusions for certain physiological context and ii) show that the simple transfer of the inhibitor binding site is obviously not sufficient for the rational design of an artificially FR-sensitive Gs protein with identical inhibition profiles as the natural FR target Gq. Moreover, our results indicate that the potential design of FR scaffold-based inhibitors that merely mimic the interaction of FR with the engineered FR-binding site in Gs proteins may therefore be insufficient to perform studies on the same scale as would be possible with Gq.

Approaches for further development of FR-sensitive Gs proteins.

One publication that provided a basis for possible further developments of chemogenetic FR-sensitive Gs proteins was the recent investigation by Jan H. Voss and Christa Müller. In their study, the aim of which was to unravel the binding mechanism and kinetics of macrocyclic Gq protein inhibitors, they provided insight about recently discovered divergent residence times of radiolabeled FR and YM. Using molecular dynamic simulations, they analyzed the structural differences associated with the presence of bound inhibitors. They observed that by binding of both inhibitors, FR and YM, two Gq exclusive amino acids, E119 and K120, localized in the loop between the helix B and helix C in the αH domain, exhibited the greatest entropy increase suggesting that these positions could be important for the inhibitory effect and thus related to the stabilizing impact of the inhibitors that prevents the domain separation between the αH and RasD domains of Gq (Voss et al. 2021). In our study, we clearly show that these two residues have no further positive impact on the inhibitory effect of FR, because the mutagenesis results of our analysis revealed that none of the new introduced Gq exclusive residues showed a superior inhibitory effect upon activation of an overexpressed and maximum activated receptor (Fig. 28).

Consequently, the lack of inhibition despite the presence of the FR-binding site suggests that FR and YM may form distinct interactions within Gq and Gs heterotrimers thus affecting GDP release.

Different hypotheses exist how GPCRs mediate G protein activation since cytoplasmic loops of many GPCRs are too short to touch Gα near its guanine nucleotide binding pocket to cause “directly” a nucleotide exchange (Bohm et al. 1997). Dror et al. suggested that Gα domain separation is necessary to provide an exit pathway for nucleotide exchange however, a separation alone is not enough for GDP release. Activated receptors promote conformational changes in the Ras domain, predominantly in the C-terminal α5 helix. Hence, an α5 movement shifts the β6- α5 loop away from the guanine ring of GDP, thereby weakening the interaction between GDP and the Ras domain, and permitting GDP to escape, once the Gα domains separate spontaneously (Dror et al. 2015). Since α5 presumably initiates the GDP release, it is might be possible that FR may prevent the movement of α5 in Gq but not in Gs 10 or in Gs 11. Although no direct interaction between α5 and FR is observed, indirect interactions could be possible that may allow the movement of the α5 helix, depending on the G protein family. Contrary to the hypothesis that Gα domain separation occurs spontaneously numerous publications propose that GPCRs use Gβy as a lever (“lever theory”) to open the guanine binding pocket and provide an exit path for GDP from the binding pocket (Iiri et al. 1998; Rondard et al. 2001; Singh et al. 2012; Majumdar et al. 2004). Nishimura et al. has depicted potential interactions between YM and the Gβ subunit (Nishimura et al. 2010a) and a dissertation from Desiree Kaufmann in 2019 (Technical University of Darmstadt), focusing on understanding the mechanism of action of FR and YM, proposed possible interactions between FR and the Gβ subunit. Thus, considering the “lever theory”, it is may possible that FR and YM in complex with the Gs mutants may form fewer stabilizing interactions with the proposed Gβ residues than in complex with Gq, allowing Gβy as a lever to pry open the nucleotide binding pocket for GDP release (Iiri et al. 1998; Majumdar et al. 2004). Thus, it may be possible that with increased receptor presence and activity, the β2AR may be capable to engage the Gβy subunit since stabilizing effects could miss between FR and the Gs mutants in contrast to Gq due to different protein dynamics. Therefore, fewer stabilizing interactions which could have a significant impact on the inhibitory power would consequently explain the lack of total inhibition upon maximum activation of an overexpressed receptor

Inhibition by FR is dependent on signal amplification.

As mentioned above, we observed that FR inhibited the Gs-mutant receptor-induced signaling either completely or partially, depending on agonist concentration and receptor density. Moreover, we also noticed that besides of agonist concentration and receptor presence, the extent of inhibition was also readout dependent. Thus, in cells expressing Gs 10 and Gs 11 together with the endogenous β2AR, DMR responses could not be completely inhibited (Fig. 26) whereas cAMP production could be successfully blunted despite comparable conditions (Fig. 15E & 17A). These results suggest that the more downstream the analyses were performed in the signaling cascade, the lower FR's inhibitory power turned out to be, since cAMP production is further upstream compared to cell mass redistribution. This observation is in line with previous reports that indicated that ligand efficacy, and consequently signaling, is significantly enhanced distal from receptor activation within the cell (Schrage et al. 2016; Colabufo et al. 2008). Such signal amplification upon receptor activation is depicted in figure 36. Consequently, this finding is highly relevant and needs to be considered when using Gs chemogenetics to unravel Gs specific physiological events.

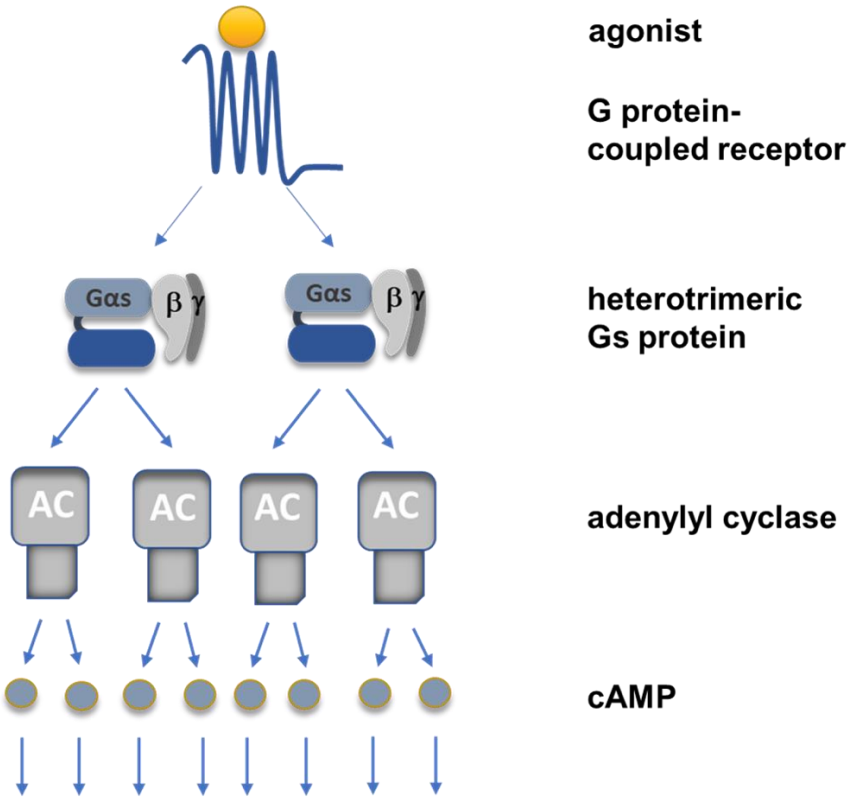

Figure 36: Signal amplification within signal pathway. Graphical illustration of cellular amplification initiated by the activation of a GPCR. As depicted a stimulated GPCR may activate more than one G protein, which can activate more than one membrane bound adenylyl cyclase isoforms (AC). ACs, in turn, catalyze the production of numerous molecules of cAMP and cAMP, in turn, binds to its effector and contributes to shaping the cellular response. Illustration adapted from Schrage et. al 2017.

Inhibition mediated by FR is superior to that by YM

In all tested conditions when analyzing the artificially FR/YM- sensitive Gs protein, we observed that FR was superior to YM. For example, we found that 30 µM FR, but not YM, was able to blunt cAMP signaling entirely upon activation of the overexpressed β2AR with an 80 % stimulating agonist concentration (Fig. 19). These findings are in line with previous observations of our group that showed that although FR and YM share a common mechanism of action by capturing the G protein in its GDP-bound form, inhibition of Gq proteins by FR and YM is distinct. Thus, Malfacini et al. observed that it was more difficult to perturb Gq inhibition with FR than with YM, as well as easier to trigger FR inhibition onto

a G16, engineered with artificial FR/YM sensitivity, than with YM (Malfacini et al. 2019). These differences are most likely due to the three additional methyl groups of FR (highlighted in yellow in figure 37) that are not present in YM.

Altogether, our data suggest that FR may be more ideal than YM as a potential scaffold for the successful design and development of specific inhibitors targeting FR insensitive Gα subunits.

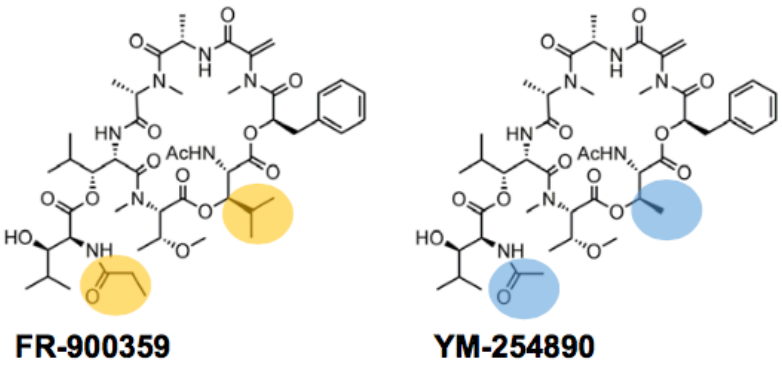

Figure 37: Structure of FR-900359 and YM-254890. Structural differences of FR and YM highlighted in yellow or blue, respectively.

A crucial residue that provides an easier exchangeable state for guanine nucleotides

Lowering the basal signaling of Gs 11 by restoring a single Gs WT residue, leucine at position 189, raises the question of how such an enormous difference in basal activity is possible from a single change. Even though the elevated basal signaling of Gs 11 hardly affects the inhibitory efficacy of FR and YM, these data provide interesting insights into G protein activation and function, thus contributing to understand which factors and structural changes within G proteins impair the kinetics of nucleotide exchange.

It is known that the flexibility of linker I and linker II, two interdomain linkers which connect the GTPase and the helical domains, regulates the GDP release rate of Gα by acting as a hinge during the opening process, when the helical domain moves away from the GTPase domain (Taniguchi et al. 2003; Taniguchi et al. 2004a; Nishimura et al. 2010a; Majumdar et

al. 2004). Therefore, it is not surprising that alterations in the linker region, such as the L189P mutation that is located in linker II, affects the nucleotide exchange rate, although it is initially surprising that a single modification has such an effect on basal signaling. However, Majumdar et al. have reported that perturbing the linker regions of transducin with a single mutation, either within linker I or II by mutating each glycine to a proline (G56P-linker I- or G179P-linker II) led to a more readily exchangeable state (Majumdar et al. 2004). This is totally in line with our results since the substitution of lysine to a proline within linker II enhanced the basal activity and thus the tendency to accelerate the nucleotide exchange. Cerione and co-workers hypothesized that the proline substitutions decrease the flexibility and, consequently, enhance the rigidity of the linkers, which causes an open state that facilitates an easier GDP release. They also suggested that glycine, lacking a side chain, displays the greatest conformational flexibility (Majumdar et al. 2004). Thus, it may be possible that proline, with its pyrrolidine ring, is less flexible than both glycine and leucine, which traps Gs 11 in an open state that leads to an increased basal rate of GDP/GTP exchange.

Later, the same group provided insights into the mechanism of G protein activation with the previously generated constitutively active Gα subunit (G56P). They observed that two amino acid residues interacted differently with GDP in the X-ray structure of G56P as compared to wild-type. First, Arg174 (positions belong to transducin), which is normally hydrogen-bonded to the α and β oxygens of the phosphate groups of GDP, appeared to interact differently. Interestingly, akin changes were observed for the corresponding residue (Arg178) of the Gi1 mutant T329A, which is known for its increased spontaneous GDP/GTP exchange as compared with Gi1 WT (Singh et al. 2012; Kapoor et al. 2009). Second, Lys266, which supports stabilization of the guanine ring of GDP through hydrogen bonds and hydrophobic interactions, undergoes weaker interactions with GDP suggesting that differences between Arg174 and GDP or Lys266 and GDP interactions contributes to a more rapid GTP/GTP exchange in constitute active G proteins (Singh et al. 2012).

Overall, even if the mentioned specific residues, which have an impact on the GDP release, do not match with Gs 11, both, the data from the literature and our own data provide insights regarding factors that might influence the kinetics of nucleotide exchange, a process which is normally tightly regulated. This knowledge could consequently help us in our search for

suitable non-Gq protein modulators. Thus, pharmacological agents that stabilize the interaction with the guanine ring of GDP, as above mentioned, could be used as inhibitors that prevent nucleotide exchange, such as FR and YM. Conversely, design of ligands that specifically promote the nucleotide exchange would allow to study G protein pathways that are able to induce GPCR-independent nucleotide exchange versus those G proteins that are constitutively active because of their GTPase deficiency. For example, studies performed on Cdc42-GTP-binding proteins have showed that constitutively active mutants that were still able to hydrolyze GTP had much stronger effects on cell growth and transformation than those mutants that were constitutively active due to their inability to catalyze GTP hydrolysis (Majumdar et al. 2004; Lin et al. 1997). Thus, cellular responses of G proteins, especially of Gα mutants with constitutive activity, could be thoroughly examined.

Biphasic inhibition pattern- a Gq dependent phenomenon.

Boesgaard et al. created several mutants in addition to Gs 11 and Gs 10 by restoring amino acids naturally occurring in Gs WT. Thus, one of their goals was to determine how many mutations in the Gs protein are required to achieve FR sensitivity. According to their results, four of the mutants displayed high-potency partial inhibition and different four mutants showed a biphasic inhibition pattern, whereas Gs 11 and Gs 10 showed total inhibition of agonist response in a normal monophasic fashion. However, our analyses showed that depending on the cellular background, biphasic inhibition pattern occurs also in the presence of Gs 11 and Gs 10 expressing cells (Fig. 10 & 11). We displayed both in the present study and in the recently published work by our group (Patt et al.) that biphasic inhibition patterns are rather a cellular background dependent than a mutant dependent phenomenon. Thus, the presence of endogenous expressed Gq in Gs ko cells causes the first inflection point since all Gq dependent signals affect or enhance cAMP formation, which could be unmasked by FR, whereas the second inflection point around 1 µM represents the inhibition of Gs dependent signaling (Patt et al. 2021). The graphical illustration (Fig.38) shows this crosstalk between both pathways and how FR prevents the stimulating impact of Gq dependent components on AC isoforms that result in a decrease in cAMP accumulation.

Therefore, this extremely relevant information needs to be considered when using artificially generated FR-sensitive Gα subunits. Thus, studies would need to be performed either in the absence of Gq or in the presence of FR-insensitive Gq mutants to preserve the physiological conditions. On the other hand, neither is necessary as long as biphasic inhibition curves are tolerated and do not interfere with the question of interest.

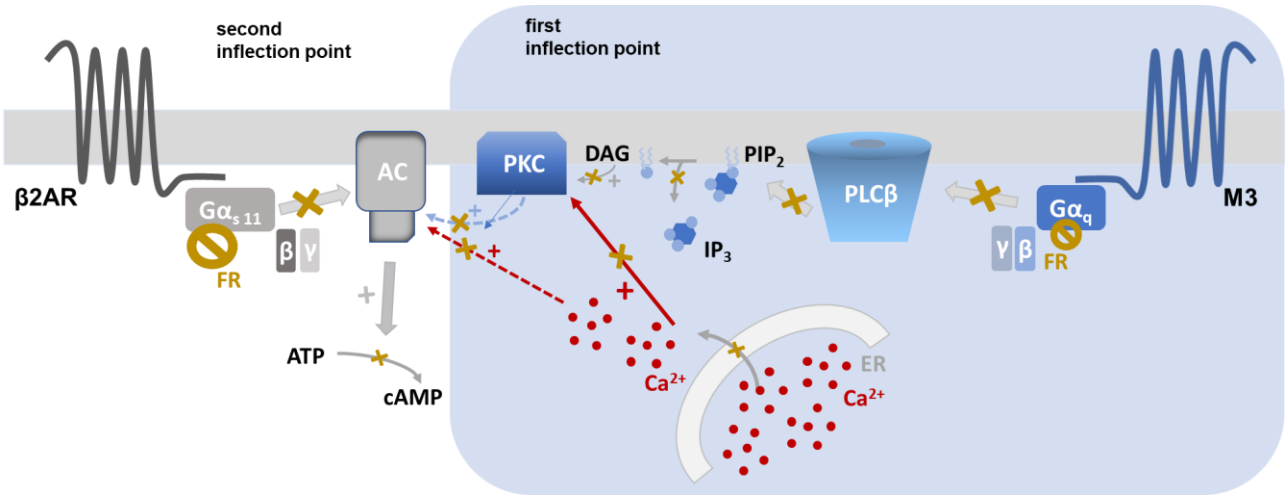

Figure 38: Biphasic inhibition pattern- a Gq dependent phenomenon. Graphical illustration of Gq contribution (right panel) to cAMP production. Red arrows with red "+" display respective positive effect on target structures. Ochre symbols represent FR targets along with the resulting inhibition effects, showed as ochre colored "x". Right panel: Gq dependent Ca^{2+} release, triggered upon inositol trisphosphate (IP_3) binding of IP_3-receptors (IP_3Rs) located in the endoplasmic reticulum (ER), sensitizes both adenylyl cyclase (AC) calcium-sensitive isoforms and membrane bound protein kinase C (PKC) along with diacyl glycerol (DAG), which in turn also activates AC isoforms. Left panel: Gs 11 dependent cAMP production via activation of AC isoforms which in turns convert ATP to cAMP. FR prevents stimulating impact of Gq dependent components on AC isoforms resulting in a decrease in cAMP accumulation.

Significance for the Gs signaling pathway.

Since 30% of FDA-approved drugs target GPCRs, G protein inhibitors, which block signaling downstream of GPCRs, are emerging as a potential basis for therapeutical tools (Annala et al. 2019; Kostenis et al. 2020; Klepac et al. 2016). FR has shown promising results in studies on cancer (Annala et al. 2019) and asthma (Matthey et al. 2017) among others. Therefore, the development of appropriate chemogenetic Gs proteins or even Gs inhibitors, based on Gs 10, and our additional provided information could help to unravel Gs linked diseases and thus in developing new treatment options.

Conclusion

In conclusion, it is undeniably that FR-sensitive Gs proteins can be created by an artificially generated inhibitor binding site, yet i) our study has provided experimental evidence that the simple transfer of the inhibitor binding site is not sufficient to carry over the properties of FR´s natural target Gq. Therefore, ii) further studies need to be done to understand why FR, despite excellent binding, cannot inhibit Gs signaling under all circumstances. We assume that iii) additional parameters beyond the direct FR epitopes need to be considered to successfully unlock inhibition of Gs. Finally, iv) we concluded that FR may be preferred over YM as scaffold in the search for specific and potent modulators targeting Gs.

Summary

G protein-mediated signaling cascades are key regulators of a variety of physiological processes, such as regulation of blood pressure or cell proliferation among many other vital functions. These cascades must function orthodoxly to ensure a controlled cellular response, otherwise pathological changes with corresponding diseases are inevitable. Considering their influence on our bodies, thorough investigations of these cascades are an important step to define their influences or contributions to specific cellular events. Such in depth studies could be performed using specific G protein inhibitors to discriminate individual signaling cascades. To date, only specific inhibition of Gi and Gq could be achieved by PTX and FR900359 (FR) / YM-25489 (YM), respectively. Creating new inhibitors or modifying available inhibitors to abrogate the signaling pathway of the two leftover G proteins, Gs and G12/13 was despite intense efforts abortively yet.

Interestingly, it has recently been reported the generation of a Gs protein, named Gs 11, which selectively interact with FR by introducing 11 amino acid replacements within the putative FR binding site. Our group suggested that Gs 11 could be instrumentalized in defining and analyzing the contribution of Gs proteins to biological processes. However, it has been reported that Gs 11 is catalytically more active than Gs WT, a feature that could affect the performance of Gs 11 towards signaling inhibition by FR and YM. Indeed, our results revealed that basal signaling of Gs 11 is as high as that of the oncogene Gs R201C, which results in elevated intracellular cAMP levels. Thus, we concluded that Gs 11 might not be an ideal designed tool for Gs pathway investigations.

Reducing the amino acid replacements by restoring a single Gs WT residue lowered the basal signal of Gs 11 tremendously. The resulting FR-sensitive mutant, termed Gs 10, was expressed in CRISPR/Cas9-generated $G\alpha_{s}$-null and $G\alpha_{s/olf/q/11/12/13/z}$ -null cells and different cutting-edge tools, such as label-free whole-cell biosensing, HTRF based cAMP accumulation and real-time BRET-based G protein activation assay systems were used to test the suitability of Gs 10 as a potential chemogenetic tool, an approach in which engineered molecules interact with previously unrecognized molecules. Surprisingly, we observed that despite the transfer of the inhibitor binding site, the inhibitory properties of FR could not be entirely transmitted to Gs 10 as well as to Gs 11. Thus, even though both

mutants bind FR and YM with the same nanomolar affinity as observed for Gq WT the reengineered inhibitor binding site was not fully functional. Gq signaling events were completely abolished by FR, whereas partial inhibition for Gs 10 and Gs 11 expressing cells were observed when β2ARs are highly abundant and exposed to high concentrations of Iso. Therefore, we concluded that the simple transfer of the FR binding site is not sufficient to carry on similar inhibitory properties, proposing that further interventions beyond the direct FR epitope need to be considered. In order to overcome this, we tried to enhance the inhibitory effect of FR by introducing into the artificial FR-sensitive Gs proteins two additional Gq exclusive amino acid residues (E119 &K120) that have been reported to undergo the greatest entropy change upon FR binding, thus suggesting the importance of both residues in providing proper inhibition. Surprisingly, none of the proposed residues improved FR´s inhibitory efficacy.

In conclusion, our study expands our general understanding of G protein activation and inhibition by demonstrating the uniqueness of each individual G protein family since although they share an identical inhibitor binding site, only Gq, but not Gs 10 and Gs 11, can be fully inhibited by FR. Clearly, further investigations are needed to better understand the mechanism of FR inhibition in artificial Gα proteins to, consequently i) generate new chemogenetic tools with more pronounced inhibition profiles and ii) FR scaffold-based inhibitors which successfully unlock inhibition of Gs besides the Gq family.

References

Alberts, Bruce (2015): Molecular biology of the cell (6th ed.). Sixth edition. New York, NY: Garland Science, Taylor and Francis Group.

Annala, Suvi; Feng, Xiaodong; Shridhar, Naveen; Eryilmaz, Funda; Patt, Julian; Yang, JuHee et al. (2019): Direct targeting of Gα(q) and Gα(11) oncoproteins in cancer cells. In: *Science signaling* 12 (573). DOI: 10.1126/scisignal.aau5948.

Ashcroft, S. J. (1997): Intracellular second messengers. In: *Advances in experimental medicine and biology* 426, S. 73–80. DOI: 10.1007/978-1-4899-1819-2_9.

Atasoy, Deniz; Sternson, Scott M. (2018): Chemogenetic Tools for Causal Cellular and Neuronal Biology. In: *Physiological reviews* 98 (1), S. 391–418. DOI: 10.1152/physrev.00009.2017.

Ayoub, Mohammed Akli; Damian, Marjorie; Gespach, Christian; Ferrandis, Eric; Lavergne, Olivier; Wever, Olivier de et al. (2009): Inhibition of heterotrimeric G protein signaling by a small molecule acting on Galpha subunit. In: *The Journal of biological chemistry* 284 (42), S. 29136–29145. DOI: 10.1074/jbc.M109.042333.

Barren, Brandy; Artemyev, Nikolai O. (2007): Mechanisms of dominant negative G-protein alpha subunits. In: *Journal of neuroscience research* 85 (16), S. 3505–3514. DOI: 10.1002/jnr.21414.

Bock, Andreas; Annibale, Paolo; Konrad, Charlotte; Hannawacker, Annette; Anton, Selma E.; Maiellaro, Isabella et al. (2020): Optical Mapping of cAMP Signaling at the Nanometer Scale. In: *Cell* 182 (6), 1519-1530.e17. DOI: 10.1016/j.cell.2020.07.035.

Boesgaard, Michael W.; Harpsøe, Kasper; Malmberg, Michelle; Underwood, Christina R.; Inoue, Asuka; Mathiesen, Jesper M. et al. (2020): Delineation of molecular determinants for FR900359 inhibition of G(q/11) unlocks inhibition of Gα(s). In: *The Journal of biological chemistry* 295 (40), S. 13850–13861. DOI: 10.1074/jbc.RA120.013002.

Bohm, A.; Gaudet, R.; Sigler, P. B. (1997): Structural aspects of heterotrimeric G-protein signaling. In: *Current opinion in biotechnology* 8 (4), S. 480–487. DOI: 10.1016/s0958-1669(97)80072-9.

Cassel, D.; Pfeuffer, T. (1978): Mechanism of cholera toxin action: covalent modification of the guanyl nucleotide-binding protein of the adenylate cyclase system. In: *Proceedings of the National Academy of Sciences of the United States of America* 75 (6), S. 2669–2673. DOI: 10.1073/pnas.75.6.2669.

Chakraborty, M.; Chatterjee, D.; Kellokumpu, S.; Rasmussen, H.; Baron, R. (1991): Cell cycle-dependent coupling of the calcitonin receptor to different G proteins. In: *Science (New York, N.Y.)* 251 (4997), S. 1078–1082. DOI: 10.1126/science.1847755.

Colabufo, Nicola Antonio; Abate, Carmen; Contino, Marialessandra; Inglese, Carmela; Ferorelli, Savina; Berardi, Francesco; Perrone, Roberto (2008): Tritium radiolabelling of PB28, a potent sigma-2 receptor ligand: pharmacokinetic and pharmacodynamic characterization. In: *Bioorganic & medicinal chemistry letters* 18 (6), S. 2183–2187. DOI: 10.1016/j.bmcl.2007.12.056.

Cooper, D. M.; Mons, N.; Karpen, J. W. (1995): Adenylyl cyclases and the interaction between calcium and cAMP signalling. In: *Nature* 374 (6521), S. 421–424. DOI: 10.1038/374421a0.

Cooper, Geoffrey M. (2000): The cell. A molecular approach. 2. ed. Washington, DC, Sunderland, Mass.: ASM Press; Sinauer Associates.

Dorsam, Robert T.; Gutkind, J. Silvio (2007): G-protein-coupled receptors and cancer. In: *Nature reviews. Cancer* 7 (2), S. 79–94. DOI: 10.1038/nrc2069.

Dror, Ron O.; Mildorf, Thomas J.; Hilger, Daniel; Manglik, Aashish; Borhani, David W.; Arlow, Daniel H. et al. (2015): SIGNAL TRANSDUCTION. Structural basis for nucleotide exchange in heterotrimeric G proteins. In: *Science (New York, N.Y.)* 348 (6241), S. 1361–1365. DOI: 10.1126/science.aaa5264.

Druey, Kirk M. (2009): Regulation of G-protein-coupled signaling pathways in allergic inflammation. In: *Immunologic research* 43 (1-3), S. 62–76. DOI: 10.1007/s12026-008-8050-0.

Duc, Nguyen Minh; Kim, Hee Ryung; Chung, Ka Young (2015): Structural mechanism of G protein activation by G protein-coupled receptor. In: *European journal of pharmacology* 763 (Pt B), S. 214–222. DOI: 10.1016/j.ejphar.2015.05.016.

Escriva, H.; Delaunay, F.; Laudet, V. (2000): Ligand binding and nuclear receptor evolution. In: *BioEssays : news and reviews in molecular, cellular and developmental biology* 22 (8), S. 717–727. DOI: 10.1002/1521-1878(200008)22:8<717::AID-BIES5>3.0.CO;2-I.

Freissmuth, M.; Boehm, S.; Beindl, W.; Nickel, P.; Ijzerman, A. P.; Hohenegger, M.; Nanoff, C. (1996): Suramin analogues as subtype-selective G protein inhibitors. In: *Molecular pharmacology* 49 (4), S. 602–611.

Fujioka, Mamoru; Koda, Shigetaka; Morimoto, Yukiyoshi; Biemann, Klaus (1988): Structure of FR900359, a cyclic depsipeptide from Ardisia crenata sims. In: *J. Org. Chem.* 53 (12), S. 2820–2825. DOI: 10.1021/jo00247a030.

Gilchrist, Annette; Li, Anli; Hamm, Heidi E. (2002): G alpha COOH-terminal minigene vectors dissect heterotrimeric G protein signaling. In: *Science's STKE : signal transduction knowledge environment* 2002 (118), pl1. DOI: 10.1126/stke.2002.118.pl1.

Gill, D. M.; Meren, R. (1978): ADP-ribosylation of membrane proteins catalyzed by cholera toxin: basis of the activation of adenylate cyclase. In: *Proceedings of the National Academy of Sciences of the United States of America* 75 (7), S. 3050–3054. DOI: 10.1073/pnas.75.7.3050.

Gold, Matthew G.; Gonen, Tamir; Scott, John D. (2013): Local cAMP signaling in disease at a glance. In: *Journal of cell science* 126 (Pt 20), S. 4537–4543. DOI: 10.1242/jcs.133751.

Haan, Lolke de; Hirst, Timothy R. (2004): Cholera toxin: a paradigm for multi-functional engagement of cellular mechanisms (Review). In: *Molecular membrane biology* 21 (2), S. 77–92. DOI: 10.1080/09687680410001663267.

Harrison, C.; Traynor, J. R. (2003): The 35SGTPgammaS binding assay: approaches and applications in pharmacology. In: *Life sciences* 74 (4), S. 489–508. DOI: 10.1016/j.lfs.2003.07.005.

Hauser, Alexander S.; Attwood, Misty M.; Rask-Andersen, Mathias; Schiöth, Helgi B.; Gloriam, David E. (2017): Trends in GPCR drug discovery: new agents, targets and indications. In: *Nature reviews. Drug discovery* 16 (12), S. 829–842. DOI: 10.1038/nrd.2017.178.

Ho, S. N.; Hunt, H. D.; Horton, R. M.; Pullen, J. K.; Pease, L. R. (1989): Site-directed mutagenesis by overlap extension using the polymerase chain reaction. In: *Gene* 77 (1), S. 51–59. DOI: 10.1016/0378-1119(89)90358-2.

Hu, Qi; Shokat, Kevan M. (2018): Disease-Causing Mutations in the G Protein Gαs Subvert the Roles of GDP and GTP. In: *Cell* 173 (5), 1254-1264.e11. DOI: 10.1016/j.cell.2018.03.018.

Hurley, J. H. (1999): Structure, mechanism, and regulation of mammalian adenylyl cyclase. In: *The Journal of biological chemistry* 274 (12), S. 7599–7602. DOI: 10.1074/jbc.274.12.7599.

Iiri, T.; Farfel, Z.; Bourne, H. R. (1998): G-protein diseases furnish a model for the turn-on switch. In: *Nature* 394 (6688), S. 35–38. DOI: 10.1038/27831.

Kapoor, Neeraj; Menon, Santosh T.; Chauhan, Radha; Sachdev, Pallavi; Sakmar, Thomas P. (2009): Structural evidence for a sequential release mechanism for activation of heterotrimeric G proteins. In: *Journal of molecular biology* 393 (4), S. 882–897. DOI: 10.1016/j.jmb.2009.08.043.

Katada, T.; Ui, M. (1982): Direct modification of the membrane adenylate cyclase system by islet-activating protein due to ADP-ribosylation of a membrane protein. In: *Proceedings of the National Academy of Sciences of the United States of America* 79 (10), S. 3129–3133. DOI: 10.1073/pnas.79.10.3129.

Katritch, Vsevolod; Fenalti, Gustavo; Abola, Enrique E.; Roth, Bryan L.; Cherezov, Vadim; Stevens, Raymond C. (2014): Allosteric sodium in class A GPCR signaling. In: *Trends in biochemical sciences* 39 (5), S. 233–244. DOI: 10.1016/j.tibs.2014.03.002.

Kaur, Harveen; Harris, Paul W. R.; Little, Peter J.; Brimble, Margaret A. (2015a): Total synthesis of the cyclic depsipeptide YM-280193, a platelet aggregation inhibitor. In: *Organic letters* 17 (3), S. 492–495. DOI: 10.1021/ol503507g.

Kaur, Harveen; Harris, Paul W. R.; Little, Peter J.; Brimble, Margaret A. (2015b): Total synthesis of the cyclic depsipeptide YM-280193, a platelet aggregation inhibitor. In: *Organic letters* 17 (3), S. 492–495. DOI: 10.1021/ol503507g.

Klepac, Katarina; Kilić, Ana; Gnad, Thorsten; Brown, Loren M.; Herrmann, Beate; Wilderman, Andrea et al. (2016): The Gq signalling pathway inhibits brown and beige adipose tissue. In: *Nature communications* 7, S. 10895. DOI: 10.1038/ncomms10895.

Kostenis, Evi; Pfeil, Eva Marie; Annala, Suvi (2020): Heterotrimeric G(q) proteins as therapeutic targets? In: *The Journal of biological chemistry* 295 (16), S. 5206–5215. DOI: 10.1074/jbc.REV119.007061.

Krumins, Andrejs M.; Gilman, Alfred G. (2006): Targeted knockdown of G protein subunits selectively prevents receptor-mediated modulation of effectors and reveals complex changes in non-targeted signaling proteins. In: *The Journal of biological chemistry* 281 (15), S. 10250–10262. DOI: 10.1074/jbc.M511551200.

Kuschak, Markus; Namasivayam, Vigneshwaran; Rafehi, Muhammad; Voss, Jan H.; Garg, Jaspal; Schlegel, Jonathan G. et al. (2019): Cell-permeable high-affinity tracers for Gq proteins provide structural insights, reveal distinct binding kinetics, and identify small molecule inhibitors. In: *British journal of pharmacology*. DOI: 10.1111/bph.14960.

Landis, C. A.; Masters, S. B.; Spada, A.; Pace, A. M.; Bourne, H. R.; Vallar, L. (1989): GTPase inhibiting mutations activate the alpha chain of Gs and stimulate adenylyl cyclase in human pituitary tumours. In: *Nature* 340 (6236), S. 692–696. DOI: 10.1038/340692a0.

Li, Jian; Ge, Yang; Huang, Jun-Xiang; Strømgaard, Kristian; Zhang, Xiaolei; Xiong, Xiao-Feng (2020): Heterotrimeric G Proteins as Therapeutic Targets in Drug Discovery. In: *Journal of medicinal chemistry* 63 (10), S. 5013–5030. DOI: 10.1021/acs.jmedchem.9b01452.

Lin, R.; Bagrodia, S.; Cerione, R.; Manor, D. (1997): A novel Cdc42Hs mutant induces cellular transformation. In: *Current biology : CB* 7 (10), S. 794–797. DOI: 10.1016/s0960-9822(06)00338-1.

Liu, Wei; Chun, Eugene; Thompson, Aaron A.; Chubukov, Pavel; Xu, Fei; Katritch, Vsevolod et al. (2012): Structural basis for allosteric regulation of GPCRs by sodium ions. In: *Science (New York, N.Y.)* 337 (6091), S. 232–236. DOI: 10.1126/science.1219218.

Longo, Patti A.; Kavran, Jennifer M.; Kim, Min-Sung; Leahy, Daniel J. (2013): Transient mammalian cell transfection with polyethylenimine (PEI). In: *Methods in enzymology* 529, S. 227–240. DOI: 10.1016/B978-0-12-418687-3.00018-5.

Lorenzen, A.; Fuss, M.; Vogt, H.; Schwabe, U. (1993): Measurement of guanine nucleotide-binding protein activation by A1 adenosine receptor agonists in bovine brain membranes: stimulation of guanosine-5'-O-(3-35Sthio)triphosphate binding. In: *Molecular pharmacology* 44 (1), S. 115–123.

Majumdar, Sharmistha; Ramachandran, Sekar; Cerione, Richard A. (2004): Perturbing the linker regions of the alpha-subunit of transducin: a new class of constitutively active GTP-binding proteins. In: *The Journal of biological chemistry* 279 (38), S. 40137–40145. DOI: 10.1074/jbc.M405420200.

Malfacini, Davide; Patt, Julian; Annala, Suvi; Harpsøe, Kasper; Eryilmaz, Funda; Reher, Raphael et al. (2019): Rational design of a heterotrimeric G protein α subunit with artificial inhibitor sensitivity. In: *The Journal of biological chemistry* 294 (15), S. 5747–5758. DOI: 10.1074/jbc.RA118.007250.

Marinissen, M. J.; Gutkind, J. S. (2001): G-protein-coupled receptors and signaling networks: emerging paradigms. In: *Trends in pharmacological sciences* 22 (7), S. 368–376. DOI: 10.1016/s0165-6147(00)01678-3.

Masuho, Ikuo; Ostrovskaya, Olga; Kramer, Grant M.; Jones, Christopher D.; Xie, Keqiang; Martemyanov, Kirill A. (2015): Distinct profiles of functional discrimination among G proteins determine the actions of G protein-coupled receptors. In: *Science signaling* 8 (405), ra123. DOI: 10.1126/scisignal.aab4068.

Matthey, Michaela; Roberts, Richard; Seidinger, Alexander; Simon, Annika; Schröder, Ralf; Kuschak, Markus et al. (2017): Targeted inhibition of G(q) signaling induces airway relaxation in mouse models of asthma. In: *Science translational medicine* 9 (407). DOI: 10.1126/scitranslmed.aag2288.

McKnight, G. S. (1991): Cyclic AMP second messenger systems. In: *Current opinion in cell biology* 3 (2), S. 213–217. DOI: 10.1016/0955-0674(91)90141-k.

Meister, Jaroslawna; Wang, Lei; Pydi, Sai P.; Wess, Jürgen (2021): Chemogenetic approaches to identify metabolically important GPCR signaling pathways: Therapeutic implications. In: *Journal of neurochemistry* 158 (3), S. 603–620. DOI: 10.1111/jnc.15314.

Miller-Gallacher, Jennifer L.; Nehmé, Rony; Warne, Tony; Edwards, Patricia C.; Schertler, Gebhard F. X.; Leslie, Andrew G. W.; Tate, Christopher G. (2014): The 2.1 Å resolution structure of

cyanopindolol-bound β1-adrenoceptor identifies an intramembrane Na+ ion that stabilises the ligand-free receptor. In: *PloS one* 9 (3), e92727. DOI: 10.1371/journal.pone.0092727.

Min, Anna de; Matera, Carlo; Bock, Andreas; Holze, Janine; Kloeckner, Jessica; Muth, Mathias et al. (2017): A New Molecular Mechanism To Engineer Protean Agonism at a G Protein-Coupled Receptor. In: *Molecular pharmacology* 91 (4), S. 348–356. DOI: 10.1124/mol.116.107276.

Mons, N.; Decorte, L.; Jaffard, R.; Cooper, D. M. (1998): Ca2+-sensitive adenylyl cyclases, key integrators of cellular signalling. In: *Life sciences* 62 (17-18), S. 1647–1652. DOI: 10.1016/s0024-3205(98)00122-2.

Newton, Alexandra C.; Bootman, Martin D.; Scott, John D. (2016): Second Messengers. In: *Cold Spring Harbor perspectives in biology* 8 (8). DOI: 10.1101/cshperspect.a005926.

Nishimura, Akiyuki; Kitano, Ken; Takasaki, Jun; Taniguchi, Masatoshi; Mizuno, Norikazu; Tago, Kenji et al. (2010a): Structural basis for the specific inhibition of heterotrimeric Gq protein by a small molecule. In: *Proceedings of the National Academy of Sciences of the United States of America* 107 (31), S. 13666–13671. DOI: 10.1073/pnas.1003553107.

Nishimura, Akiyuki; Kitano, Ken; Takasaki, Jun; Taniguchi, Masatoshi; Mizuno, Norikazu; Tago, Kenji et al. (2010b): Structural basis for the specific inhibition of heterotrimeric Gq protein by a small molecule. In: *Proceedings of the National Academy of Sciences of the United States of America* 107 (31), S. 13666–13671. DOI: 10.1073/pnas.1003553107.

Oakley, R. H.; Laporte, S. A.; Holt, J. A.; Barak, L. S.; Caron, M. G. (1999): Association of beta-arrestin with G protein-coupled receptors during clathrin-mediated endocytosis dictates the profile of receptor resensitization. In: *The Journal of biological chemistry* 274 (45), S. 32248–32257. DOI: 10.1074/jbc.274.45.32248.

O'Hayre, Morgan; Vázquez-Prado, José; Kufareva, Irina; Stawiski, Eric W.; Handel, Tracy M.; Seshagiri, Somasekar; Gutkind, J. Silvio (2013 Jun): The emerging mutational landscape of G proteins and G-protein-coupled receptors in cancer.

Okashah, Najeah; Wright, Shane C.; Kawakami, Kouki; Mathiasen, Signe; Zhou, Joris; Lu, Sumin et al. (2020): Agonist-induced formation of unproductive receptor-G(12) complexes. In: *Proceedings of the National Academy of Sciences of the United States of America* 117 (35), S. 21723–21730. DOI: 10.1073/pnas.2003787117.

Oldham, William M.; Hamm, Heidi E. (2008): Heterotrimeric G protein activation by G-protein-coupled receptors. In: *Nature reviews. Molecular cell biology* 9 (1), S. 60–71. DOI: 10.1038/nrm2299.

Onken, Michael D.; Makepeace, Carol M.; Kaltenbronn, Kevin M.; Kanai, Stanley M.; Todd, Tyson D.; Wang, Shiqi et al. (2018): Targeting nucleotide exchange to inhibit constitutively active G protein α subunits in cancer cells. In: *Science signaling* 11 (546). DOI: 10.1126/scisignal.aao6852.

Patt, Julian; Alenfelder, Judith; Pfeil, Eva Marie; Voss, Jan Hendrik; Merten, Nicole; Eryilmaz, Funda et al. (2021): An experimental strategy to probe Gq contribution to signal transduction in living cells. In: *The Journal of biological chemistry* 296, S. 100472. DOI: 10.1016/j.jbc.2021.100472.

Pfeil, Eva Marie; Brands, Julian; Merten, Nicole; Vögtle, Timo; Vescovo, Maddalena; Rick, Ulrike et al. (2020): Heterotrimeric G Protein Subunit Gαq Is a Master Switch for Gβγ-Mediated Calcium

Mobilization by Gi-Coupled GPCRs. In: *Molecular cell* 80 (6), 940-954.e6. DOI: 10.1016/j.molcel.2020.10.027.

Prévost, Grégoire P.; Lonchampt, Marie O.; Holbeck, Susan; Attoub, Samir; Zaharevitz, Daniel; Alley, Mike et al. (2006): Anticancer activity of BIM-46174, a new inhibitor of the heterotrimeric Galpha/Gbetagamma protein complex. In: *Cancer research* 66 (18), S. 9227–9234. DOI: 10.1158/0008-5472.CAN-05-4205.

Reher, Raphael; Kühl, Toni; Annala, Suvi; Benkel, Tobias; Kaufmann, Desireé; Nubbemeyer, Britta et al. (2018a): Deciphering Specificity Determinants for FR900359-Derived G(q) α Inhibitors Based on Computational and Structure-Activity Studies. In: *ChemMedChem* 13 (16), S. 1634–1643. DOI: 10.1002/cmdc.201800304.

Reher, Raphael; Kuschak, Markus; Heycke, Nina; Annala, Suvi; Kehraus, Stefan; Dai, Hao-Fu et al. (2018b): Applying Molecular Networking for the Detection of Natural Sources and Analogues of the Selective Gq Protein Inhibitor FR900359. In: *Journal of natural products* 81 (7), S. 1628–1635. DOI: 10.1021/acs.jnatprod.8b00222.

Rensing, Derek T.; Uppal, Sakshi; Blumer, Kendall J.; Moeller, Kevin D. (2015a): Toward the Selective Inhibition of G Proteins: Total Synthesis of a Simplified YM-254890 Analog. In: *Organic letters* 17 (9), S. 2270–2273. DOI: 10.1021/acs.orglett.5b00944.

Rensing, Derek T.; Uppal, Sakshi; Blumer, Kendall J.; Moeller, Kevin D. (2015b): Toward the Selective Inhibition of G Proteins: Total Synthesis of a Simplified YM-254890 Analog. In: *Organic letters* 17 (9), S. 2270–2273. DOI: 10.1021/acs.orglett.5b00944.

Rodbell, M. (1980): The role of hormone receptors and GTP-regulatory proteins in membrane transduction. In: *Nature* 284 (5751), S. 17–22. DOI: 10.1038/284017a0.

Rondard, P.; Iiri, T.; Srinivasan, S.; Meng, E.; Fujita, T.; Bourne, H. R. (2001): Mutant G protein alpha subunit activated by Gbeta gamma: a model for receptor activation? In: *Proceedings of the National Academy of Sciences of the United States of America* 98 (11), S. 6150–6155. DOI: 10.1073/pnas.101136198.

Rosenbaum, Daniel M.; Rasmussen, Søren G. F.; Kobilka, Brian K. (2009): The structure and function of G-protein-coupled receptors. In: *Nature* 459 (7245), S. 356–363. DOI: 10.1038/nature08144.

Roth, Bryan L. (2016): DREADDs for Neuroscientists. In: *Neuron* 89 (4), S. 683–694. DOI: 10.1016/j.neuron.2016.01.040.

Sassone-Corsi, Paolo (2012): The cyclic AMP pathway. In: *Cold Spring Harbor perspectives in biology* 4 (12). DOI: 10.1101/cshperspect.a011148.

Schrage, R.; Min, A. de; Hochheiser, K.; Kostenis, E.; Mohr, K. (2016): Superagonism at G protein-coupled receptors and beyond. In: *British journal of pharmacology* 173 (20), S. 3018–3027. DOI: 10.1111/bph.13278.

Schrage, Ramona; Schmitz, Anna-Lena; Gaffal, Evelyn; Annala, Suvi; Kehraus, Stefan; Wenzel, Daniela et al. (2015): The experimental power of FR900359 to study Gq-regulated biological processes. In: *Nature communications* 6, S. 10156. DOI: 10.1038/ncomms10156.

Schröder, Ralf; Janssen, Nicole; Schmidt, Johannes; Kebig, Anna; Merten, Nicole; Hennen, Stephanie et al. (2010): Deconvolution of complex G protein-coupled receptor signaling in live cells using dynamic mass redistribution measurements. In: *Nature biotechnology* 28 (9), S. 943–949. DOI: 10.1038/nbt.1671.

Schröder, Ralf; Schmidt, Johannes; Blättermann, Stefanie; Peters, Lucas; Janssen, Nicole; Grundmann, Manuel et al. (2011): Applying label-free dynamic mass redistribution technology to frame signaling of G protein-coupled receptors noninvasively in living cells. In: *Nature protocols* 6 (11), S. 1748–1760. DOI: 10.1038/nprot.2011.386.

Seibel-Ehlert, Ulla; Plank, Nicole; Inoue, Asuka; Bernhardt, Guenther; Strasser, Andrea (2021): Label-Free Investigations on the G Protein Dependent Signaling Pathways of Histamine Receptors. In: *International journal of molecular sciences* 22 (18). DOI: 10.3390/ijms22189739.

Seifert, R.; Lee, T. W.; Lam, V. T.; Kobilka, B. K. (1998): Reconstitution of beta2-adrenoceptor-GTP-binding-protein interaction in Sf9 cells--high coupling efficiency in a beta2-adrenoceptor-G(s alpha) fusion protein. In: *European journal of biochemistry* 255 (2), S. 369–382. DOI: 10.1046/j.1432-1327.1998.2550369.x.

Simon, M. I.; Strathmann, M. P.; Gautam, N. (1991): Diversity of G proteins in signal transduction. In: *Science (New York, N.Y.)* 252 (5007), S. 802–808. DOI: 10.1126/science.1902986.

Singh, Garima; Ramachandran, Sekar; Cerione, Richard A. (2012): A constitutively active Gα subunit provides insights into the mechanism of G protein activation. In: *Biochemistry* 51 (15), S. 3232–3240. DOI: 10.1021/bi3001984.

Steiner, Debora; Saya, Daniella; Schallmach, Ester; Simonds, William F.; Vogel, Zvi (2006): Adenylyl cyclase type-VIII activity is regulated by G(betagamma) subunits. In: *Cellular signalling* 18 (1), S. 62–68. DOI: 10.1016/j.cellsig.2005.03.014.

Stone, Laura S.; Molliver, Derek C. (2009): In search of analgesia: emerging roles of GPCRs in pain. In: *Molecular interventions* 9 (5), S. 234–251. DOI: 10.1124/mi.9.5.7.

Syrovatkina, Viktoriya; Alegre, Kamela O.; Dey, Raja; Huang, Xin-Yun (2016a): Regulation, Signaling, and Physiological Functions of G-Proteins. In: *Journal of molecular biology* 428 (19), S. 3850–3868. DOI: 10.1016/j.jmb.2016.08.002.

Syrovatkina, Viktoriya; Alegre, Kamela O.; Dey, Raja; Huang, Xin-Yun (2016b): Regulation, Signaling, and Physiological Functions of G-Proteins. In: *Journal of molecular biology* 428 (19), S. 3850–3868. DOI: 10.1016/j.jmb.2016.08.002.

Takasaki, Jun; Saito, Tetsu; Taniguchi, Masatoshi; Kawasaki, Tomihisa; Moritani, Yumiko; Hayashi, Kazumi; Kobori, Masato (2004): A novel Galphaq/11-selective inhibitor. In: *The Journal of biological chemistry* 279 (46), S. 47438–47445. DOI: 10.1074/jbc.M408846200.

Tang, W. J.; Gilman, A. G. (1991): Type-specific regulation of adenylyl cyclase by G protein beta gamma subunits. In: *Science (New York, N.Y.)* 254 (5037), S. 1500–1503. DOI: 10.1126/science.1962211.

Taniguchi, Masatoshi; Nagai, Koji; Arao, Nakako; Kawasaki, Tomihisa; Saito, Tetsu; Moritani, Yumiko et al. (2003): YM-254890, a novel platelet aggregation inhibitor produced by

Chromobacterium sp. QS3666. In: *The Journal of antibiotics* 56 (4), S. 358–363. DOI: 10.7164/antibiotics.56.358.

Taniguchi, Masatoshi; Suzumura, Ken-Ichi; Nagai, Koji; Kawasaki, Tomihisa; Takasaki, Jun; Sekiguchi, Mitsuhiro et al. (2004a): YM-254890 analogues, novel cyclic depsipeptides with Galpha(q/11) inhibitory activity from Chromobacterium sp. QS3666. In: *Bioorganic & medicinal chemistry* 12 (12), S. 3125–3133. DOI: 10.1016/j.bmc.2004.04.006.

Taniguchi, Masatoshi; Suzumura, Ken-Ichi; Nagai, Koji; Kawasaki, Tomihisa; Takasaki, Jun; Sekiguchi, Mitsuhiro et al. (2004b): YM-254890 analogues, novel cyclic depsipeptides with Galpha(q/11) inhibitory activity from Chromobacterium sp. QS3666. In: *Bioorganic & medicinal chemistry* 12 (12), S. 3125–3133. DOI: 10.1016/j.bmc.2004.04.006.

Taylor, S. S.; Knighton, D. R.; Zheng, J.; Eyck, L. F. ten; Sowadski, J. M. (1992): Structural framework for the protein kinase family. In: *Annual review of cell biology* 8, S. 429–462. DOI: 10.1146/annurev.cb.08.110192.002241.

Uemura, Toshio; Takamatsu, Hajime; Kawasaki, Tomihisa; Taniguchi, Masatoshi; Yamamoto, Eisaku; Tomura, Yuichi et al. (2006): Effect of YM-254890, a specific Galphaq/11 inhibitor, on experimental peripheral arterial disease in rats. In: *European journal of pharmacology* 536 (1-2), S. 154–161. DOI: 10.1016/j.ejphar.2006.02.048.

Voss, Jan H.; Nagel, Jessica; Rafehi, Muhammad; Guixà-González, Ramon; Malfacini, Davide; Patt, Julian et al. (2021): Unraveling binding mechanism and kinetics of macrocyclic Gα(q) protein inhibitors. In: *Pharmacological research* 173, S. 105880. DOI: 10.1016/j.phrs.2021.105880.

Wacker, Daniel; Stevens, Raymond C.; Roth, Bryan L. (2017): How Ligands Illuminate GPCR Molecular Pharmacology. In: *Cell* 170 (3), S. 414–427. DOI: 10.1016/j.cell.2017.07.009.

Wettschureck, Nina; Offermanns, Stefan (2005): Mammalian G proteins and their cell type specific functions. In: *Physiological reviews* 85 (4), S. 1159–1204. DOI: 10.1152/physrev.00003.2005.

Wilson, C. H.; McIntyre, R. E.; Arends, M. J.; Adams, D. J. (2010): The activating mutation R201C in GNAS promotes intestinal tumourigenesis in Apc(Min/+) mice through activation of Wnt and ERK1/2 MAPK pathways. In: *Oncogene* 29 (32), S. 4567–4575. DOI: 10.1038/onc.2010.202.

Wong, M. P.; Cooper, D. M.; Young, K. W.; Young, J. M. (2000): Characteristics of the Ca(2+)-dependent inhibition of cyclic AMP accumulation by histamine and thapsigargin in human U373 MG astrocytoma cells. In: *British journal of pharmacology* 130 (5), S. 1021–1030. DOI: 10.1038/sj.bjp.0703411.

Xiong, Xiao-Feng; Zhang, Hang; Underwood, Christina R.; Harpsøe, Kasper; Gardella, Thomas J.; Wöldike, Mie F. et al. (2016): Total synthesis and structure-activity relationship studies of a series of selective G protein inhibitors. In: *Nature chemistry* 8 (11), S. 1035–1041. DOI: 10.1038/nchem.2577.

Zhang, Hang; Nielsen, Alexander L.; Boesgaard, Michael W.; Harpsøe, Kasper; Daly, Norelle L.; Xiong, Xiao-Feng et al. (2018a): Structure-activity relationship and conformational studies of the natural product cyclic depsipeptides YM-254890 and FR900359. In: *European journal of medicinal chemistry* 156, S. 847–860. DOI: 10.1016/j.ejmech.2018.07.023.

Zhang, Hang; Nielsen, Alexander L.; Boesgaard, Michael W.; Harpsøe, Kasper; Daly, Norelle L.; Xiong, Xiao-Feng et al. (2018b): Structure-activity relationship and conformational studies of the natural product cyclic depsipeptides YM-254890 and FR900359. In: *European journal of medicinal chemistry* 156, S. 847–860. DOI: 10.1016/j.ejmech.2018.07.023.

Zhang, Hang; Xiong, Xiao-Feng; Boesgaard, Michael W.; Underwood, Christina R.; Bräuner-Osborne, Hans; Strømgaard, Kristian (2017a): Structure-Activity Relationship Studies of the Cyclic Depsipeptide Natural Product YM-254890, Targeting the G(q) Protein. In: *ChemMedChem* 12 (11), S. 830–834. DOI: 10.1002/cmdc.201700155.

Zhang, Hang; Xiong, Xiao-Feng; Boesgaard, Michael W.; Underwood, Christina R.; Bräuner-Osborne, Hans; Strømgaard, Kristian (2017b): Structure-Activity Relationship Studies of the Cyclic Depsipeptide Natural Product YM-254890, Targeting the G(q) Protein. In: *ChemMedChem* 12 (11), S. 830–834. DOI: 10.1002/cmdc.201700155.

Zhu, Hu; Roth, Bryan L. (2014): DREADD: a chemogenetic GPCR signaling platform. In: *The international journal of neuropsychopharmacology* 18 (1). DOI: 10.1093/ijnp/pyu007.

Abbreviations

AC	adenylyl cyclase
ATP	adenosine-5'-triphosphate
BRET	bioluminescence resonance energy transfer
cAMP	cyclic adenosine monophosphate
CCh	carbachol
cDNA	complementary DNA
CRISPR	Clustered Regularly Interspaced Short Palindromic Repeats
DAG	diacylglycerol
DMR	dynamic mass redistribution
DNA	desoxyribonucleic acid
ER	endoplasmatic reticulum
e.coli	Escherichia coli
pEC_{50}	concentration of half maximum effect
pEC_{80}	effect concentration at 80%
FBS	fetal bovine/calf serum
FR	FR900359
GAP	GTPase-activating proteins
GDP	guanine diphosphate
GDI	guanine nucleotide exchange factor

GPCR	G protein-coupled receptor
GTP	guanine triphosphate
HBSS	Hanks balanced salt solution
HEK	human embryonic kidney cells, HEK293 cells
HEPES	4-(2-hydroxyethyl)-1-piperazineethane- sulfonic acid
HTRF	homogeneous time resolved fluorescence
pIC_{50}	half-maximal inhibitory concentration
IP_3	inositol-1,4,5-trisphosphate
Iso	isoprenaline
PCR	Polymerase chain reaction
PIP_2	phosphoinositol-4,5-bisphosphate
PKA	protein kinase A
YM	YM-254890

List of Figures

Publications

1. Patt, J., Alenfelder, J., Pfeil, E.M**.**, Voss, J.H., Merten, N., **Eryilmaz, F.**, Heycke, N., Rick, U., Inoue, A., Kehraus, S., Deupi, X., Müller, C.E., König, G.M., Crüsemann, M., and Kostenis, E. An experimental strategy to probe Gq contribution to signal transduction in living cells. **The Journal of Biological Chemistry** 2021, p. 100472. DOI: 10.1016/j.jbc.2021.100472

2. Davide Malfacini, Julian Patt, Suvi Annala, Kasper Harpsøe, **Funda Eryilmaz**, Raphael Reher, Max Crüsemann, Wiebke Hanke, Hang Zhang, Daniel Tietze, David E. Gloriam, Hans Bräuner-Osborne, Kristian Strømgaard, Gabriele M. Könnig, Asuka Inoue, Jesus Gomeza, and Evi Kostenis. Rational design of a heterotrimeric G protein subunit with artificial inhibitor sensitivity. **The Journal of Biological Chemistry 2019,** DOI 10.1074/jbc.RA118

3. Annala, S.; Feng, X.; Shridhar, N.; **Eryilmaz, F.;** Patt, J.; Yang, J.; Pfeil, E. M.; Cervantes-Villagrana, R. D.; Inoue, A.; Häberlein, F.; Slodczyk, T.; Reher, R.; Kehraus, S.; Monteleone, S.; Schrage, R.; Heycke, N.; Rick, U.; Engel, S.; Pfeifer, A.; Kolb, P.;König, G.; Bünemann, M.; Tüting, T.; Vázquez-Prado, J.; Gutkind, J. S.; Gaffal, E.;Kostenis, E. Direct targeting of Gαq and Gα11 oncoproteins in cancer cells. **Science signaling** 2019, *12* (573). DOI: 10.1126/scisignal.aau5948